

Departamento de Ciencias Experimentales y de la Salud
Facultad de Ciencias de la Salud y de la Vida
Universidad Pompeu Fabra

"Characterization of *SNAIL1* and *PTEN* transcriptional regulation by snail1 : new insights into Epithelial-to-Mesenchymal transition and cell resistance to apoptosis"

Memoria presentada por
María Escrivá Izquierdo
para optar al Grado de Doctor,
Barcelona, Junio de 2008.

Trabajo realizado bajo la dirección del Dr. Antonio García de Herreros Madueño y de la Dra. Sandra Peiró Sales, en el "Institut Municipal d'Investigació Mèdica" (IMIM-Hospital del Mar), dentro del "Programa de Recerca en Càncer".

Antonio García de Herreros Madueño
(Director de la Tesis)

Sandra Peiró Sales
(Directora de la Tesis)

María Escrivá Izquierdo
(Doctoranda)

“Science is always wrong, it never solves a problem without creating ten more.”

George Bernard Shaw

ACKNOWLEDGMENTS

(Agradecimientos)

La cotidianidad es tal vez nuestro mejor aliado y nuestro más temido enemigo. Envueltos en ella corremos el riesgo de no apreciar cada segundo y sin embargo, sin ella no podríamos encontrar ese ambiente en el que nos dejamos ser quien somos, como somos. Es curioso cómo, en el transcurso de la redacción de esta tesis, uno se distancia de esa cotidianidad para sumergirse en otra y es precisamente entonces cuando se hace patente la suerte que se ha tenido al estar rodeado de todos aquellos a los que se echa en falta. A esa gente, a cada uno de los que ocupa un buen recuerdo en la memoria, es a quien dedico esta tesis.

No puedo dejar, sin embargo, de hacer mención a aquellos que de una manera directa han hecho que este día sea posible. No sólo quiero agradecer a los miembros del tribunal el que hayan aceptado compartir conmigo esta experiencia y regalarme algunos sabios consejos, sino que también quiero agradecer, y muy especialmente, su ayuda a mis directores de tesis. A Antonio le deberé siempre la oportunidad que me brindó de unirme a su grupo, sus esfuerzos iniciales por pedir una beca cuando nos separaba el océano Atlántico y su apoyo constante a lo largo de estos cuatro años. Este trabajo que hoy concluyo no existiría de no ser por su habilidad para saber guiar los esfuerzos en la buena dirección. Gracias no sólo por eso, sino también permitir mi incursión docente, una experiencia muy positiva que he compartido con buenos amigos. Para Sandra es difícil tener palabras; ni en el mejor de mis sueños hubiera imaginado una compañera de fatigas y consejera mejor. Gracias por enseñarme con una paciencia inacabable, por buscar el lado positivo de cada resultado, por tu incansable inquietud por seguir mejorando y tu apoyo cuando me encontraba en unos

de esos agujeros en que, a veces, cuesta ver la luz. Gracias por ser una amiga.

No quisiera dejar pasar esta ocasión sin hacer mención especial a mis padres, las personas más generosas que conozco y cuyo apoyo incansable no conoce kilómetros. Gracias por el esfuerzo cotidiano a lo largo de los años, por enseñarme el mundo y preocuparos por hacerme un hueco en él. No tengo palabras, no hay palabras. A mi hermano Tomás, compañero de juegos y amigo. Tu ingenuidad y optimismo, tu capacidad para escuchar y tu habilidad para transmitir la ilusión que llevas dentro son tu mejor atributo. Cómete el mundo y guarda un rato para escuchar historias raras de laboratorios y células verdes (aunque sea en la distancia que rompe la webcam). Al resto de mi familia, a Jose y Joaquín, a Carmen y "las niñas" (que hace tiempo que dejaron de serlo). Gracias por los ánimos, las visitas y las tartas de chocolate con galleta. A mi familia catalana-toledana, por hacer un hueco en sus vidas y hacerme sentir como en casa desde el primer día. A "los de Alicante" como yo os llamo, por haber aprendido a conllevar la amistad en la distancia, por reservaros las nocheviejas, por mantener viva una relación que tiene más años que memoria tenemos nosotros. Y a la "secta", como se refieren a nosotros los que nos envidian. Gracias a esos padres y madres, vecinos y vecinas, amigos y amigas, que nos han criado con el espanto y orgullo de vernos crecer y llegar a compartir una copa de cava en las noches de Junio. A los que llegaron por casualidad y me hicieron un hueco en "Monistrol" y en sus vidas. A los que se dejan seducir por un partido del FCB emitido por "los chinos", a los que, más con paciencia que éxito (por mi culpa, sin duda), me enseñaron sevillanas, a los que les falta tiempo para montar una escapada a esquiar o un partidillo de fútbol. Gracias a todos. A mis "niñas" Montse y Gina, por la grata sorpresa de no descubrirlas demasiado tarde como para no compartir las alegrías y miserias de estos últimos años. A las chicas del fútbol, que con la excusa de jugar cada jueves, hoy puedo llamar amigas. A su inacabable paciencia para

dejarme jugar de delantera cuando no doy pie con bola y a las caipirinhas tóxicas que hemos compartido.

A los compañeros del laboratorio, a los que se fueron y a los que ahora llegan. Gracias por compartir "rotus", células y algunas "farras". Os deseo mucha suerte. A la ya extinta UBCM, a todos y cada uno de los que habéis compartido estos años conmigo. Gracias por las conversaciones en cultivos, los partidos de voley playa y los ánimos cuando se acercaba el temido seminario UBCM.

A todos aquellos que merecen unas líneas que no escribiré, y sin embargo, mantienen intacto su lugar en mis recuerdos.

A Arnau, por la paciencia infinita del convivir cotidiano, por compartir mis triunfos y curar mis tristezas. Por el futuro que compartimos.

Barcelona, 27 de abril de 2008.

TABLE OF CONTENTS

TABLE OF CONTENTS	11
FIGURE INDEX	11
ABBREVIATION AND ACRONIM INDEX	17
INTRODUCTION	19
I.1. General insights into embryonic development.....	21
I.1.a. From cell to embryo.....	21
I.1.b. Epithelial-to-Mesenchymal Transition (EMT) during embryonic development.....	22
I.1.b.i. Gastrulation.....	24
I.1.b.ii. Neural crest delamination.....	25
I.2. Cancer: what lessons can we take from embryo development?.....	28
I.2.a. Generalities about cancer.....	28
I.2.b. Mechanisms shared by development and cancer.....	30
I.2.c. EMT and cancer.....	31
I.3. The transcriptional regulation of EMT.....	34
I.3.a. The zeb family of transcription factors and EMT.....	35
I.3.b. The bHLH family of transcription factors and EMT.....	35
I.3.c. The snail superfamily of transcription factors and EMT.....	36
I.4. The snail1 transcription factor.....	40
I.4.a. Snail1 protein structure.....	41
I.4.b. SNAIL1 gene structure and transcriptional regulation.....	42
I.5. Snail1 and cancer.....	43
I.6. Cell survival and cancer: the importance of apoptosis.....	45
I.6.a. The importance of apoptosis in tissue homeostasis and tumor progression.....	45
I.6.b. The two apoptotic pathways.....	47
I.6.c. The role of p53 protein in cell cycle arrest and apoptosis.....	48
I.6.a. The PI3K-Akt/PKB pathway and cell survival.....	50
I.7. The role of snail family members in apoptosis and cell damage response.....	51
OBJECTIVES	55
RESULTS	57

RESULTS 1. REPRESSION OF PTEN PHOSPHATASE BY SNAIL1 TRANSCRIPTIONAL FACTOR DURING γ RADIATION-INDUCED APOPTOSIS.....	59
R.1.1. Snail1 prevents PTEN γ radiation-induced up-regulation.	59
R.1.2. Snail1 induces resistance to γ -radiation-induced apoptosis.	61
R.1.3. Up-regulated Akt activity and decreased levels of PTEN mRNA are also detected in RWP-1 cells transfected with snail1.	64
R.1.4. Contrary distribution of snail1 and PTEN in murine embryos.	65
R.1.5. Relevance of <i>PTEN</i> repression in the resistance to γ radiation-induced apoptosis caused by snail1.	67
R.1.6. Snail1 binds to <i>PTEN</i> promoter and represses its activity.	70
R.1.7. Binding of snail1-HA to <i>PTEN</i> promoter is modulated after γ radiation.	72
R.1.8. Summary to Chapter 1.	75
RESULTS 2. POST-TRANSLATIONAL MODULATION OF SNAIL1 PROTEIN IN RESPONSE TO γ RADIATION	77
R.2.1. Snail1 protein is stabilized in response to γ radiation.	77
R.2.2. Chk1 phosphorylates snail1 "in vitro".	80
R.2.3. Relevance of Ser246 in snail1 stabilization, E-cadherin repression and resistance to apoptosis promotion.....	82
R.2.4. Summary to Chapter 2.	85
RESULTS 3. SNAIL1 BINDS TO ITS OWN PROMOTER AND GENERATES A NEGATIVE FEED-BACK LOOP THAT CONTROLS ITS EXPRESSION IN EPITHELIAL CELLS.....	87
R.3.1. Snail1 expression is stimulated by serum.	87
R.3.2. Characterization of three E-boxes within <i>SNAIL1</i> promoter.....	89
R.3.3. Ectopic snail1 represses <i>SNAIL1</i> promoter and down-regulates snail1 mRNA levels.	91
R.3.4. Snail1 protein binds to <i>SNAIL1</i> promoter.	93
R.3.5. A snail1 inhibitory feed-back loop is active in cell culture.....	95
R.3.6. Summary to Chapter 3.	97
RESULTS 4. SNAIL1 EFFECTS ON <i>SNAIL1</i> TRANSCRIPTION ARE CELL DEPENDENT.....	99
R.4.1. Snail1 activates in its own promoter independently of the E-box.	99
R.4.2. E-cadherin controls the activation of <i>SNAIL1</i> promoter by snail1.	104
R.4.3. Snail1 stimulation of <i>SNAIL1</i> promoter requires NF κ B transcriptional activity.	107
R.4.4. Summary to Chapter 4.	109

MATERIALS & METHODS	111
MM.1. Cell culture.	113
MM.2. DNA constructs and transfection.	114
MM.3. Fluorescence Activated Cell Sorter (FACS) analysis and determination of cell cycle and cell death.	117
MM.4. Analysis of protein expression by Western Blot.	119
Analysis of endogenous snail1 and annexin-2 in NIH-3T3 cells	119
Determination of the exogenous snail1 protein in transfected cells	120
Determination of exogenous E-cadherin protein in transfected cells	121
Determination of endogenous proteins in transfected cells	121
MM.5. Phosphorylated protein purification and western blot analysis	122
MM.6. Immunofluorescence protocol	122
MM.7. Luciferase reporter assays	123
MM.8. Chromatin immunoprecipitation assay (ChIP)	124
MM.9. Gel retardation assays	128
MM.10. Semi quantitative and quantitative RT-PCR analysis	129
MM.11. Immunohistochemistry	131
MM.12. "In vitro" phosphorylation assays	132
DISCUSSION	135
The PI3K/Akt/PTEN interplay and how snail1 fits in between to promote cell survival.	137
The importance of snail1-induced resistance to apoptosis.	145
The complex network of <i>SNAIL1</i> transcriptional control.	152
New strategies by which snail1 promotes EMT and cell migration.	156
General overview of this thesis: our working model.	159
ANNEX	163
A.1. ChIP-on-CHIP	165
A.2. Sequence of the -883/+305 PTEN promoter and its representative motifs.	177
A.3. Sequence of the different <i>SNAIL1</i> promoters used in this study and its representative motifs.	179
A.4. p53MH software analysis of mouse snail2 transcript and human snail1 transcript.	181
BIBLIOGRAPHY	185
PUBLISHED PAPERS	203

FIGURE INDEX

INTRODUCTION

FIGURE I-1. Derivative tissues from the three embryonic layers (ectoderm, mesoderm and endoderm).	21
FIGURE I-2. Examples of EMT during embryonic development.	24
FIGURE I-3. Amnion structure and cell movements during human gastrulation.	25
FIGURE I-4. Major derivatives of the ectoderm germ layer.	26
FIGURE I-5. Neural crest cell migration in the trunk of the chick embryo.	27
FIGURE I-6. Localization of two different cadherins during the formation of the mouse neural tube.	28
FIGURE I-7. Acquired capabilities of cancer.	30
FIGURE I-8. The EMT cell traits.	32
FIGURE I-9. Scheme of the pathways involved in EMT.	33
FIGURE I-10. EMT-MET in tumor progression and metastasis.	34
FIGURE I-11. Scheme of the most relevant domains existent in Zeb1 and Zeb2.	35
FIGURE I-12. Scheme of the most relevant domains existent in the bHLH twist1 protein.	36
FIGURE I-13. The snail superfamily members.	37
FIGURE I-14. Scheme of the C2H2 type zinc fingers.	38
FIGURE I-15. Scheme of the most relevant domains existent in two snail family members: snail1 and snail2 (slug).	39
FIGURE I-16. Scheme of the snail1 protein.	42
FIGURE I-17. Death receptor (extrinsic) and intrinsic pathways of apoptosis.	48
FIGURE I-18. Effects of ionizing radiation on normal cells and cancer p53 (-/-) cells.	49
FIGURE I-19. p53-mediated activation of apoptosis via the intrinsic signaling pathway.	50

RESULTS

FIGURE R-1. Snail1 inhibits PTEN up-regulation and prevents the decrease in Akt activity in response to γ radiation.	60
FIGURE R-2. Snail1 transfection prevents MDCK cells to undergo apoptosis in response to γ radiation.	63
FIGURE R-3. Transfection of snail1 to RWP-1 cells up-regulates Akt activity and decreases PTEN mRNA levels.	65

FIGURE R-4. Snail1 and PTEN proteins display an inverse expression pattern in murine embryos.....	67
FIGURE R-5. Ectopic manipulation of PTEN protein levels affects cell death and snail1 response.....	70
FIGURE R-6. Snail1 represses PTEN promoter activity.....	72
FIGURE R-7. Snail1 is recruited to the PTEN promoter "in vivo" in response to γ radiation.	74
FIGURE R-8. Snail1 protein is stabilized in response to γ radiation.	78
FIGURE R-9. Nuclear Snail1 endogenous protein is increased in response to γ radiation in NIH-3T3 cells.	80
FIGURE R-10. Recombinant Chk1 phosphorylates snail1-GST "in vitro".....	81
FIGURE R-11. Snail1 S246A mutant (unlike wild type snail1) is not able to promote resistance to γ radiation-induced apoptosis.	82
FIGURE R-12. Snail1 S246A is located in the nucleus of MDCK.	83
FIGURE R-13. Snail1 S246A cannot bind PTEN probe in vitro.....	84
FIGURE R-14. Snail1 S246A protein is stabilized in response to γ radiation in MDCK-snail1 (S246A) cells but is unable to repress E-Cadherin.	85
FIGURE R-15. Snail1 expression is stimulated by serum.	88
FIGURE R-16. Scheme of the different SNAIL1 promoters used in this study.....	89
FIGURE R-17. <i>SNAIL1</i> promoter contains an E-box that binds a repressor.	90
FIGURE R-18. Ectopic snail1 represses the activity of SNAIL1 promoter.	92
FIGURE R-19. Ectopic snail1 murine protein down-regulates human endogenous snail1 mRNA.	93
FIGURE R-20. Snail1 binds to <i>SNAIL1</i> promoter in vitro.	94
FIGURE R-21. Snail1 binds to SNAIL1 promoter "in vivo".	95
FIGURE R-22. Snail1 represses its own expression generating a negative feed-back loop.....	97
FIGURE R-23. Ectopic murine snail1 protein upregulates human endogenous snail1 mRNA in mesenchymal cells.	100
FIGURE R-24. Ectopic snail1 activates the activity of SNAIL1 promoter.....	101
FIGURE R-25. Ectopic snail1 activates the activity of <i>SNAIL1</i> promoter.....	102
FIGURE R-26. ChIP analysis confirms snail1 binding to SNAIL1 in SW-480 cells.....	103
FIGURE R-27. The negative feed-back loop is functional in mesenchymal cells.	103
FIGURE R-28. ILK promotes EMT in IEC cells and switches SNAIL1 responsiveness from repression to activation.	104

FIGURE R-29. Overexpression of E-cadherin blocks snail1 activation of -194/+59
SNAIL1 promoter..... 106

FIGURE R-30. Overexpression of E-cadherin blocks snail1 mRNA transcription. 107

FIGURE R-31. NFkB signalling is increased in snail1 expressing cells and can be
 blocked by E-cadherin over-expression..... 108

FIGURE R-32. SNAIL1 induction by snail1 requires NFkB signaling..... 109

DISCUSSION

FIGURE D-1. PI3K pathway: Akt activation. 138

FIGURE D-2. Cell response to ionizing radiation..... 146

FIGURE D-3. Model of the conserved pathway by which snail1 and snail2
 antagonize p53-mediated apoptosis..... 150

FIGURE D-4. Effects of PTEN on migration and motility. 158

ABREVIATION AND ACRONIM INDEX

BSA: Bovine Serum Albumin	HNSCC: Head and Neck Squamous Cell Carcinoma
CDH1: E-cadherin Gene	HPRT: Hypoxanthine Guanine Phosphoribosyl Transferase
CLC: Colorectal Cancer	IDC: Infiltrating Ductal Carcinoma
CMV: cytomegalovirus	IGF: Insuline Growth Factor
CNS: Central Nervous System	IL: Interleukin
CSK: Cytoskeleton	ILK: Integrin Linked Kinase
CY: Cyclophilin	KO: Knock Out
DDR: DNA Damage Response	LEF1: lymphoid enhancer-binding factor 1
DMEM: Dulbecco's Modified Eagle's Medium	LOXL2: Lysyl Oxidase-Like 2
Dpc: Days Post Coitum	MAb: Monoclonal Antibody
DSB: Double Strand Breaks	MDCK: Madin Darby Canine Kidney
ECM: Extracellular Matrix	MET: Mesenchymal-to-Epithelial Transition
EGF: Epidermal Growth Factor	NES: Nuclear Export Signal
EMT: Epithelial-to-Mesenchymal Transition	PBS: Phosphate Buffered Saline
ER: Estrogen Receptor	PI: Propidium Iodide
ESCC: Esophageal Squamous Cell Carcinoma	PIP2: Phophatidil-Inositol-diphosphate
FACS: Fluorescent Activated Cell Sorting	PIP3: Phophatidil-Inositol-triphosphate
FAK: Focal Adhesion Kinase	PNS: Peripheral Neural System
FBS: Fetal Bovine Serum	RTK: Receptor Tyrosine Kinase
FGF: Fibroblast Growth Factor	SD: Standard Deviation
FN: Fibronectin	TGFβ: Transforming Growth Factor beta
GFP: Green Fluorescent Protein	TNFα: Tumor Necrosis Factor alpha
GST: Gluthathione-S-Transferase	VDR: Vitamin D Receptor
HCC: Human Hepatocellular Carcinoma	WB: Western Blot
HDAC: Hystone Deacetylase	
HGF: Hepatocyte Growth Factor	

INTRODUCTION

I.1. General insights into embryonic development.

I.1.a. From cell to embryo.

The complex and co-ordinate process of building a whole organism from one single cell has thrilled scientists and laymen since a long time ago. In the last century, the scientific community has gathered a lot of information that has helped us understanding some of the mechanisms involved. As **FIGURE I-1** summarizes, a single "totipotent" cell, the zygote, will give rise to all the different tissues that conform the organism.

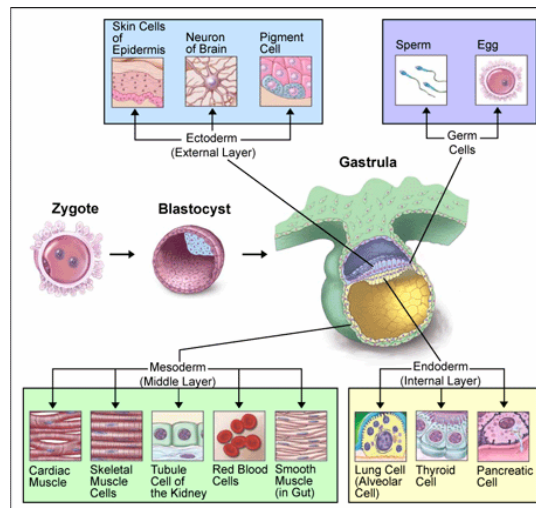


FIGURE I-1. Derivative tissues from the three embryonic layers (ectoderm, mesoderm and endoderm). http://www.ncbi.nlm.nih.gov/About/primer/genetics_cell.html

In an effort to summarize this complex process, it is generally accepted the existence of 4 stages of embryonic development, that are: (1) Cleavage, (2) Patterning, (3) Differentiation and (4) Growth.

The cleavage implies several processes of mitosis and cytokinesis of the zygote (large cell) to generate an increasing number of smaller cells, each

Introduction

with an exact copy of the genome present in the zygote. At this time, the zygotic genes are not expressed yet, and it is the maternal mRNAs and proteins the ones that promote this cleavage, that ends with the formation of the blastula. The subsequent organization of the cells in the blastula will give rise to the pattern of the future animal (patterning). For this to happen, a crucial process called gastrulation and driven by the zygotic genes occurs, generating the so called “three germ layers” (ectoderm, mesoderm and endoderm) **FIGURE I-1** and thus, the three body axis and the left and right sides of the future organism. Once the three germ layers have been formed, the cells that form them will start to differentiate, to acquire the specialized structures and functions that they will have in the adult. Finally, once the system is formed, most embryos undergo a period of growth, by the formation of new cells and more extracellular matrix resembling the existent ones.

1.1.b. Epithelial-to-Mesenchymal Transition (EMT) during embryonic development.

Changes in cell phenotype are the result of several cellular processes that need to be perfectly orchestrated during embryonic development, but also in the adult organism.

On the one hand, the phenotype of a cell is the result of the dynamic equilibrium state reached between the cell's transcription and transduction machinery and the local environment [1]. Among the modulators of cell phenotype, the molecules involved in cell-to-cell adhesion have arisen as central players. Knock out (KO) mice for several adhesion genes result in early embryonic lethality, such as E-cadherin KO, that fails to form trophectoderm epithelium and dies around the time of implantation [2], Plakoglobin KO, that dies of severe heart effect [3] or β -catenin KO [4], that dies after implantation but prior to gastrulation.

On the other hand, early embryos and primitive adults of the chordate phylum consist of epithelial tissue. A second type of tissue, (mesenchyme)

arises by the so-called Epithelial-to-Mesenchymal transition (EMT) in higher chordates, such as vertebrates [5]. Mesenchymal cells (vs. epithelial cells) are able to invade and migrate through the extracellular matrix (ECM). This process of EMT not only requires the down-regulation of cell-to-cell adhesion molecules in order to move to new environments and, eventually, differentiate into distinct cell types; but it is also characterized by many other conserved hallmarks that will be addressed later in this introduction.

The primary mesenchymal cells in amniote vertebrates originate and migrate from the primitive streak to differentiate into the mesoderm. Definitive mesenchyme (with connective tissue and muscle potential) arises from the mesoderm at about the same time as the neural crest mesenchyme forms from the ectoderm [5]. During embryogenesis, once the cells that have undergone EMT find their appropriate niche elsewhere, they differentiate into various cell types, including, in some cases, epithelial cells and thus, reverting EMT in a so-call Mesenchymal-to-Epithelial transition (MET).

The molecular hallmarks of EMT can be summarized as follows; (1) on the one hand, cells activate putative mesenchymal master genes, (2) cells turn off epithelial genes and (3) cells acquire motility machinery that allows them to interact with the ECM via actin cortex while sliding their endoplasm into their new front ends [5]. Opposite to EMT, MET is possible because the primary mesenchymal cells can (1) reactivate epithelial regulatory genes, such as E-cadherin, (2) turn off the motility machinery and (3) regenerate apical-basal polarity.

To put this process of EMT into context, it is important to now that these transitions have been shown to be crucial in several situations during embryonic development ([5-9] that are summarized in **FIGURE I-2**.

Introduction

	Stage (Mouse)	Transition	
Gastrulation	6.5d	Epiblast	Three cell layers
Pre-valvular mesenchyme (Heart formation)	8d	Endothelium	Atrial and ventricular septum
Neural crest cells	8d	Neural plate	Several derivatives (bone, muscle, PNS, etc)
Somitogenesis and sclerotome differentiation	9d	Somite walls	Sclerotome
Palate formation	3.5d	Oral epithelium	Mesenchymal and epithelial cells, combined with apoptosis
Mullerian tract regression	15d	Mullerian tract	Mesenchymal cells, combined with apoptosis

FIGURE I-2. Examples of EMT during embryonic development. Adapted from [1].

Among the processes reflected in **FIGURE I-2**, I will pay special attention to two of them; the process of gastrulation and the delamination of the neural crest., because the study of them has become of important relevance for understanding EMT and the genes involved in it.

I.1.b.i. Gastrulation.

As it has already been mentioned above, the process of gastrulation is a pivotal step in the formation of the vertebrate body plan. One of the most important developmental biologists, Prof. Lewis Wolpert from the University College of London, refers to gastrulation with the statement *“It is not birth, marriage, or death, but gastrulation, which is truly the most important time in your life”* [10].

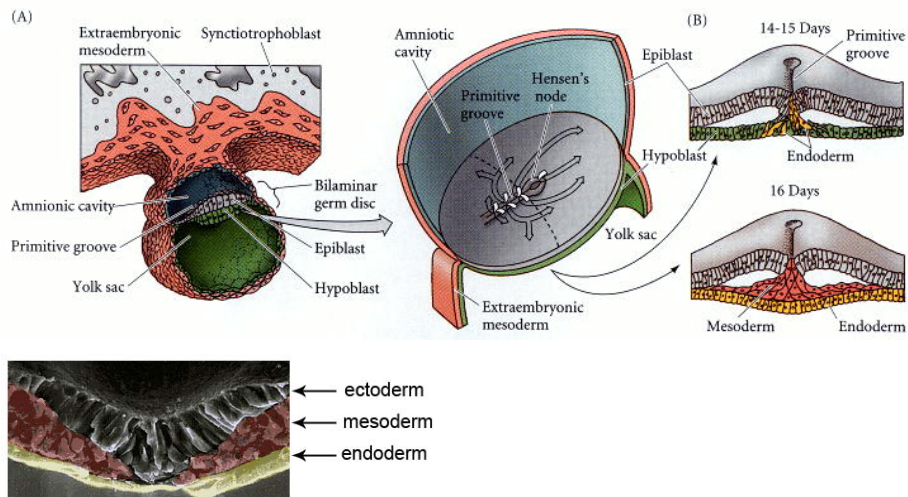


FIGURE I-3. Amnion structure and cell movements during human gastrulation. (A) Human embryo and uterine connections at day 15 of gestation. In the upper view, the embryo is cut sagittally through the midline; the lower view looks down upon the dorsal surface of the embryo. (B) The movements of the epiblast cells through the primitive streak and Hensen's node and underneath the epiblast are superimposed on the dorsal surface view. At days 14 and 15, the ingressing epiblast cells are thought to replace the hypoblast cells (which contribute to the yolk sac lining), while at day 16, the ingressing cells fan out to form the mesodermal layer. [11]. <http://www.ncbi.nlm.nih.gov/books/bv.fcgi?highlight=gastrulation&rid=dbio.figgrp.2624>. (C) Electron micrograph of a human embryo at day 16. The three germ layers can be identified (endoderm, in yellow, mesoderm in red and ectoderm, not labeled).

The correct orchestration of gastrulation will result into the generation of the mesoderm thanks to the Epithelial-to-Mesenchymal transition undergone by the epithelial cells of the epiblast, which invaginate and move inwards. (FIGURE I-3).

I.1.b.ii. Neural crest delamination.

The generation of the neural crest is one of the most relevant events in the development of vertebrates. Neural crest cells are characterized by their high motility, which allows them to populate distant tissues and contribute to the formation of many organs and tissues (FIGURE I-4) such as the peripheral nervous system (generating neurons and glia), heart, blood vessels, bone, ear,

eyes, skin, teeth, meninges, skeletal muscle and adrenal gland. Some connective tissue components of the pituitary, lachrymal, salivary, thyroid and parathyroid glands, and thymus are also derived from the neural crest [12,13].

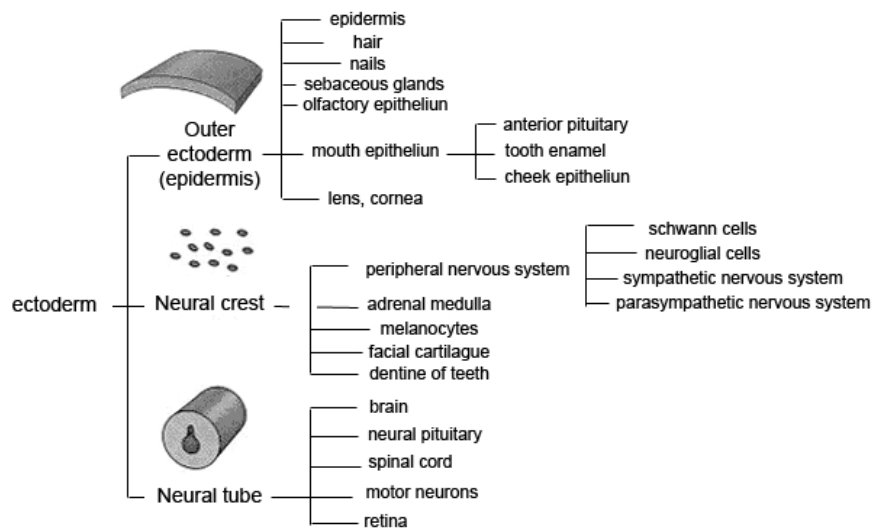


FIGURE I-4. Major derivatives of the ectoderm germ layer. The ectoderm is divided into three major domains (1) the surface ectoderm, (2) the neural tube, and the (3) neural crest. Adapted from: <http://www.ncbi.nlm.nih.gov/books/bv.fcgi?highlight=neural%20crest&rid=dbio.figgrp.2869>.

After gastrulation, the neural crest originates from the neural folds and/or the dorsal neural tube in which cells are induced to differentially express proteins driving EMT and the detachment from the neural primordium in a process called “delamination”. It is then, that the neural crest cells start migrating either ventrally close to the neural tube or dorso-laterally in proximity to the somatic ectoderm (FIGURE I-5), [14-16].

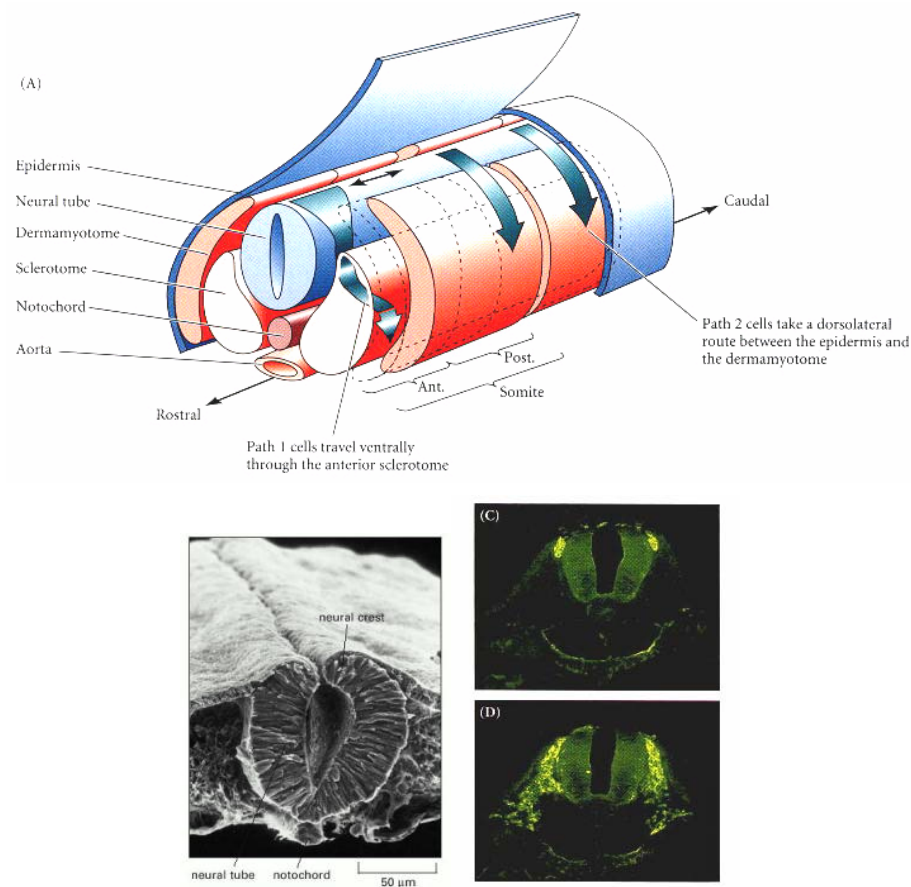


FIGURE 1-5. Neural crest cell migration in the trunk of the chick embryo. (A) Schematic diagram of neural crest cell migration. In Path 1 (the ventral pathway), cells travel ventrally through the anterior of the sclerotome (that portion of the somite that generates vertebral cartilage). Those cells initially opposite the posterior portions of the sclerotomes migrate along the neural tube until they come to an opposite anterior region. These cells contribute to the sympathetic and parasympathetic ganglia as well as to the adrenal medullary cells and dorsal root ganglia. Other trunk neural crest cells enter Path 2 (the dorsolateral pathway) somewhat later. These cells travel along a dorsolateral route beneath the ectoderm, and become pigment-producing melanocytes. (Migration pathways are shown on only one side of the embryo). (B) Formation of the neural tube. The scanning electron micrograph shows a cross section through the trunk of a 2-day chick embryo. The neural tube is about to close and pinch off from the ectoderm. <http://www.ncbi.nlm.nih.gov/books/bv.fcgi?highlight=tube,neural&rid=mboc4.figgrp.3969>. (C, D) Cross sections, showing extensive migration of the neural crest cells [17]. <http://www.ncbi.nlm.nih.gov/books/bv.fcgi?highlight=neural%20crest&rid=dbio.figgrp.3118>.

Introduction

By largely unknown mechanisms, neural crest cells stop migrating and subsequently differentiate into the variety of cell types shown above (FIGURE I-4).

As it has been mentioned above, note that this process of delamination and migration requires an EMT where the migrating cells are forced to down-regulate their cell-to-cell adhesion molecules (among other), in order to move to the target location. FIGURE I-6 shows the localization of E-cadherin and N-cadherin at that stage of development. Note the absence of E-cadherin labeling in the cells that later will give migrate.

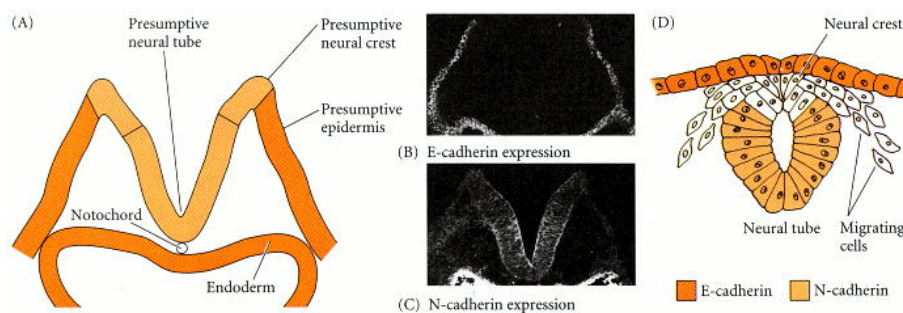


FIGURE I-6. Localization of two different cadherins during the formation of the mouse neural tube. (A) Double immunofluorescent staining is used to localize E-cadherin (B) and N-cadherin (C) in the same transverse section of an 8.5-day embryonic mouse hindbrain, revealing that the outer ectoderm expresses predominantly E-cadherin, while the invaginating neural plate ceases E-cadherin expression and instead expresses N-cadherin. (D) When the neural tube has formed, it expresses N-cadherin, the epidermis expresses E-cadherin, and the neural crest cells between them express neither.

<http://www.ncbi.nlm.nih.gov/books/bv.fcgi?highlight=neural%20crest&rid=dbio.figgrp.390>.

1.2. Cancer: what lessons can we take from embryo development?

1.2.a. Generalities about cancer.

The first descriptions of the word "cancer" come from the earliest Antiquity. Hippocrates (460-370 BC) already used the Greek words "carcinosis" and "carcinoma" to refer to chronic ulcers or growths that seemed to be

malignant tumors. Later, a roman doctor called Celsus (28 BC-50 AC), translated the Greek word "carcinos" into the Latin word "cancer" [18]. Along the human History, the concept and definition of "cancer" has been constantly revised and nowadays, the word "cancer" encloses a big amount of different complex processes, which render an abnormal behavior of the cell, which can, in its later step of development; compromise the life of the harboring organism. Indeed, it applies to a large number of different diseases with a variety of etiologies and appearances that require different cares and treatments and that will have a very variable prognosis.

In the last thirty years, the research in cancer has generated a rich and complex body of knowledge, revealing cancer to be a disease involving dynamic changes in the genome. We now know that tumorigenesis is a multistep process and that these steps reflect genetic alterations that drive the progressive transformation of normal cells into highly malignant derivatives [19]. Furthermore, some researchers have postulated that tumor development proceeds via a process formally analogous to Darwinian evolution, in which a succession of genetic changes, each conferring one or another type of growth advantage, leads to the progressive conversion of normal human cells into cancer cells [20,21]. In an effort to summarize, Douglas Hanahan and Robert A. Weinberg suggest that the vast catalogue of cancer cell genotypes is a manifestation of six essential alterations in cell physiology that collectively dictate malignant growth (**FIGURE 1-7**): (1) self-sufficiency in growth signals, (2) insensitivity to growth-inhibitory (antigrowth) signals, (3) evasion of programmed cell death (apoptosis), (4) limitless replicative potential, (5) sustained angiogenesis, and (6) tissue invasion and metastasis.

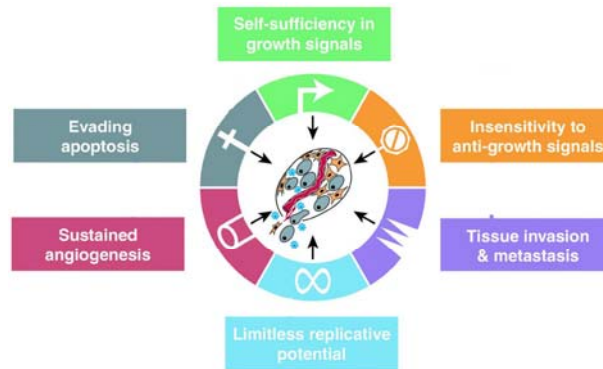


FIGURE I-7. Acquired capabilities of cancer. Most cancers acquire the same set of functional capabilities during their development, albeit through various mechanistic strategies [19].

Cancers are classified by the type of cell that resembles the tumor and, therefore, by the tissue presumed to be the origin of the tumor. Carcinomas are malignant tumors derived from epithelial cells. Among them, we find some of the most common cancers, including the breast, prostate, lung and colon cancer. Sarcomas are malignant tumors derived from connective tissue, or mesenchymal cells, whereas those malignancies derived from the hematopoietic cells are called lymphoma or leukemias. In some cases, the tumor resembles an immature or embryonic tissue and is called blastic tumor.

1.2.b. Mechanisms shared by development and cancer.

Cancer, as an abnormal state of one or more cell populations that interferes with the normal biological functioning, is often characterized by a reversion to a less differentiated, more developmentally primitive state. In fact, cancer has been called a "developmental disorder" [22] where some of the molecular players involved in controlling development might be implicated. Many of the genes involved in embryogenesis are important for the control of cell proliferation and differentiation. Mutations in these genes may contribute to the progression of cancer later in the life of the organism. Thus, research into the molecular mechanisms involved in development is

important not only for understanding embryogenesis, but also for understanding, and managing, cancer, as we will see below.

1.2.c. EMT and cancer.

The concept of EMT has been already introduced. Despite its importance for many developmental processes (**FIGURE I-3**) such as gastrulation and neural crest migration, its de-regulation in cancer cells leads to tumor progression. In other words, one of the most common causes of death, metastatic cancer, mirrors a set of cellular, molecular and genetic changes of the beginnings of life (quoting E. Thomson). In the past 20 years, the increasing information generated, points to the loss of the restricted spatio-temporal regulation of EMT during development, as the mechanism by which solid tissue epithelial cancer invade and metastasize.

E-cadherin plays a pivotal role in EMT. Its down-regulation is not only necessary during embryonic development (remember that E-cadherin KO displays an early embryonic lethality), but it is also particularly relevant in the transition from adenoma to carcinoma, since a causal relationship between loss of expression of this protein and the invasive properties of some tumors has been established [23,24].

Besides E-cadherin down-regulation, the molecular traits of EMT are many and involve changes in a lot of relevant functions for the cell. **FIGURE I-8** summarizes the up-to-now known hallmarks of EMT [25-27].

Introduction

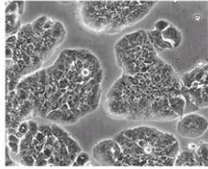
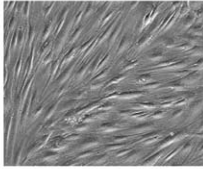
Epithelial cells				Mesenchymal cells
Apical/Basolateral polarity	MORPHOLOGY		Leading/Trailing edge asymmetry	
Cell adhesion & contact inhibition	PHYSICAL CHARACTERISTICS		Cell motility & invasiveness	
Adherens junctions (AJ) Tight junctions (TJ) Gap junctions (GJ) Desmosomes (D)	INTERCELLULAR JUNCTIONS		Focal adhesions (FA) Transient Gap junctions (tGJ)	
E-cadherin (AJ) Occludin, claudin (TJ) Desmoplakin (D)	MOLECULAR MARKERS		N-cadherin	
F-actin cytokeratins			Stress fibers vimentin	
			Matrix metalloproteinases (MMP-1,2,3,7,14)	
membrane β -catenin			nuclear β -catenin	
Muc-1 Vit3R			Rho GTPases Zeb-1 Lef-1	

FIGURE I-8. The EMT cell traits. The figure reflects the changes in cellular morphology, physical characteristics, type of intercellular junctions and molecular markers of epithelial cells, compared to those that have undergone EMT.

In the context of EMT, the tumor microenvironment behaves as an active partner in tumor progression, that is, EMT is not only triggered as a result of cell autonomous processes, but it also requires several paracrine initiating signals. The complexity of molecular cascades that can lead to EMT is so extensive that it is preferred to talk about the so-called EMT regulatory network. **FIGURE I-9** is a simplified schematic of the most representative pathways involved in EMT [25-28].

A single glance at it is enough to realize about the complexity of the EMT network. Miss-regulation of the main cellular signaling pathways results in the acquisition of a malignant phenotype, characterized by the loss of cell-to-cell adhesion, increase in cell motility and resistance to apoptosis, which will be discussed later in the introduction.

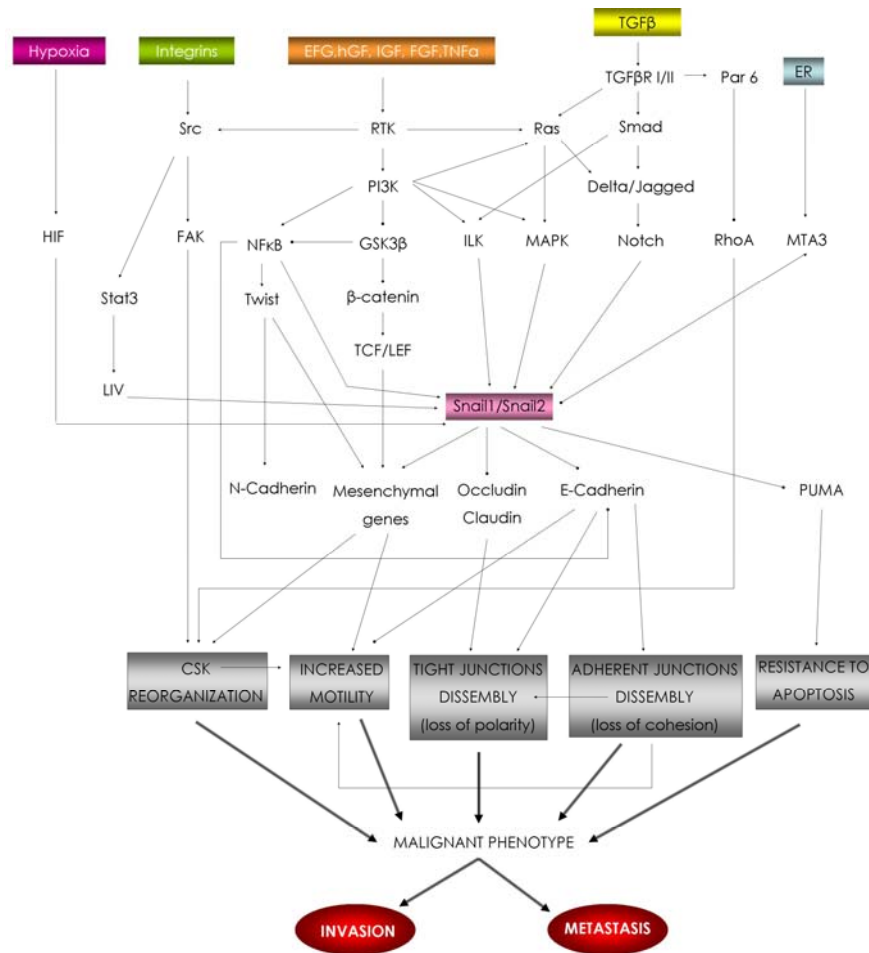


FIGURE I-9. Scheme of the pathways involved in EMT. Up, in color boxes, the signals that can promote EMT. In the pink box, snail1 and snail2, the converging point for many of these upstream signals. The result of snail1 and snail2 function is shown in grey and its consequences, in red. Activation, arrow; inhibition, dot.

Taken together, this new capabilities of the malignant cells allow them to migrate to other tissues, escape the classical cell cycle control and proliferate, giving rise, in the worst case scenario, to a metastasis (FIGURE I-10).

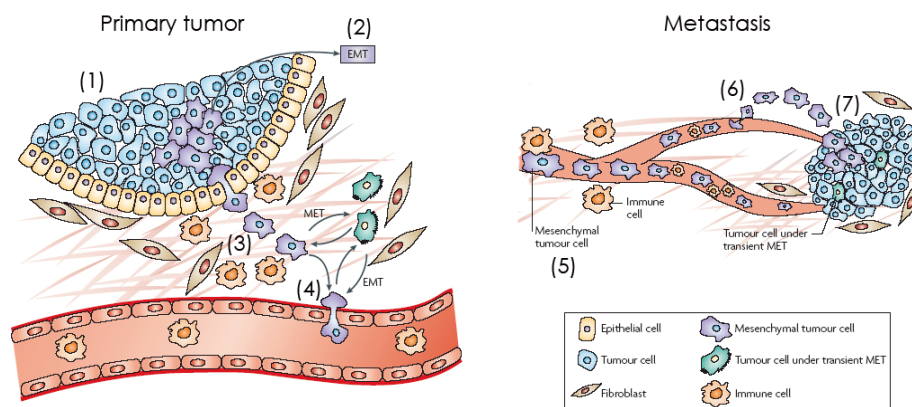


FIGURE I-10. EMT-MET in tumor progression and metastasis. Adapted from [29]. Schematic diagram summarizing the steps that lead to the formation of a distant metastasis. (1) Conversion from normal tissue to adenoma, (2) EMT, repression of E-cadherin that facilitates detachment from other neighboring cells, conversion to early carcinoma, (3) increased migration, (4) intravasation, (5) tumor mesenchymal cells circulation, (6) extravasation and (7) mesenchymal micrometastasis that undergo MET to proliferate and give rise to a secondary metastasis.

I.3. The transcriptional regulation of EMT.

The leading role of E-cadherin down-regulation in EMT explains the interest of scientists in the determination of new molecules or processes involved in it. Since the first reports on E-cadherin direct transcriptional repression by snail1 were published [30,31], some other transcriptional repressors have been found to do it as well. The most important repressors of E-cadherin belong to the snail family of transcription factors. However other families of transcription factors have also been shown to be able to repress E-cadherin, such as the zeb transcription family or some bHLH proteins.

1.3.a. The *zeb* family of transcription factors and EMT

The *zeb* family of transcription factors consists of two members: *zeb1* (δ EF1) and *zeb2* (SIP1). Their protein structure is characterized by the presence of two zinc finger domains (3 or 4 zinc fingers of the C2H2 and C3H type) at each of the protein ends and a central homeodomain (FIGURE I-11).

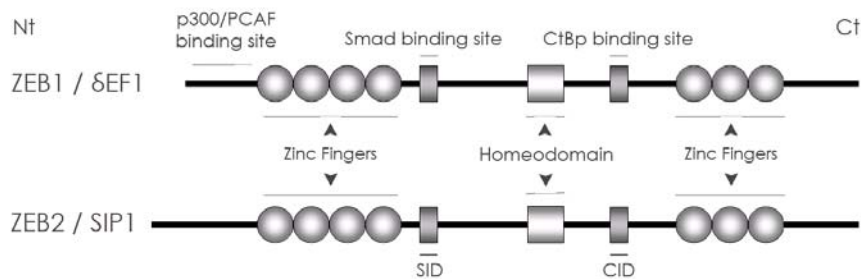


FIGURE I-11. Scheme of the most relevant domains existent in *zeb1* and *zeb2*. The two of them share the tandem DNA binding zinc fingers and the homeodomain. Note, the Smad (SID), CtBp, p300 and PCAF binding sites.

They interact with the DNA through the simultaneous binding of the two zinc-finger domains to binding sites composed of bipartite E-boxes (CACCT and CACCTG) whose orientation and spacing vary among targets [32-34]. *Zeb* factors function by the recruitment of either co-activators (PCAF or p300 for *zeb1*) or co-repressors (CTBP for *zeb2*) [33]. Their expression during development is found in the central nervous system (CNS), heart, skeletal muscle, and hematopoietic cells. *Zeb1* and *zeb2* are thought to play common roles, that is, the functional deficiency in one of these *zeb* factors can be overcome by the other. However, *zeb2* KO mice die during embryogenesis, and display defects in the neural crest emigration that can not be compensated for by *zeb1*[35].

1.3.b. The *bHLH* family of transcription factors and EMT

This family displays a common protein structure consisting of two parallel amphipathic α -helices linked by a loop that is required for dimerization. This

structure can be found as described or together with a basic domain, giving rise to the so-called bHLH transcription factors.

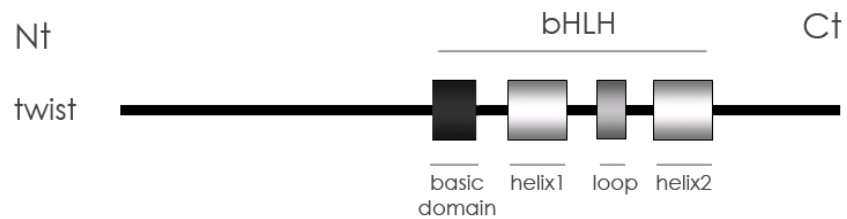


FIGURE I-12. Scheme of the most relevant domains existent in the bHLH twist1 protein.

These proteins bind to DNA as homo- or heterodimers [36] through a consensus E-box (CANNTG) site. Among them, TCF3 (E12 and E47 isoforms) [37-40] and Twist1 (FIGURE I-12) [38,41] have been found to repress E-cadherin.

1.3.c. The snail superfamily of transcription factors and EMT.

The snail superfamily of transcription factors plays a key role in morphogenesis. From the study along the past years, we know that they are involved in the development of the mesoderm during gastrulation [7,42-49], but also in large scale movements, such as those required for the formation of the neural crest [7,8,50-52]. The first member of the snail superfamily, snail, was discovered in *Drosophila melanogaster* [53]. Subsequently, many other homologues in different species were cloned and characterized (FIGURE I-13), reviewed in [54].

Species	Common name	Gene	Synonyms	Accession no.	Map
<i>Caenorhabditis elegans</i>	Nematode	<i>ces1*</i> <i>snail-like</i> <i>scratch-like*</i>	K02D7.2 C55C2.1	AAF01678 T32983 T15225	I:2.9 IV:-26.1 I:-9.3
<i>Helobdella robusta</i>	Leech	<i>snail1</i> <i>snail2</i>	<i>Hro-sna1</i> <i>Hro-sna2</i>	AF410864 AF410865	
<i>Patella vulgata</i>	Limpet	<i>snail1</i> <i>snail2</i>	Pv-sna1 Pv-sna2	AY049727 AY049791	
<i>Drosophila melanogaster</i>	Fruitfly	<i>snail</i> <i>escargot</i> <i>worniu</i> <i>scratch*</i> <i>scratch-like1*</i> <i>scratch-like2*</i>	CG12605 CG17181	S06222 AAF12733 S33639 AAA91035 AAF47818 AAF47394	35D2-3 35D1 35D2-3 64A2-3 64A1 61C7
<i>Lytechinus variegatus</i>	Sea urchin	<i>Snail</i>		AAB67715	
<i>Halocynthia roretzi</i>	Ascidia	<i>Snail</i>		BAA75811	
<i>Ciona intestinalis</i>	Ascidia	<i>Snail</i>		AAB61226	
<i>Branchiostoma floridae</i>	amphioxus	<i>Snail</i>		AAC35351	
<i>Takifugu rubripes</i>	Pufferfish	<i>Snail1</i> <i>Snail2</i>		CAB54535 CAB54536	
<i>Danio rerio</i>	Zebrafish	<i>snail1</i> <i>snail2</i> <i>slug</i> <i>scratch*</i>		CAA52795 AAA87196 AI722148 AI883776	
<i>Xenopus laevis</i>	African clawed toad	<i>Snail</i> <i>Slugα</i> <i>Slugβ</i>	<i>Xsna</i> <i>Xslu</i> <i>Xsluβ</i>	P19382 AF368041 AF368043	
<i>Silurana tropicalis</i>	Western clawed frog	<i>Slug</i>	<i>Xslug</i>	AF368038	
<i>Gallus gallus</i>	Chicken	<i>Snail</i> <i>Slug</i>	<i>SnR</i>	CAA71033 CAA54679	
<i>Mus musculus</i>	Mouse	<i>Snail</i> <i>Slug</i> <i>Scratch*</i> <i>Smuc</i>	<i>Slugh</i> Zfp293	Q02085 AAB38365 AY014997 NP038942	Chr.2-97.0 Chr.16-9.4
<i>Homo sapiens</i>	Human	<i>SNAIL</i> <i>SNAILP</i> <i>SLUG</i> <i>SCRATCH1*</i> <i>SCRATCH2*</i>	<i>SNAIL1, SNAILH</i> <i>SNAILP</i> <i>SLUGH, SNAIL2</i>	AF155233 AF153502 AAC34288 AY014996 AL121758	20q13.1 2q34 8q11 8q24.3 20p12.3-1:

FIGURE I-13. The snail superfamily members. Note that the superfamily is divided into two families (1) snail and (2) scratch (marked with an asterisk). The accession numbers in column #5 are from Entrez (<http://www.ncbi.nlm.nih.gov/sites/gquery?itool=toolbar>), [54].

Introduction

They all share a similar structure, with a highly conserved C-terminal region, which contains the C₂H₂ type zinc fingers (**FIGURE I-14**), (from four to six, in a variable number among the different homologues) responsible for the binding to the DNA, and a more divergent N-terminal region.

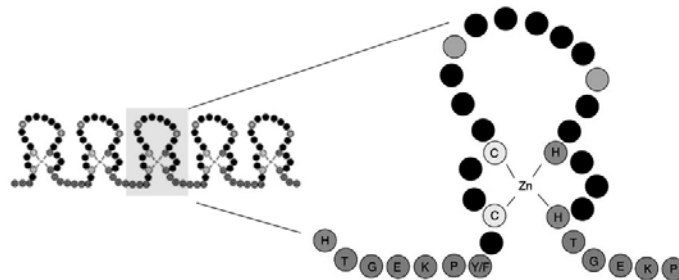


FIGURE I-14. Scheme of the C₂H₂ type zinc fingers. Among 4 to 6 are present in the members of the snail superfamily of transcription factors and responsible for DNA binding in the major groove.

The consensus binding site for all these related genes is formed by a 6 bases core 5'-CAGGTG-3' [30,31,55-58] identical to that of the bHLH transcription factors binding site (also called E-box), with which the snail superfamily of transcription factors might compete.

Upon the binding of snail superfamily members to this E-box, these proteins behave as transcriptional repressors. Though DNA binding is necessary for this repression, it is not sufficient. Two additional motifs located within the N-terminal region of the protein are also required for the observed transcriptional repression. First, the SNAG domain, conserved in all vertebrate snail genes, and required for the recruitment of chromatin-remodeling molecules such as histone deacetylase (HDAC) 1 and 2, and mSin3A co-repressor [59]. Second, the consensus binding site for the carboxy-terminal binding protein (CtBp), necessary for the repression activity of those snail superfamily members that lack the SNAG domain (i.e. *Drosophila* snail).

The snail superfamily of transcription factors is divided into the (a) snail and (b) scratch families. The three vertebrate members belonging to the snail family have been called snail1, snail2 and less characterized snail3. They all share the general structure named above and function as transcriptional repressors. Their high homology within the C-regulatory domain contrasts with the variability of their N-regulatory domain (**FIGURE I-15**). Besides the SNAG domain, the so-called serine-proline-rich domain is highly divergent.

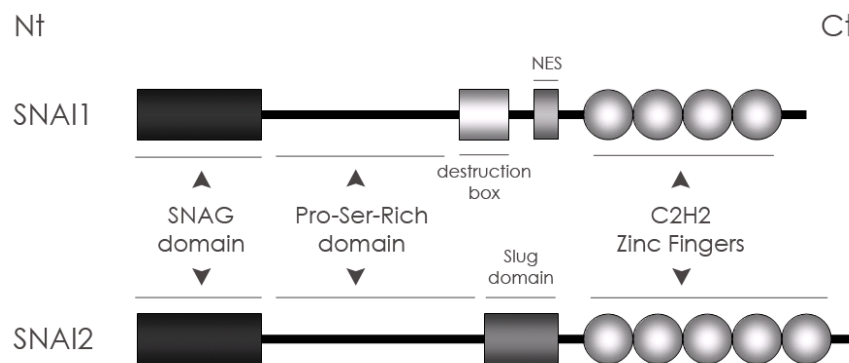


FIGURE I-15. Scheme of the most relevant domains existent in two snail family members: snail1 and snail2 (slug). The two of them share the DNA binding zinc fingers and the SNAG domain. Note, however, the NES (nuclear export signal) and the destruction box that targets snail1 for degradation and the slug domain within snail2, with still unclear functions.

The physiological relevance of this family of transcription factors in embryo development has been known for long. Besides the most well characterized target of snail1, E-cadherin, other target genes of snail1 during development are the Rho-GTPases. During the neural-crest generation in the chick, RhoB up-regulation is necessary [60]. In this model, it has been shown that slug (snail2), (which has been shown to be equivalent to snail1 in mouse) over-expression is able to induce RhoB [61], providing a link between this transcription factor and the small GTPase, which might explain the dramatic changes in cell phenotype observed during EMT, and necessary for the migration of cells. Furthermore, the snail family of transcription factors has

Introduction

been linked to the cell cycle [62,63], cell survival [57,64] and protection against cell death [65]. This matter will be thoroughly discussed below.

In the last decade, however, the involvement of these transcription factors in cancer progression through similar mechanism of those observed during development has become unquestionable. Among all the members, snail1 and snail2 have turned out to be essential for triggering EMT during tumor progression (**FIGURE I-9**), [27,29,54,65].

I.4. The snail1 transcription factor

Among the members of the snail family, snail1 emerges as a one of the most well characterized homologs. This is, in great part, due to its relevance beyond embryonic development, and more in detail, because of its importance for EMT and cancer progression. As it has been already mentioned, in mammals, snail1 blocks E-cadherin expression by binding to specific 5'-CACCTG-3' boxes in its promoter [30,31]. Nevertheless, the effects of snail1 expression in epithelial cells are not limited to E-cadherin repression. Moreover, snail1 is also able to induce a complete EMT [31,66]. Accordingly, some other epithelial genes are directly repressed by snail1 as MUC1 and cytokeratin 18 [66], and the tight junction proteins claudins and occludin [67]. Other snail1 targets are vitamin D3 receptor [68], the β -subunit of the Na⁺, K⁺ ATPase [69], and two genes presumably responsible for the resistance to apoptosis and decreased proliferation observed in cells transfected with snail1; p53 [70] and cycD2 [63]. Furthermore, snail1 stimulates the expression of matrix proteases [71], Wnt5a factor [72], transcriptional factors Zeb1 and Lef-1 [66,72] and the mesenchymal markers vimentin and fibronectin (FN) [30,66].

There is a lot of information in the literature about the requirements for the direct snail1-dependent repression of target genes. Explained in a simple

manner, (1) all the target genes contain, at least, one snail1 consensus binding sequence 5'-CACCTG-3' in their promoter, (2) the integrity of the zinc fingers must be conserved, (3) the SNAG domain must be able to recruit histone deacetylases, and (4) the subcellular localization of the protein must be nuclear.

Note the fact that the members of the snail family of transcription are known to repressors. However, snail1 has been shown to act as an activator in certain promoters. Besides the possibility of an indirect activation (i.e. repressing a repressor), the molecular mechanism for this activation remains unknown. In the last months, however, some papers have enlightened new putative mechanism that will be addressed in the Discussion.

1.4.a. Snail1 protein structure.

Snail1 protein is a 264 aminoacid protein composed by two well defined domains that interact with each other [73]. The C-terminal domain is responsible for DNA binding and presents specificity for sequences with a 5'-CACCTG-3' core. The N-terminal is required for transcriptional repression and can recruit histone deacetylase (HDAC) family members [74]. Snail1 repressive activity can be modulated by at least two molecular mechanisms. In the one hand, by phosphorylation in a proline-serine-rich sequence situated in the regulatory domain. Two phosphorylation motifs have been allocated in this subdomain, one involved in snail1 export from the nucleus, and the other in its ubiquitinylation and degradation [73,75]. GSK3 β kinase seems to be responsible for the modification of both motifs [75]. In the other hand, oxidation of residues K98 and K137 by lysyl oxidase-like 3 enzyme (LOXL2) has been shown to be essential for the function and stability of the protein [76]. They propose that LOXL2 catalyzes the oxidative deamination of the two lysines, leading to the formation of covalent cross-links into snail1 and inducing a conformational change that would mask GSK3 β phosphorylation motifs [77]. Moreover, the C-terminus of snail1 protein can be phosphorylated

Introduction

by PAK-1 kinase [78] resulting in protein retention in the nucleus. Subcellular distribution of snail1 is also sensitive to the expression of the STAT3-target LIV1 Zn transporter [79]. **FIGURE I-16** shows a scheme of the human snail1 protein and the motifs related to its regulation.

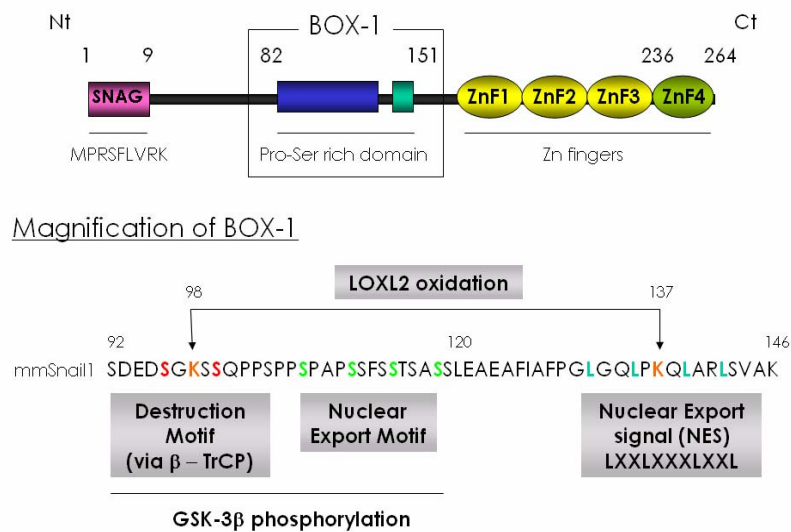


FIGURE I-16. Scheme of the snail1 protein. The regulatory elements present in BOX-1 are magnified below for a better appreciation.

1.4.b. SNAIL1 gene structure and transcriptional regulation.

Up-regulated expression *SNAIL1* gene has been detected in several experimental conditions in which cells are forced to adopt a mesenchymal phenotype [59,80-86]. This phenomenon has been also observed during gastrulation and neural crest migration [43,44,54,86,87]. Transcriptional regulation of snail1 has also been proposed to happen in the infiltration front of epithelial tumors [88]. Apparently, this increase in the transcription of *SNAIL1* is related to the presence of EMT inducers either from the tumor or the adjacent tissue [89-91].

However, little is known about the promoters driving snail family members' expression, and even in the case that some information is available; it cannot be easily extrapolated among species. Note that, contrary to codifying sequences, promoter homology tends to be low [92].

The characterization of a human *SNAI1* promoter (-869/+59, respect to the transcription start) has revealed its dependence on ERK2 and GSK-3 β /NF κ B pathways activity [85,93]. Furthermore, it has been demonstrated that PI3 kinase (PI3K) activity also controls *SNAI1* transcription and promoter activity [59], probably acting on the same pathway than GSK-3 β /NF κ B. The activity of this *SNAI1* promoter (-869/+59) mimics the expression of snail1 during EMT, however, the pathways named above are not only active in epithelial cells, but also in mesenchymal cells, and do not entirely explain the specificity of *SNAI1* expression in mesenchymal cells. The existence of three putative 5'-CACCTG-3' E-boxes in this promoter prompted us to study their relevance in the transcription of *SNAI1* gene, as it will be shown in the Results chapter.

1.5. Snail1 and cancer.

Given the substantial information available about snail1 and the solid and well characterized link to E-cadherin and other targets in cell models, the lack of definitive studies that prove the role of snail1 in human cancer is surprising. Few works have addressed this issue, in part because of the absence of good antibodies, an issue shortly overcome [94]. Nevertheless, since snail1 was originally shown to be expressed in invasive carcinoma cells, and responsible for E-cadherin repression, some publications have successfully addressed snail1 role in different human cancers, among which, the more prevalent ones are included.

Introduction

In several series of human breast carcinomas, the expression of snail1 and that of molecules of the E-cadherin/catenin complexes correlate with the pathological features of the tumors and inversely correlates with the grade of differentiation of the tumors. Furthermore, snail1 is expressed in infiltrating ductal carcinomas (IDC) presenting lymph node metastases and in some dedifferentiated tumors with a negative nodal status [88]. In addition to that, this inverse correlation observed in human tumor between E-cadherin and snail1 can be linked to the existence of transcriptional mechanisms that lead to E-cadherin promoter hypermethylation and increased expression of snail1 in breast cancer tumors [95]. The importance of snail1 in breast cancer has also been associated with cancer recurrence, a fundamental clinical manifestation of tumor progression that represents the principal cause of death from this disease. EMT is promoted by spontaneously up-regulation of transcriptional repressor snail1 in these recurrent tumors and consistent with this observation, snail1 high levels predict decreased relapse-free survival in women with breast cancer [96]. This observations have been also described in metastatic ovarian cancer by in situ hybridization and immunocytochemistry in which snail1 presence is associated with extremely poor survival rates [97].

Snail1 mRNA is also expressed in cancer tissues different from breast carcinomas. In samples of human hepatocellular carcinoma (HCC) cells (but not in bile duct cells, blood vessels or infiltrating leukocytes), expression of snail1 mRNA also correlates with E-cadherin down-regulation and tumor invasiveness [98]. The same is true for primary human gastric cancers [99]. In addition to that, hypermethylation of the E-cadherin promoter and snail1 over-expression have been detected in 61% cases of esophageal squamous cell carcinoma (ESCC). In this case, hypermethylation and snail1 over-expression correlated significantly with E-cadherin down-regulation but snail1 over-expression was unrelated to clinicopathologic factors (versus E-cadherin expression, that correlated with tumor and vascular invasion) [100]. In head

and neck squamous cell carcinoma (HNSCC) samples, co-expression of NBS1/snail1 in primary tumors correlate with metastasis and the worst prognosis [101]. Nevertheless, this results are not backed by other works, in which no correlation for nuclear snail1 expression and tumor grade, tumor stage or tumor size has been found in adenocarcinoma samples of the upper gastrointestinal tract: esophagus, cardia and stomach; and that suggest a minor role for snail1 in this type of tumors [102].

The studies that have faced the role of snail1 in colorectal cancer (CLC) samples have shown that its expression is associated with the transcriptional down-regulation of E-cadherin and vitamin D receptor (VDR). A correlation between (1) down-regulation of VDR and poor differentiation and (2) down-regulation of *CDH1* and poor differentiation, vascular invasion, presence of lymph node metastases and advanced stages has been observed [103-105].

So far, the relationship between snail1 and cancer has been shown to exist in epithelial derived tumors; however, some recent studies have revealed that snail1 is highly expressed in sarcomas and fibrosarcomas (mesenchymal derived tumors). In this same study, they show how, in epithelial tumors, snail1 is presented in a limited distribution, where it is restricted to the stromal cells placed in the vicinity of the tumor and to tumoral cells in the same areas. These results demonstrate that snail1 is present in activated mesenchymal cells, and point to its putative relevance in the communication between tumor and stroma, suggest that snail1 can promote the conversion of carcinoma cells to stromal cells [94].

I.6. Cell survival and cancer: the importance of apoptosis.

I.6.a. The importance of apoptosis in tissue homeostasis and tumor progression.

The term "apoptosis" is derived from the greek *apo-* (away from) and *-ptosis* (falling, a fall, death). Apoptosis or programmed cell death is a

Introduction

genetically controlled and biochemically active process (ATP and protein synthesis-dependent), necessary for the multicellular organisms to keep their homeostasis. Apoptosis is triggered in a wide variety of physiological circumstances such as tissue homeostasis or embryo development and also a defense against pathogens, as a cell response to DNA damage or cancer.

At a molecular level, apoptosis consists of a proteolytic pathway that results in cell dismantling by the cleavage of cellular proteins. The whole apoptotic machinery can be classified into two groups: the sensors and the effectors. The sensors monitor the extracellular and intracellular environment for normality or abnormality that will result in the decision of whether a cell should live or not. By doing this, they regulate the effectors of apoptotic death. Among the extracellular survival sensors we find IGF-1R or IL-3R [106] and among the extracellular death sensors, FAS and TNF α receptors [107]. All of them respond to extracellular ligand binding, triggering an intracellular response. In addition to them, intracellular sensors are also in charge of detecting abnormalities such as DNA damage, imbalanced signaling provoked by oncogene activation, survival factor insufficiency or hypoxia [108]. Last, the correct disposition of the ECM and cell-to-cell contacts promotes survival signals, the abrogation of which promotes apoptosis [109,110].

Many of the signals that will elicit apoptosis converge in the mitochondria, where either the pro-apoptotic Bcl-2 family members (Bax, Bak, Bid, Bim) or the anti-apoptotic Bcl-2 family members (Bcl-2, Bcl-XL, Bcl-W) modulate the release of cytochrome C, a potent inductor of apoptosis [111].

The final effectors of apoptosis, a group of intracellular proteases (caspases) [112] respond to activated FAS receptor or cytochrome C. Caspases 8 and 9 are known as "gatekeeper" caspases, their activation triggers the subsequent activation of other effector caspases, that will

execute the death program (selective destruction of subcellular structures and DNA).

It is not difficult to understand how miss-regulation of apoptosis is tightly related to disease. Many pathologies account for an increase or decrease in this process: among them, cancer [19]. The link between cancer and apoptosis was first described in 1972 [113]. Since then, the vast amount of published papers has revealed several strategies by which cancer cells bypass apoptosis. The most commonly occurring loss of a pro-apoptotic regulator accounts for p53 inactivation (with a 50% overall inactivation in cancer). This results in the removal of a pivotal player of the DNA damage sensor pathway that, in turn, cannot be activated [114]. Additionally, the PI3K-Akt/PKB pathway is also able to foster anti-apoptotic signals and has also been shown to be involved in carcinogenesis.

1.6.b. The two apoptotic pathways.

Depending on the eliciting signal, two main apoptotic pathways (the intrinsic or the extrinsic) can be activated (**FIGURE 1-17**). The intrinsic pathway integrates a wide variety of signals, such as DNA damage, loss of adhesion, growth factor withdrawal, oxidative stress and others, whereas the extrinsic pathway is dependent on the activation of a subset of specific cell surface receptors upon binding of their cognate ligands. Even though the two pathways involve different molecules, they share the final effectors: the caspases.

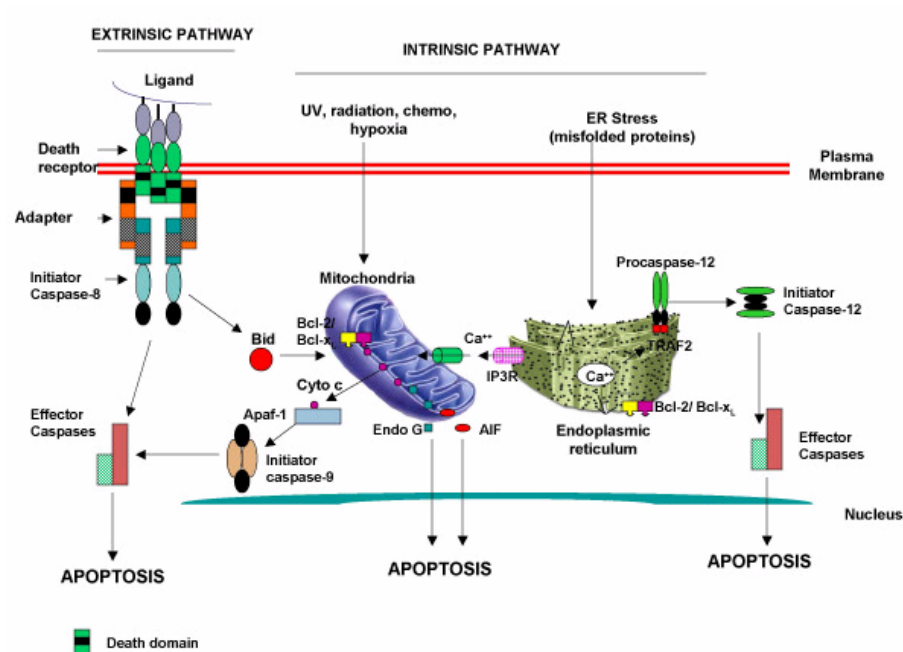


FIGURE I-17. Death receptor (extrinsic) and intrinsic pathways of apoptosis. Intrinsic pathway is mediated by the mitochondrial and the endoplasmic reticulum pathways. Note that distinct initiator caspases are activated in each pathway of apoptosis [115].

1.6.c. The role of p53 protein in cell cycle arrest and apoptosis.

The p53 tumor repressor protein plays a critical role when it comes to the cell to decide whether to promote apoptosis or cell cycle arrest. In response to cell damage, i.e. γ radiation, the double-strand breaks (DSB) generated activate the sensor kinases ATM, ATR and DNA-PK. In the cell, the levels of p53 are modulated by MDM2 [116], however, in response to cell damage, this repressor is phosphorylated by ATM and targeted for destruction. The role of ATM in p53 activation goes beyond MDM2 degradation [117]. ATM, together with ATR, also phosphorylates p53 in two serine residues (S15 and S20). Moreover, Chk1 and 2 have been also shown to phosphorylate p53 in S20 and T18 residues [118]. The overall result of all this phosphorylations is p53

accumulation and increased transcriptional activity of its activated target genes.

The main functions of p53 in the cell are related to its transcriptional activity, even though some p53 transcriptional independent functions have also been reported. The most well characterized transcriptional target of p53 is p21^{WAF1/Cip1} protein. Its accumulation results in cell cycle arrest through inhibition of cdk2/cyclinE complexes.

However, if the cell is too harmed to restore its homeostasis, the role of p53 in promotion of apoptosis emerges as a last chance for the cell not to survive with an uncertain quantity of DNA irregularities (such as loss or gain of several nucleotides) that can lead to cancer initiation (**FIGURE I-18**). In this case, p53 activates the transcription of pro-apoptotic genes BAX, PUMA and NOXA to promote apoptosis, as **FIGURE I-19** shows.

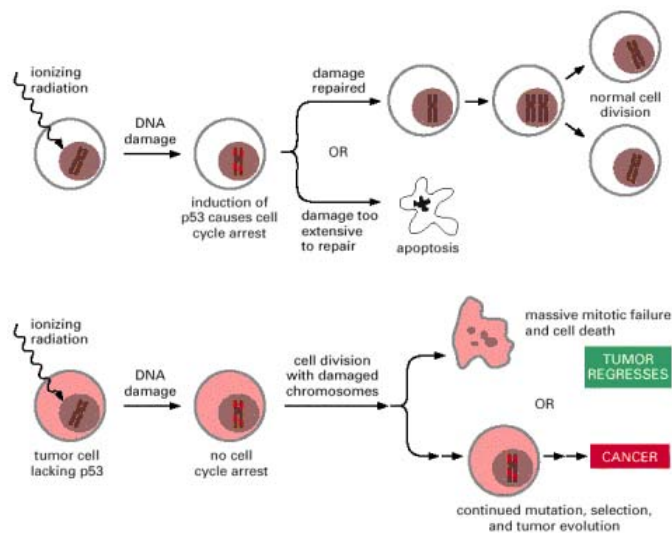


FIGURE I-18. Effects of ionizing radiation on normal cells and cancer p53 (-/-) cells. Cancer cells that lack p53 are more susceptible than normal cells to the damaging effects of ionizing radiation because they cannot arrest the cell cycle and make the necessary DNA repairs. Unfortunately, the

same genetic defects may render some cancer cells resistant to radiation treatment, as they may also be less adept at activating apoptosis in the face of DNA damage.
<http://www.ncbi.nlm.nih.gov/books/bv.fcgi?highlight=apoptosis&rid=mboc4.figgrp.4355>

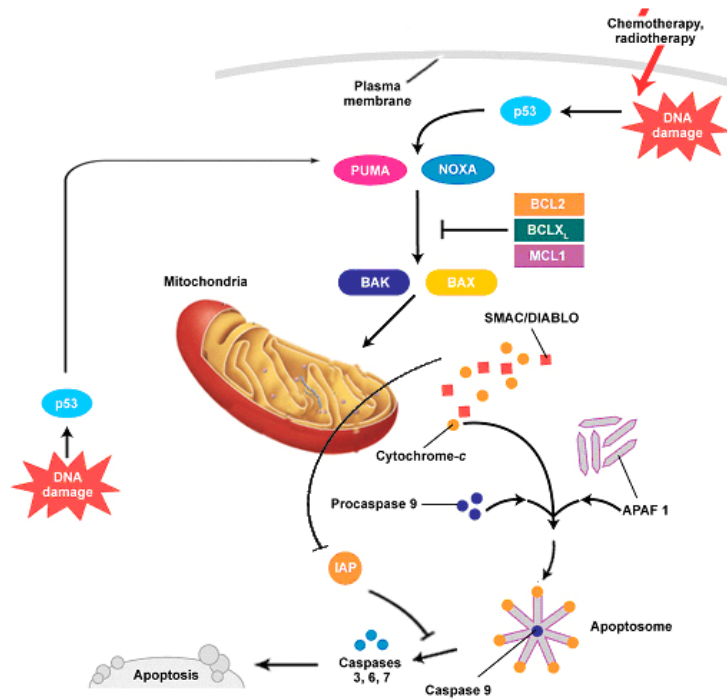


FIGURE I-19. p53-mediated activation of apoptosis via the intrinsic signaling pathway. Adapted from [119].

1.6.a. The PI3K-Akt/PKB pathway and cell survival.

The first indication that PI3K activation protects from cell death dates from 1996 [120]. This cytosolic complex consists of an 85kDa regulatory subunit and a 110kDa catalytic subunit (p110a). In response to ligand-mediated activation of receptor tyrosine kinases (RTKs), the P85–P110 complex is recruited to the RTK where it is activated. The primary consequence of PI3-K activation is the generation of phosphatidylinositol 3,4,5-triphosphate (PIP3) which functions as a membrane bound second messenger that recruits

Akt/PKB kinase through the binding to its pleckstrin-homology (PH)-domain [121]. The relevance of Akt/PKB activation by PI3K [122-124] and the link of these two with the resistance to UV irradiation and IL-3 withdrawal-induced death respectively, was soon reported [125,126].

The cellular counterweight for Akt activation is a protein called PTEN. Phosphatase and Tensin homolog deleted in chromosome ten (PTEN) is a lipid phosphatase able to convert PIP3 to PIP2, and abrogate PI3K signaling via Akt.

1.7. The role of snail family members in apoptosis and cell damage response.

Along this introduction, the physiological relevance of the snail family genes has been addressed. However, and for a better understanding of this text, an additional role for this family of transcription factors remains to be explained. Some snail family members have the ability to confer protection against apoptosis, a capacity observed almost since the very first snail family members were characterized.

The *Caenorhabditis elegans ces-1* gene encodes a snail family zinc finger protein homolog to the *Drosophila* Scratch. Upon *ces-1* transcriptional down-regulation by *ces-2* (a protein closely related to the vertebrate PAR family of bZIP transcription factors), the cell-death activator EGL-1 is no longer repressed and can, in turn, repress the anti-apoptotic *ced-9* protein, allowing the action of apoptotic proteins CED-4 and CED-3 and promoting cell death [64]. Note that human homologs for each one of these proteins had been characterized, suggesting a possible parallel role for them in mammals, as it was later shown. *snail2* (*slug*) protein, bears a close homology to the CES-1 protein of *Caenorhabditis elegans*. Consistent with the role of CES-1 as an anti-apoptotic transcription factor; *snail2*, an E2A-HLF oncoprotein responsive element, was nearly as active as Bcl-2 or Bcl-x_L in promoting the survival of IL-

Introduction

3-dependent murine pro-B cells deprived of the cytokine, giving an explanation to the observed E2A-HLF dependent survival and eventual malignant transformation of mammalian pro-B cells otherwise slated for apoptotic death [57]. Moreover, studies performed with hematopoietic cells also indicate a role for snail2 as a survival factor, protecting normal progenitor cells from radiation-induced DNA damage [127]. In fact, snail2 has been shown to repress the transcription of p53-up-regulated modulator of apoptosis (PUMA), a member of the Bcl-2 family, and a potent inducer of p53-induced apoptosis [128]. PUMA, the mammal homolog for the *Caenorhabditis elegans* EGL-1 protein, is in charge for initiating the cell-death cascade modulating the pro-apoptotic Bax activity that results in cytochrome c release from the mitochondria.

Although some data point snail1 as a protein involved in cell resistance to apoptosis, the available data are far from being as conclusive as those available for snail2. *Snail1* gene expression protects certain cells from apoptosis, such as the neural crest cells [63] or the epithelial cells at the medial edge of the palate when the palate fails to fuse [129]. Moreover, in *min* mice (mouse model for colonic neoplasia), snail1 down-regulation by antisense oligonucleotides increases cell death in colon tumors [130].

The underlying molecular mechanisms for this observations remain mostly unknown, although snail1-promoted resistance to apoptosis has been associated with its ability to up-regulate the activity of the PI3K pathway [63]. Snail1 interference with p53 function has also been reported in epithelial tumor cell lines. To date, however, this point remains unclear. On the one side, some reports claim that snail1 can repress the expression of p53 [70]. On the other side, however, some reports show no effects of snail1 on p53 activity, even in cells where snail1 is able to induce radioprotection [131].

Taken together, the results above suggest a role for snail1 in the coordination of several processes such as cell movement, survival and invasion, both during embryo development and tumor progression. In the context of cancer, by snail1 expression, the primary tumor cells acquire a selective advantage and the ability to migrate. Once the migrating cells stop being protected by the survival signals that are present in their original tissue and move towards new territories, they can come across with several apoptotic factors. Their "succeed" in reaching their final destination and give rise to a metastasis depends, in part, on snail1-mediated cell capacity to overcome this apoptotic signals [65].

OBJECTIVES

The aim of this project was the **characterization of new snail1 transcriptional targets**. Our start point was a chromatin immunoprecipitation assay coupled to CpG rich DNA array (ChIP-on-CHIP). This experiment resulted in a group of candidate gene promoters that might be regulated by snail1. A thorough study of the candidates prompted us to focus on PTEN phosphatase, a tumor suppressor gene that exerts its functions, mainly, through the negative modulation of the serine/threonine kinase Akt.

RESULTS

RESULTS 1. REPRESSION OF PTEN PHOSPHATASE BY SNAIL1 TRANSCRIPTIONAL FACTOR DURING γ RADIATION-INDUCED APOPTOSIS**R.1.1. Snail1 prevents γ radiation-induced up-regulation of *PTEN*.**

In our search to identify novel snail1 transcriptional target genes, a series of ChIP-on-CHIP analysis were performed. This type of experiment consists in the combination of two well established techniques: the chromatin immunoprecipitation followed by DNA array hybridization. First, the cells (SW480-snail1) are treated with a solution that cross-links the protein-DNA associations. Then, the chromatin (and the proteins cross-linked to it) is obtained. Next, the chromatin extracts are subjected to an immunoprecipitation with a snail1 antibody. After this step, the immunoprecipitated DNA-snail1 protein are forced to reverse their cross-linkage and the DNA sequences are purified. The last step is the hybridization of these DNA sequences against a human CpG-rich array (note that gene promoters are highly enriched in CpG islands), which revealed that *PTEN* promoter sequences (among others) were highly enriched in the snail1 immunoprecipitate. Technical information about this ChIP-on-chip analysis is given in the Annex (p165). Because the regulation of Akt by PTEN phosphatase is crucial for the apoptotic response, we tested whether snail1 is able to modify PTEN levels in Madin Darby Canine Kidney (MDCK) cells. We reasoned that such an effect would be maximal in those conditions when the cells are forced to undergo apoptosis, such as in response to γ radiation exposure. As shown in **FIGURE R-1A and B**, in MDCK control cells, γ radiation induces an increase in PTEN protein that is maximal after 8h, preceding the down-regulation in Akt activity. This increase in PTEN protein turns out to be much smaller in snail1 MDCK clones when compared to control MDCK cells, and as expected, correlates with the higher persistence of active Akt in snail1 transfectants. Closely resembling the results obtained at the protein level, PTEN mRNA is also increased in irradiated MDCK cells (**FIGURE R-1C**), but not in snail1 MDCK transfectants, suggesting that snail1 affects *PTEN* transcription.

Results

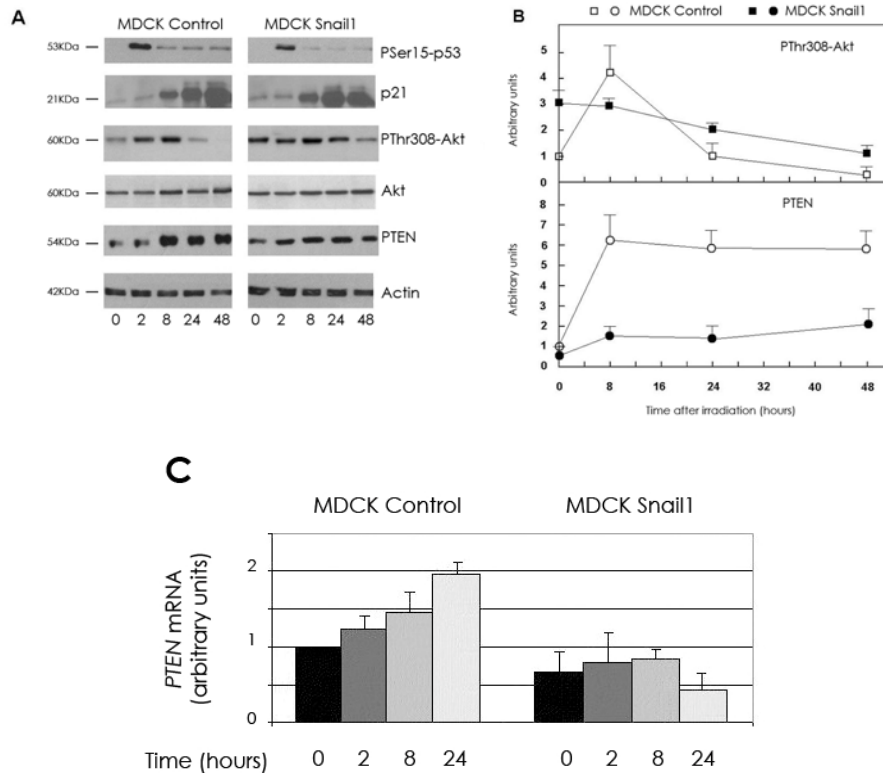


FIGURE R-1. Snail1 inhibits *PTEN* up-regulation and prevents the decrease in Akt activity in response to γ radiation. (A) MDCK control and MDCK-snail1 cells were subjected to a 20Gy dose of γ radiation and samples were collected at the times indicated. Cytosolic or total cell extracts were prepared, and p53 phosphorylation (PSer15-p53), Akt phosphorylation (PThr308-Akt), or total AKT, p21, PTEN and actin (as loading control) protein levels were determined by Western blot (WB) analysis. (B) The figure shows the result of a representative experiment of three performed. The autoradiograms were scanned, and the measures obtained for PThr308-Akt and PTEN represented respect to the value of non-irradiated control MDCK cells. Averages \pm ranges (error bars) are shown. (C) Snail1 prevents PTEN mRNA up-regulation in response to γ radiation in MDCK cells. Control and MDCK-snail1 cells were irradiated and mRNAs were purified at the indicated times. The levels of endogenous PTEN were detected by quantitative RT-PCR as described in Materials and Methods. Results are presented as the averages \pm SDs (error bars) from a minimum of three independent experiments. Levels of PTEN mRNA in another clone of MDCK-snail1 cells 24h after γ radiation were 0.8 ± 0.15 (average \pm range of two experiments; relative to the initial value of PTEN mRNA in control non-irradiated cells). With respect to the value at time zero, the PTEN mRNA increase in control cells is significant at 8h ($P < 0.05$) and at 24h ($P < 0.01$); when we compare the levels of PTEN mRNA between control and snail1 MDCK cells at the same time-points, the differences are significant at 8 and 24h with a P value of 0.01.

In addition to that, the induction of cell death by DNA damage is preceded, in MDCK cells, by a rise in the activity of p53, promoted by the phosphorylation of the protein in the Ser15 residue and thus, reducing its interaction with its negative regulator MDM2 [116]. As shown in **FIGURE R-1A**, an increase in P-Ser15-p53 is detected in MDCK control cells 2h after γ radiation. MDCK-snail1 clones show a similar increase in this parameter, suggesting that p53 activity is not altered by snail1 presence. Accordingly, after γ radiation, both control and MDCK-snail1 clones display similar increases in the p53 target gene p21^{WAF1/cip1} (**FIGURE R-1A**).

Because PTEN protein modulates the levels of activated Akt in the cell, we reasoned that Akt phosphorylation and subsequent activation should be affected by the observed PTEN up-regulation. Control MDCK cells respond to γ radiation with a rapid increase in the activity of Akt (detected with a specific MAb against residue P-Thr308), which rises its maximum 2h after γ irradiation. The phosphorylation of this amino acid by PDK1 is required for the activation of Akt [132]. At later time-points, the activity of Akt decays and 48h after the γ radiation is clearly lower than that of non-irradiated cells (**FIGURE R-1A** and **FIGURE R-1B**). On the contrary, prior to γ radiation, MDCK-snail1 cells present higher levels of active Akt than control cells (approximately threefold), (**FIGURE R-1A** and **FIGURE R-1B**). After γ radiation, the phosphorylation pattern of residue Thr308 is slightly modified by this damage; that is, the initial rise detected in control cells is not detected and the amount of phosphorylated Thr308 decreases slower. As a consequence, the activity of Akt is substantially higher in MDCK-snail1 cells than in control cells 24h after γ radiation (**FIGURE R-1**).

R.1.2. Snail1 induces resistance to γ -radiation-induced apoptosis.

Because snail1 up-regulation of the PI3K pathway has been found relevant to confer resistance to apoptosis, we characterized the response of our MDCK clones against γ radiation.

Results

MDCK control or snail1 stable clones were subjected to γ radiation to analyze their response to this classical apoptotic stimulus. 15h after seeding, the cells were challenged to a 20Gy γ radiation dose and 8h later, subjected to Fluorescence Activated Cell Sorting (FACS) with propidium iodide (PI). Our results show that after γ radiation 80% of the cells are in G2 (**FIGURE R-2A**), suggesting that they have been arrested at the G2-M checkpoint, whereas non-irradiated cells progress normally through the cell cycle. At longer time-points (48h) after γ radiation, MDCK cells re-enter the cell cycle (**FIGURE R-2A**) and start to undergo apoptosis (see below). As reported previously [63], MDCK-snail1 clones display a higher number of cells in G1 in the moment of γ radiation than control cells (40% versus 20%) (**FIGURE R-2A**, lower panel). Although delayed, γ radiation also induces G2-M cell cycle arrest in MDCK-snail1 cells. Even 48h after γ radiation, a significant percentage of the MDCK-snail1 cell population rests in G2 phase (56% [**FIGURE R-2A**]), suggesting that this checkpoint is still functional.

In a characteristic experiment, 30 to 35% percent of the control MDCK cells are undergoing apoptosis 48h after γ radiation. These cells present traits of programmed cell death, such as cytoplasmic vacuolization, increased intracellular staining for trypan blue and an elevated proportion of cells with DNA content lower than 2n, when examined by FACS (**FIGURE R-2B**). These three features are less abundant in MDCK-snail1 clones, with only 8 to 10% of cells undergoing apoptosis 48h after of γ radiation (**FIGURE R-2B**). To deepen into the role of snail1 in the resistance to apoptosis, snail1 protein was down-regulated by using a shRNA specific for this gene. As observed in (**FIGURE R-2C**), the transfection of this interferent RNA significantly represses the levels of snail1-HA in MDCK-snail1 clones. After being γ irradiated, these cells with decreased levels of ectopic snail1 display a higher sensitivity to γ radiation-induced apoptosis than snail1-expressing clones do (**FIGURE R-2D**), indicating that the resistance to cell death is partially a consequence of snail1 expression.

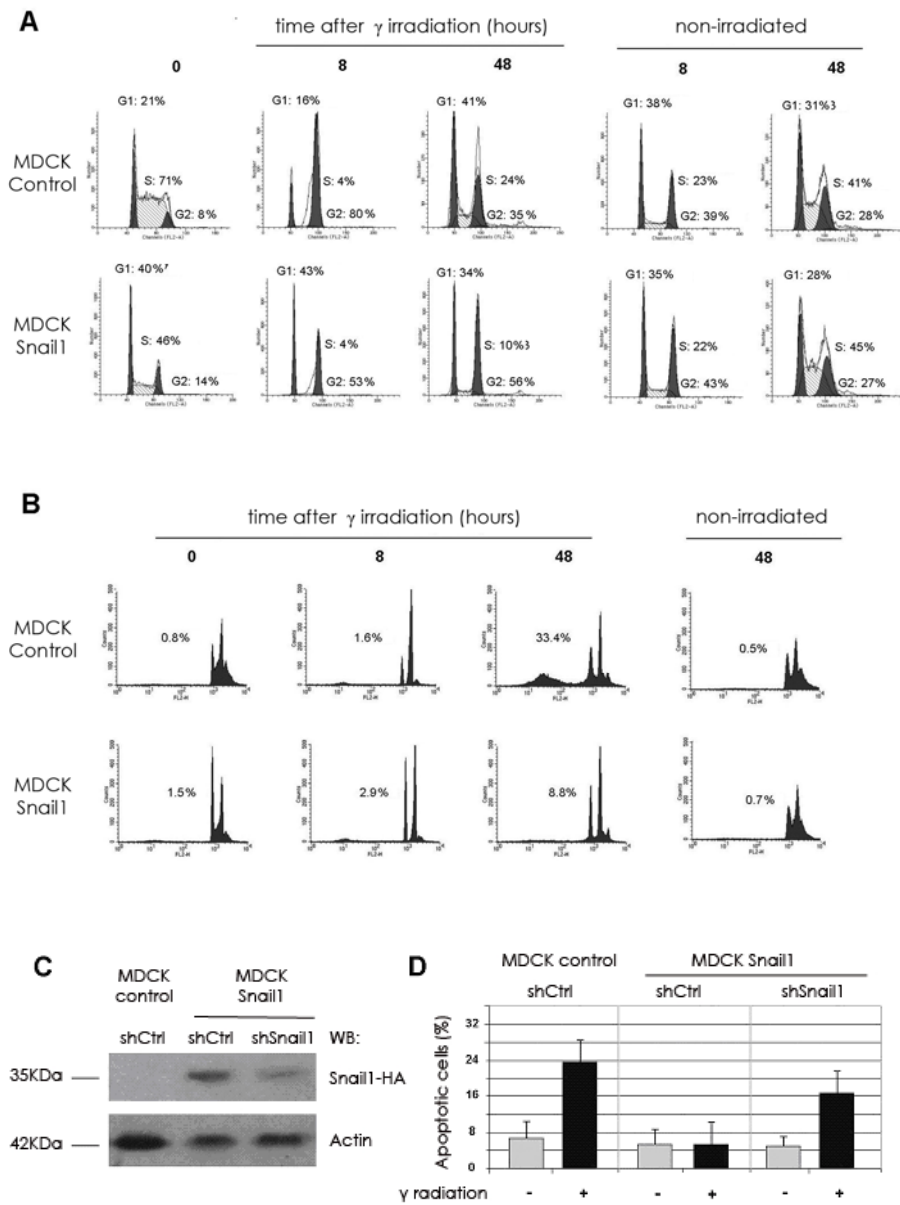


FIGURE R-2. Snail1 transfection prevents MDCK cells to undergo apoptosis in response to γ radiation. (A) γ radiation arrests MDCK control and MDCK-snail1 cells at the G2/M checkpoint. Representative diagrams show the DNA content of MDCK control or MDCK-snail1 cells at the times indicated after γ radiation (20Gy). Cells were seeded on tissue culture plates, irradiated 15h later, and at the indicated times, harvested, stained with propidium iodide (PI) and analyzed by Fluorescence

Results

Activated Cell Sorting (FACS). (B) MDCK-snail1 cells are resistant to γ radiation-induced apoptosis. The induction of apoptosis was determined by propidium iodide staining followed by FACS at the times indicated after γ radiation (20Gy). The figure shows the result of a representative experiment of three performed. Similar results were obtained with another clone of MDCK-snail1 for which a number of apoptotic cells after γ radiation was 5.6-fold lower than that of control cells. (C) MDCK control or MDCK-snail1 cells were transfected with control or snail1 shRNAs as indicated in Materials and Methods. A clone with decreased expression of snail1-HA was selected. The down-regulation of snail1-HA expression with respect to a representative clone transfected with the control shRNA was analyzed by Western blotting (WB). The molecular masses of snail1-HA and annexin 2, used as loading control, are indicated. (D) Control MDCK cells transfected with control shRNA or MDCK-snail1 cells transfected with control or snail1 shRNA were irradiated, and the percentage of apoptotic cells determined after 48h is indicated. The figure shows the averages \pm ranges (error bars) of two experiments performed. -, absence of; +, presence of.

Taken together, the results in **FIGURE R-1** and **FIGURE R-2** not only are in agreement with the previous data, but also suggest a new potential role for snail1 in promoting cell survival through the down-regulation of *PTEN* and the subsequent Akt over-activation.

R.1.3. Up-regulated Akt activity and decreased levels of PTEN mRNA are also detected in RWP-1 cells transfected with snail1.

We checked whether the differences in Akt activity and PTEN expression were detected in other cell lines. As shown in **FIGURE R-3A**, RWP-1 cells stably transfected with snail1 also present a higher resistance to apoptosis after γ radiation than control RWP-1 cells do. Typically, 40 to 50% of control cells undergo apoptosis 24h after γ radiation, whereas around 20% of RWP-1-snail1 cells do. Accordingly, a characteristic marker of apoptosis, the processed form of caspase 3, is detected at higher levels in control cells than in snail1-HA expressing cells after γ radiation **FIGURE R-3B**. In a similar manner to that observed in MDCK cells, RWP-1 cells transfected with snail1 present higher levels of active Akt, both before and 24h after γ radiation **FIGURE R-3B**. In the same way, PTEN mRNA is down-regulated in RWP-1 snail1 cells with respect to the control **FIGURE R-3C**. In a different manner from that of control MDCK cells, the increase in PTEN mRNA after γ radiation is very minor in RWP-1 cells; however, since snail1 down-regulation of this mRNA is patent before the insult,

the differences in PTEN mRNA between control and snail1 transfectants are significant at all times examined.

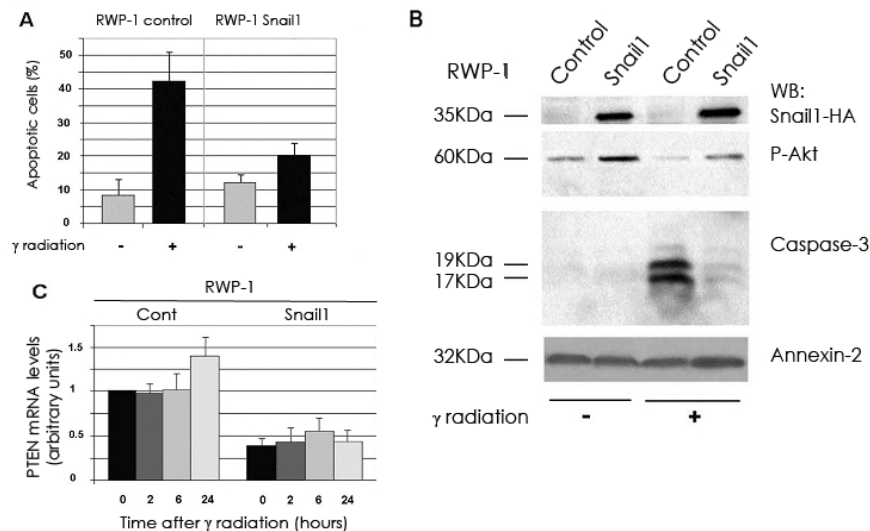


FIGURE R-3. Transfection of snail1 to RWP-1 cells up-regulates Akt activity and decreases PTEN mRNA levels. Control RWP-1 cells stably transfected with pcDNA3 or with pcDNA3-snail-HA were irradiated and analyzed. (A) Apoptosis was determined, as previously described, for non-irradiated cells (-) or for cells 24h after γ radiation (+). The figure shows the average ranges of three experiments performed. (B) Total cell extracts were prepared from non-irradiated cells (-) or 24h after γ radiation (+) and analyzed by Western blotting (WB) with MAb against HA, PThr308-Akt, caspase 3 (Casp-3) or annexin 2 (as loading control). (C) mRNA was prepared from RWP-1 cells at the indicated time-points, and levels of PTEN mRNA were detected by quantitative RT-PCR. Results are presented as the averages \pm SDs (error bars) of three independent experiments. When we compared the levels of PTEN mRNA between control and snail1-expressing cells at the same time-points, the differences were significant at all time-points with a P value of 0.01.

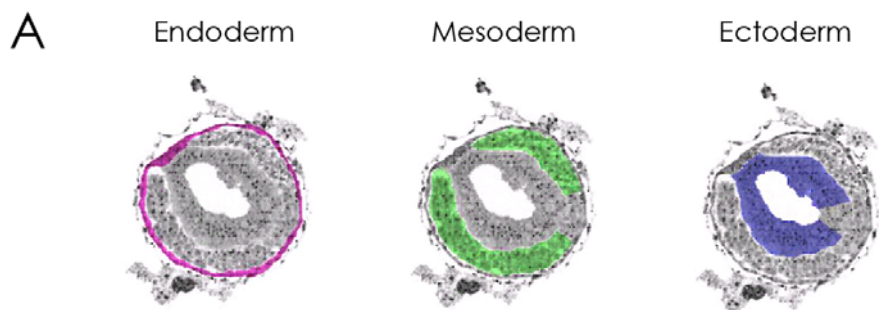
R.1.4. Contrary distribution of snail1 and PTEN in murine embryos.

To try to extrapolate our results from our cell model to an animal model, we took profit of mouse embryos at early stages of development, in which snail1 expression is essential and easier to detect than in the adult tissue. The expression of snail1 and PTEN proteins was analyzed by immunohistochemistry and the results are shown in **FIGURE R-4A**. Snail1 is expressed in the mesoderm of

Results

wild-type murine embryos (7.5 dpc), (**FIGURE R-4A**, upper left panel), whereas, as expected, no labeling is observed in *snail1* null embryos (**FIGURE R-4A**, bottom left panel). PTEN protein expression displays an inverse pattern to that of *snail1* at this stage of development, being restricted to the ectoderm (**FIGURE R-4A**, upper middle panel). In *snail1*-deficient embryos, PTEN protein pattern is not restricted to this embryonic layer, although the alterations in the mutant embryo architecture (a consequence of its incapability to undergo gastrulation) preclude further statements. In these mutant embryos, fewer cells are stained by anti-PThr308-Akt MAb (only $36\% \pm 5\%$ [average \pm SD of four determinations] with respect to the number observed in control embryo sections), (**FIGURE R-4A**, bottom right panel), indicating that the activation of this kinase is also reduced in *snail1* mutants.

Altogether, these data indicate that *snail1* expression is contrary to that of PTEN, in our mouse embryos, and suggest that *snail1* regulation of PTEN expression is an active mechanism during embryonic development.



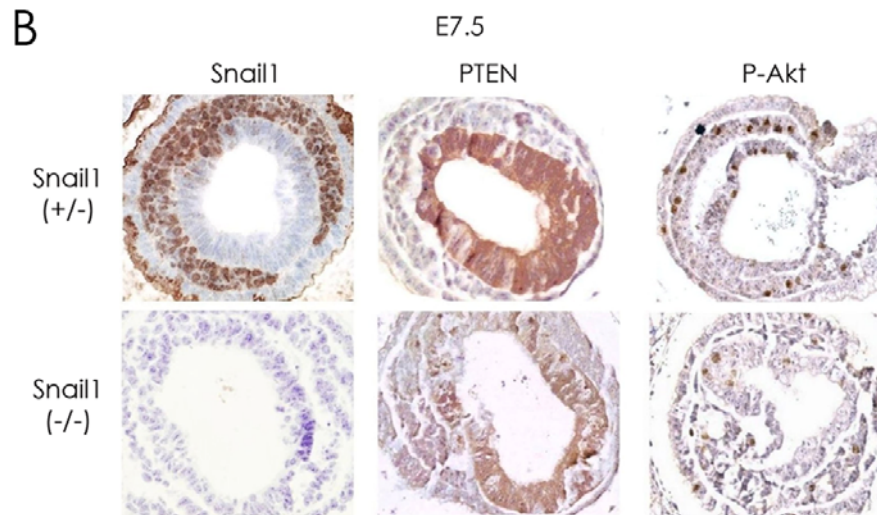


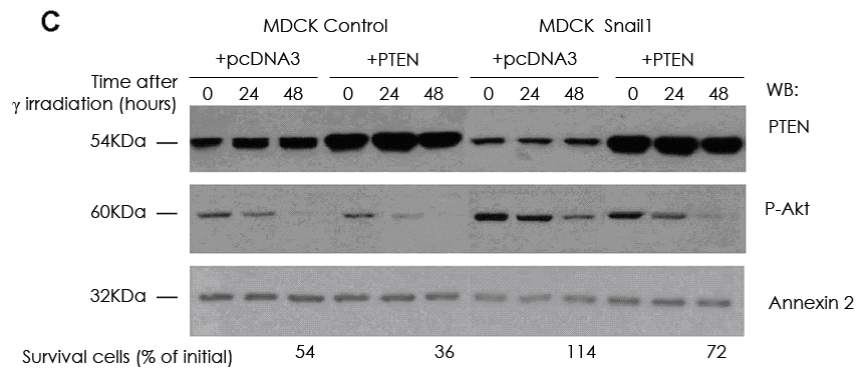
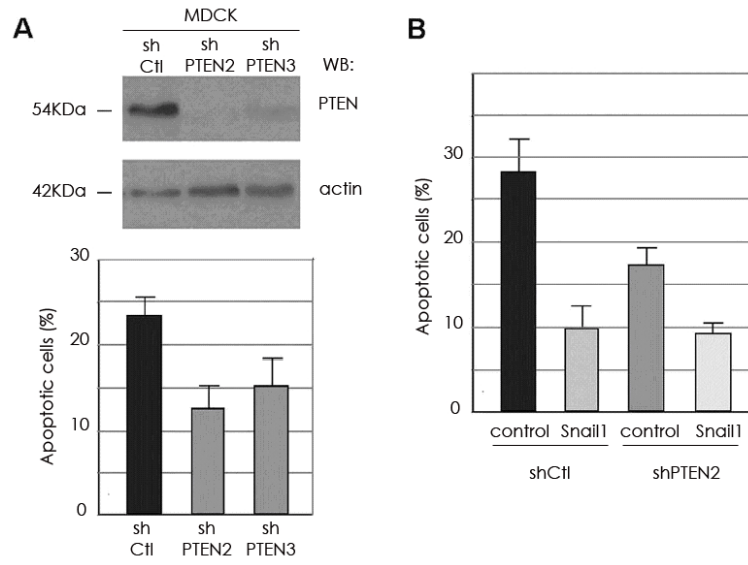
FIGURE R-4. Snail1 and PTEN proteins display an inverse expression pattern in murine embryos. (A) Schematic of a murine embryo at stage 7.5 dpc. The transverse cut reveals the three embryonic layers: endoderm (purple), mesoderm (green) and ectoderm (blue). (B) Presence of snail1, PTEN, or P308-Akt was determined in wild-type or snail1-null 7.5 dpc embryos (E7.5) by immunohistochemistry using specific MAbs and the conditions indicated in Materials and Methods. Original magnification, x150.

R.1.5. Relevance of *PTEN* repression in the resistance to γ radiation-induced apoptosis caused by snail1.

We determined the relevance of *PTEN* repression in the resistance to γ -radiation-induced apoptosis. Cell clones showing down-regulated expression of *PTEN* were generated by transfecting MDCK cells with a plasmid that generates a shRNA specific for *PTEN*. As shown in **FIGURE R-5A**, the depletion of *PTEN* protein correlates with an increased resistance to apoptosis, since 48h after γ radiation, the number of apoptotic cells is lower in MDCK cells expressing shPTEN than in the corresponding controls. This result indicates that *PTEN* plays a relevant role in the promotion of cell death in MDCK cells. However, the protection conferred by this shPTEN is not as complete as that provided by the expression of snail1, suggesting that this transcription factor also acts on other elements than *PTEN*. Accordingly, the expression of snail1

Results

increases the resistance to apoptosis even in cells with undetectable levels of PTEN (**FIGURE R-5B**). To confirm this result, PTEN was over-expressed in MDCK or RWP-1 cells either in control cell populations or in cell populations ectopically expressing snail1. As shown in **FIGURE R-5C and FIGURE R-5D**, the transfection of PTEN slightly increases the amount of control cells undergoing cell death after radiation. For instance, in RWP-1 cells, at 24h, the number of dead cells increases from 54% to 73% in the representative experiment shown in **FIGURE R-5D**. Similarly, the number of surviving cells decreases in MDCK cells after ectopic expression of PTEN from 54% to 36% (**FIGURE R-5D**). As shown above, the expression of snail1 decreases the extent of apoptosis in cells transfected with pcDNA3 (from 54% to 30% in RWP-1 cells) and also does so in cells over-expressing PTEN (from 73% to 53%). An analysis of Akt activity also correlates with these data. The expression of snail1 up-regulates the levels of active Akt (**FIGURE R-5C and FIGURE R-5D**), whereas PTEN ectopic expression accelerates the decrease in Akt activity observed after γ radiation (**FIGURE R-5C**, compare lanes 2 and 5). However, even in cells with a high expression of PTEN, snail1 transfectants present higher levels of active Akt than control cells (**FIGURE R-5C**, compare lanes 4 to 6 with lanes 10 to 12, or D, compare lanes 5 to 6 with 7 to 8). Altogether, these results suggest that although *PTEN* down-regulation caused by snail1 expression affects resistance to apoptosis and Akt activity, additional elements also contribute to the full snail1 response.



Results

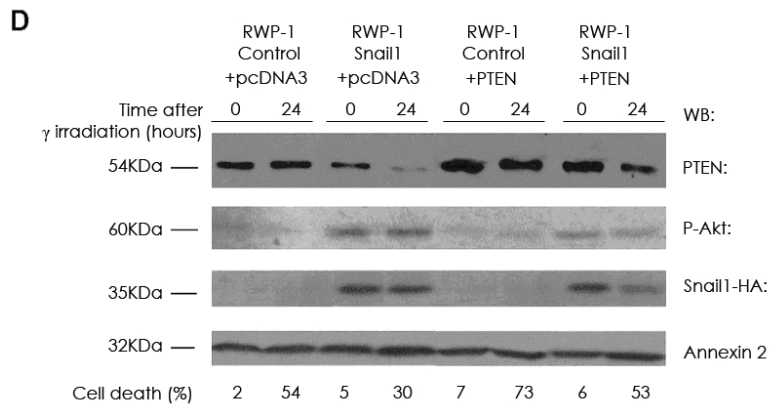


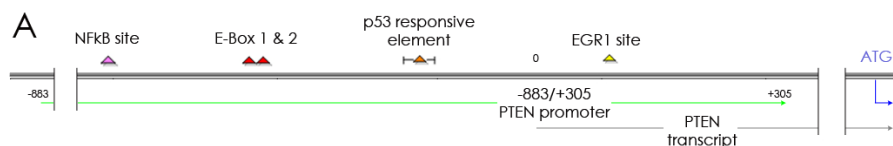
FIGURE R-5. Ectopic manipulation of PTEN protein levels affects cell death and snail1 response.

Stable clones expressing a shRNA specific for PTEN or expressing a shRNA control were generated in MDCK cells. (A) Expression of PTEN was checked by Western blot (WB) analysis (top panels). The indicated cells were irradiated and cultured for 48h. The percentage of apoptotic cells was analyzed by flow cytometry (bottom panel). The averages \pm SDs (error bars) of three experiments performed are shown. (B) MDCK shCtrl or shPTEN (clone 2) cells were transfected with pcDNA3 or pcDNA3-snail1-HA and selected, and the resistance to apoptosis of the four different subpopulations was analyzed. The averages \pm ranges (error bars) of two experiments performed are shown. (C) MDCK control or snail1 cells were transfected with a GFP expression plasmid and PTEN cDNA or a control (cont) plasmid. After 24h of expression, the cells were irradiated and cultured for an additional 48 h. The percentage of apoptotic cells was analyzed by determining the number of GFP-positive cells by flow cytometry and referred to the number of cells at the time of γ radiation. In parallel, cell extracts were prepared and analyzed by Western blotting with the indicated antibodies. (D) RWP-1 control or RWP-1 snail1-HA cells were transfected with pcDNA3 or pcDNA3-PTEN plasmids, and the double-transfectant populations were selected. Cells were irradiated and the percentage of apoptotic cells was determined. The figure shows the result of one experiment of two performed with similar results.

R.1.6. Snail1 binds to *PTEN* promoter and represses its activity.

In order to analyze the mechanism responsible for the lower expression of PTEN in snail1 transfectants, we cloned a fragment of the human *PTEN* promoter (positions -883/+305 bp), (FIGURE R-6A). This DNA fragment displays a high activity in epithelial cells, such as the MDCK cells used in our assays and its activity lowers to $61\% \pm 3\%$, (shown as mean \pm standard deviation [SD]) in MDCK-snail1 cells, indicating that snail1 effect on PTEN mRNA levels is transcriptional. Similar results are obtained when the activity of this promoter fragment is examined in RWP-1 snail1 transfectants. Transient transfections of snail1 cDNA in MDCK cells substantially repress the activity of the *PTEN*

promoter in a dose-response manner (**FIGURE R-6B**). The snail1 P2A mutant (already introduced as a deficient repressor) of snail1 target genes, is unable to repress *PTEN* promoter activity in this reporter assay (**FIGURE R-6B**). The *PTEN* promoter contains two putative binding elements (also called E-boxes) for the snail1 transcriptional factor with a core sequence 5'-CACCTG-3'. These two E-boxes are placed at positions -351/-345 and -337/-332 from the transcription start. As shown by electrophoretic gel shift assays (**FIGURE R-6C**), snail1 recombinant protein strongly binds to an oligonucleotide containing the two E-boxes. Such binding is competed by a 10-fold excess of unlabeled oligonucleotide but not by a mutant oligonucleotide in which the two boxes are replaced by 5'-AACCTA-3'. A similar mutation has been reported to block snail1 binding to E-cadherin and other target promoters [31,66,68]. We checked whether the two E-boxes are relevant for snail1 repression of the *PTEN* promoter. As shown in (**FIGURE R-6B**), a promoter form in which the two boxes are mutated to 5'-AACCTA-3' is insensitive to snail1 expression in the luciferase reporter assays, indicating that these sequences are mediating the effects of snail1 on *PTEN* transcription. snail2 (Slug) and Zeb1 are two transcriptional factors that also repress E-cadherin through the binding to the same elements as snail1, although with lower potency [66,133]. The transfection of these two cDNAs at a same concentration than snail1 does not significantly repress *PTEN* promoter activity (**FIGURE R-6B**), indicating that snail1 is much more efficient in the control of *PTEN* expression than these two other repressors.



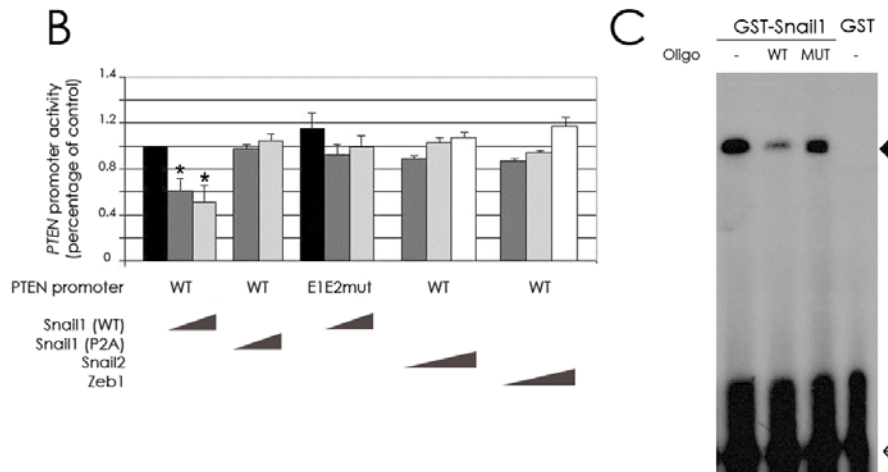


FIGURE R-6. Snail1 represses *PTEN* promoter activity. (A) Scheme of *PTEN* promoter. In green, the -883/+295 fragment cloned. The different responsive elements are labeled in color boxes (B) snail1 represses *PTEN* promoter in a dose-dependent manner. The activity of the wild type or the E1E2-mutant *PTEN* promoter was determined in MDCK cells by transient transfection. When indicated, wild-type or P2A snail1 mutant, wild-type snail2, or zeb1 cDNAs were cotransfected at several concentrations: 0.1 (dark gray bars), 1 (light gray bars), and 10ng (white bars). Black bars correspond to the activity of each promoter in the absence of repressors. The figure shows the averages \pm SDs (error bars) of three independent experiments performed in triplicate. Asterisks indicate differences that were significant at a *P* value of 0.05. (C) snail1 binds to *PTEN* promoter. The GST-snail1 fusion protein or the GST protein was incubated with a double-stranded ³²P-radiolabeled probe corresponding to a DNA fragment within which the two E-boxes of *PTEN* promoter are present. Binding experiments were carried out with 150ng of GST-snail1 without competitor (-) or competing with an excess of unlabeled wild-type (WT) or mutant oligonucleotide (MUT). Arrow, free probe; arrowhead, specific shifted band.

R.1.7. Binding of snail1-HA to *PTEN* promoter is modulated after γ radiation.

The binding of snail1-HA to *PTEN* promoter was also determined by ChIP assay (FIGURE R-7). In MDCK cells, *PTEN* promoter sequences are detected in the fraction precipitated with a MAb against the HA tag labeling the ectopically expressed snail1. As shown in (FIGURE R-7A), the binding of *PTEN* promoter to snail1 is also detected if endogenous snail1 is immunoprecipitated from SW-620 cells with a snail1 MAb prepared in our lab [94], discarding the possibility of an unspecific binding of snail1 to *PTEN* promoter due to the over-expression of the protein. As a positive control of

our ChIP experiments, the association of snail1 to *PTEN* promoter with performed in parallel to that of another well-established target promoter of this transcriptional factor, E-cadherin [74]. The results are displayed in **FIGURE R-7A**, and reflect no significant differences between this two target genes.

Though we had been able to show the binding of snail1 to *PTEN* promoter, our data did not completely match. We had observed no differences in *PTEN* protein expression in non-irradiated MDCK control vs. MDCK-snail1 cells (**FIGURE R-1A** and **FIGURE R-1B**); however, our ChIP experiments suggested that, under these conditions, snail1 could bind to *PTEN* promoter. To address the matter of whether snail1-HA binding to *PTEN* promoter is modulated by γ radiation we performed ChIP experiments at several time-points after γ radiation (20Gy). As shown in **FIGURE R-7B**, the amount of the *PTEN* promoter immunoprecipitated with snail1-HA from MDCK cells is significantly increased 2h after γ radiation. Furthermore, given that *PTEN* transcriptional activity has been reported to be dependent on p53 binding to *PTEN* promoter [134], we would expect this mechanism to be fostered by p53 phosphorylation after DNA damage (i.e. γ radiation). We hypothesized that snail1 could prevent p53 association to *PTEN* promoter. By ChIP assays, and prior to γ radiation, very little binding of p53 to *PTEN* promoter is detected, either in control or in snail1 MDCK cells (**FIGURE R-7C**). This association is greatly increased in control cells 2h after γ radiation (**FIGURE R-7C**), correlating with the detected up-regulation of P^{Ser15}-p53 (**FIGURE R-1A**). However, this binding is not observed in MDCK-snail1 cells, indicating that snail1 inhibits p53 interaction to the *PTEN* promoter (**FIGURE R-7C**).

We also analyzed whether snail1 modulated the expression of the apoptosis regulator *PUMA*, another p53 target gene reported to be sensitive to snail2 (Slug) in hematopoietic cells [128]. *PUMA* mRNA levels prior to γ radiation are not significantly different in MDCK-snail1 in comparison with MDCK control cells. After γ radiation, *PUMA* mRNA levels are increased, as

Results

expected, but in a similar manner in both cell lines, that is, not being affected by the presence of snail1 (FIGURE R-7D). Moreover, the presence of *PUMA* promoter sequences is not detected in snail1 immunoprecipitates (data not shown), suggesting that snail1 does not bind to *PUMA* promoter.

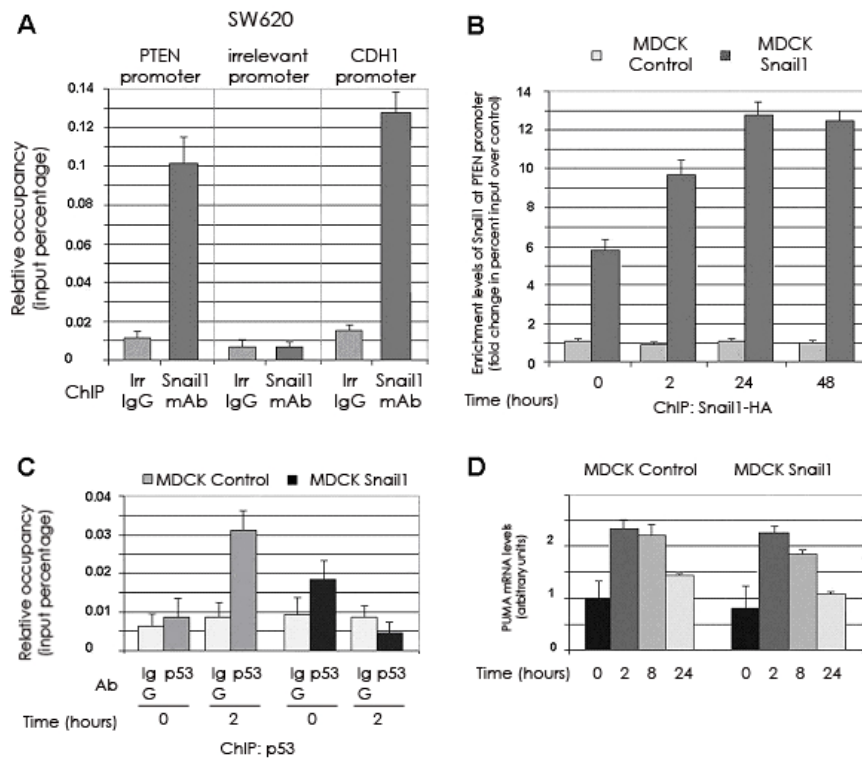


FIGURE R-7. Snail1 is recruited to the *PTEN* promoter "in vivo" in response to γ radiation. (A) Snail1 binds to the *PTEN* promoter in SW-620 cells. ChIP assays were carried out by using a MAb specific for snail1 or an irrelevant (irr) IgG as described in Materials and Methods. The presence of sequences corresponding to *PTEN*, E-cadherin (CDH1), or an irrelevant promoter was analyzed and represented as relative occupancy (percent input). (B) Binding of snail1 to the *PTEN* promoter is up-regulated after γ radiation. ChIP assays were performed by immunoprecipitating snail1-HA with an anti-HA MAb or an irrelevant IgG from MDCK-snail1 cells at different times after γ radiation. Enrichment levels in snail1 at the *PTEN* promoter correspond to the change in the percentage input calculated with respect to the amount detected in the immunoprecipitation carried out with an irrelevant IgG. In a representative experiment, the percentages of input obtained with the IgG or with anti-HA MAb in the control (cont) clones (not expressing snail1) varied between 0.005 and 0.007; the values obtained with anti-HA MAb in MDCK-snail1 cells at 0, 2, 24, and 48 h after γ radiation were 0.035, 0.07, 0.08, and 0.07, respectively. Similar results were obtained when the binding of snail1-HA to *PTEN* promoter was analyzed in another clone of MDCK-snail1 cells. (C) Snail1 prevents the interaction of p53 with *PTEN* promoter in response to γ radiation. ChIP assays were performed by immunoprecipitating p53 from the indicated cells either before or 2h after γ . Data are represented as described for panel A. Panels A to C of this figure show the averages \pm SDs (error bars) of three

independent experiments. (D) Snail1 does not prevent PUMA up-regulation in response to γ radiation in MDCK cells. The levels of endogenous PUMA were detected by quantitative RT-PCR, as described in Materials and Methods, using mRNA isolated from the indicated cells prior and after γ radiation. Results are presented as the averages \pm SDs (error bars) from three independent experiments.

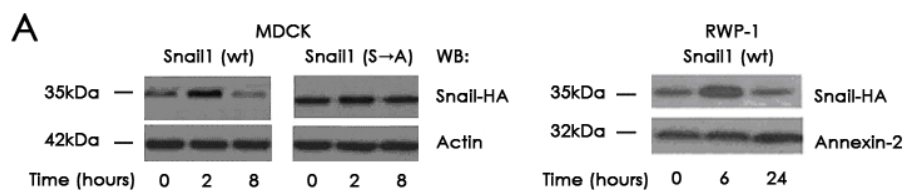
R.1.8. Summary to Chapter 1.

We have characterized a novel molecular mechanism responsible, at least in part, for the already reported snail1-induced resistance to apoptosis. Snail1 prevents PTEN up-regulation in response to γ radiation at the transcriptional level by (a) binding and repressing *PTEN* promoter and (b) avoiding p53 binding to *PTEN* promoter.

**RESULTS 2. POST-TRANSLATIONAL MODULATION OF SNAIL1 PROTEIN IN
RESPONSE TO γ RADIATION**

R.2.1. Snail1 protein is stabilized in response to γ radiation.

While trying to elucidate the mechanism leading to the up-regulated binding of snail1 to the *PTEN* promoter after γ radiation, we observed that, in MDCK-snail1 cells, the levels of ectopic snail1 rise after γ radiation, temporally correlating with the increased binding to the *PTEN* promoter (FIGURE R-8A, left panel). This increase in snail1 protein is transient and can be reproduced in other models such as RWP-1 snail1 cells (FIGURE R-8A, right panel). This enhanced expression of snail1 is detected in the nucleus (FIGURE R-8B), suggesting that the process of export and subsequent degradation of snail1 protein [75,135] is blocked in the irradiated cells. To test our hypothesis, we used a snail1-HA mutant (snail1 Ser \rightarrow Ala) in which the serine residues required for the export and degradation of the protein, placed in the Pro-Ser-rich domain, are replaced by alanines [73] conferring this mutant protein with a higher stability than the wild-type form. As shown in FIGURE R-8A, left panel, the levels of this mutant are not significantly increased after γ radiation, supporting our theory that γ radiation is somehow inhibiting the degradation of snail1 protein.



Results

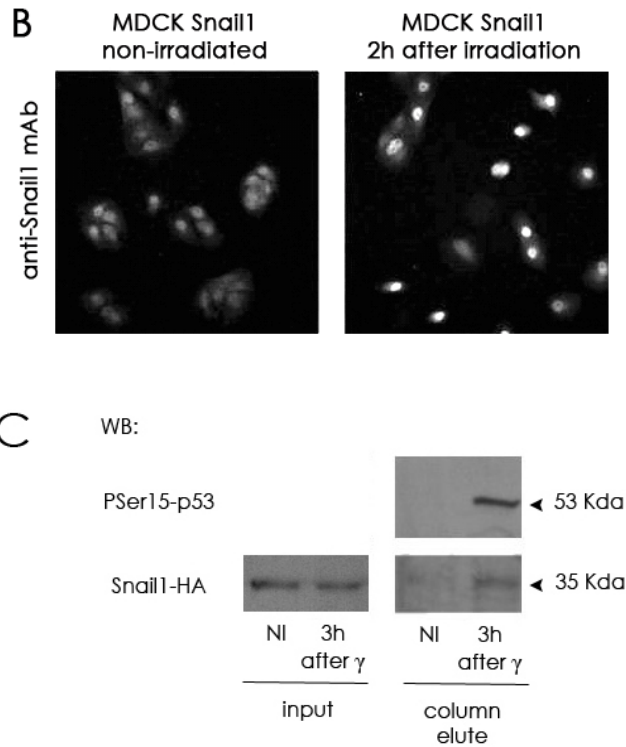


FIGURE R-8. Snail1 protein is stabilized in response to γ radiation. (A) Protein levels and (B) cellular distribution of snail1 were determined at the indicated times after γ irradiation in MDCK-snail1 (wild-type), MDCK-snail1 (Ser \rightarrow Ala mutant) or RWP-1-snail1 (wild-type) cells by Western blotting (A) or immunofluorescence (B). (C) Phosphorylation of snail1 protein was determined in stable MDCK-snail1 transfectants 3h after γ radiation and compared with the phosphorylation of the same non-irradiated MDCK-snail1 cells (NI). The purification of phosphorylated snail1-HA was performed as indicated in Materials and Methods.

As described above, snail1 export and subsequent degradation has been reported to be mediated by snail1 phosphorylation within the Pro-Ser-rich domain. To test whether the stabilization observed in response to γ radiation is due to a dephosphorylation in this domain, we checked by affinity chromatography if the amount of phosphorylated snail1 in MDCK irradiated cells is lower than in non-irradiated cells. The validity of our purification system (PhosphoProtein purification kit, Qiagen) was proofed by the increase in

PSer15-p53 detected in the column-bound fraction (**FIGURE R-8C**) and in accordance with our previous observations showing that, in our MDCK-snail1 model, the induction of p53 phosphorylation happens shortly (2h) after γ radiation (**FIGURE R-8A**). To our surprise, the amount of phospho-snail1 purified after γ radiation is higher (**FIGURE R-8C**). This result, though not being conclusive because a stabilization of snail1 by means of another mechanism could explain our observations without meaning an increase in phosphorylation, suggests that the stabilization of snail1 protein is not due to the dephosphorylation of residues.

Though ectopic snail1 stabilization in MDCK snail1 cells is a highly reproducible experiment, we were concerned about the possibility that this accumulation might be an artifact due to snail1 over-expression. To solve this problem, we addressed the study of endogenous snail1 in response to γ irradiation. Because of the low expression of endogenous snail1 in MDCK cells, we chose another cell model, the NIH-3T3 fibroblast, where endogenous snail1 can be detected by immunofluorescence and western blot. NIH-3T3 cells were seeded on coverslips and 24h later challenged to a 20Gy γ radiation dose. The coverslips were fixed at different times after γ irradiation and the immunofluorescence against endogenous snail1 protein performed as explained in Materials & Methods. **FIGURE R-9A** shows our preliminary results obtained for time-points 0h and 9h in which endogenous snail1 nuclear staining is significantly increased.

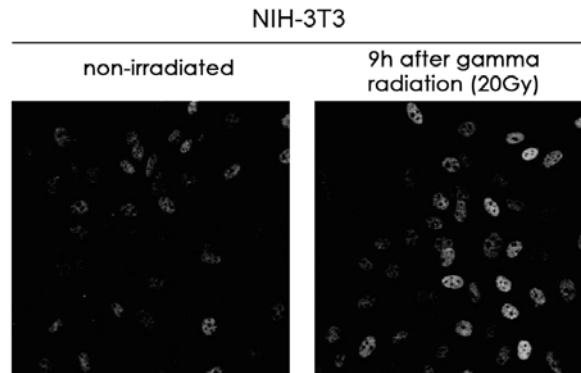


FIGURE R-9. Nuclear Snail1 endogenous protein is increased in response to γ radiation in NIH-3T3 cells. (A) Cellular distribution of snail1 endogenous protein was determined at the indicated times after γ irradiation in NIH-3T3 cells by immunofluorescence.

R.2.2. Chk1 phosphorylates snail1 “in vitro”.

The relevance of snail1 stabilization has been introduced above. We have seen that, at least for the case of *PTEN* promoter, snail1 stabilization occurs concomitantly with a higher binding to *PTEN* promoter (**FIGURE R-7B**), which blocks *PTEN* transcription in response to γ radiation. Our experiments with the snail1 (Ser \rightarrow Ala) mutant in which the serine residues within the Pro-Ser-rich domain cannot be phosphorylated, seem to discard this region as the putative region responsible for snail1 stabilization observed. To approach the search of new regions within snail1 that might be responsible for its stabilization, we first performed an “in silico” phosphorylation assay (<http://scansite.mit.edu/>). The results of this assay point Chk1, among others such as PAK, as a putative kinase able to phosphorylate snail1 (this issue will be addressed below). We are particularly interested in Chk1 because its relevance in the early response to cell damage has been known for long [136]. To confirm this prediction “in silico” and to narrow the residue(s) phosphorylated by Chk1, an “in vitro” phosphorylation assay followed by

enzyme digestion and mass spectrometry is currently being performed and its results will be soon available.

In the meantime, another approach to the study of snail1 stabilization has arisen from the observation of some previous evidence. It has been reported that, besides the phosphorylation events within the Pro-Ser-rich domain, which have been related to snail1 subcellular localization and targeting for degradation [73,75]; phosphorylation of Ser246, placed in the C terminus of snail1 protein, promotes contrary effects to those of the serine residues located in the Pro-Ser-rich domain [78]. The phosphorylation of this Ser can be catalyzed by PAK1, a protein kinase known to be activated by ionizing γ radiation [137]. We show here, by "in vitro" phosphorylation assay (**FIGURE R-10**), that other kinases (such as Chk1) might also be able to phosphorylate this residue "in vivo". We have also performed the same "in vitro" phosphorylation assay with the recombinant snail1 (S246A)-GST in the presence of Chk1 and shown that, by avoiding phosphorylation in this Ser246 residue, the overall phosphorylation of snail1 protein is drastically lowered though not completely, (suggesting the existence of more than one phosphorylation site for Chk1 in snail1 protein), (**FIGURE R-10**).

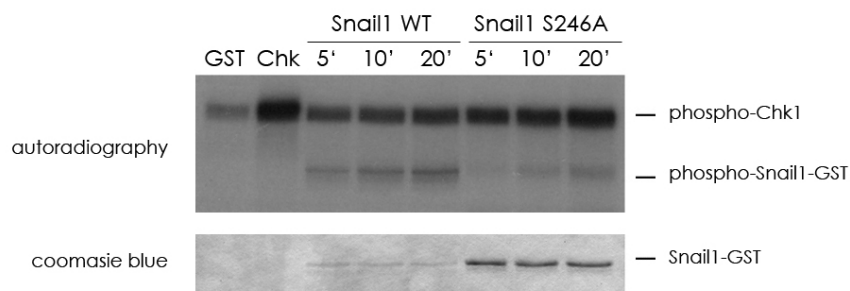


FIGURE R-10. Recombinant Chk1 phosphorylates snail1-GST "in vitro". A time course of wild type snail1-GST or snail1 (S246A)-GST phosphorylation by Chk1 was performed. Recombinant Chk1 (1 μ g), GST alone, snail1-GST or snail1 (S246A)-GST proteins were incubated for the indicated times in the presence of 32 P-ATP. The specific bands are labeled to distinguish them from the degradation bands present.

R.2.3. Relevance of Ser246 in snail1 stabilization, E-cadherin repression and resistance to apoptosis promotion.

The results in **FIGURE R-10** encouraged us to establish a MDCK-snail1 S246 stable cell line and determine whether these cells respond to γ radiation different from MDCK-snail1. As shown in **FIGURE R-11**, MDCK-snail1 (S246A) challenged with a 20Gy dose behave as control MDCK cells and undergo apoptosis (vs. MDCK-snail1 cells).

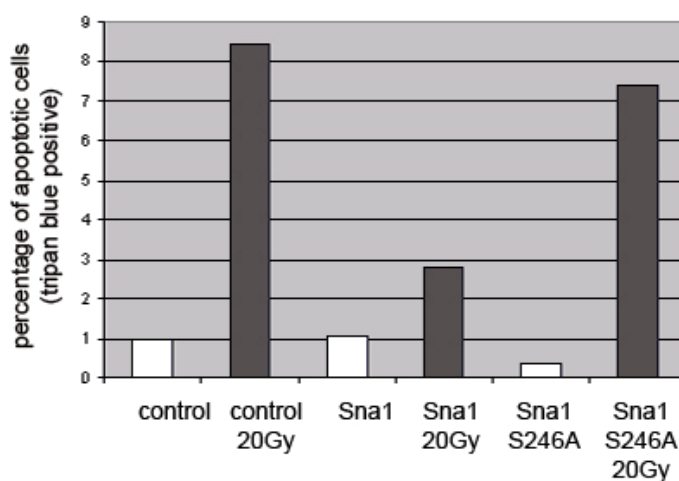


FIGURE R-11. Snail1 S246A mutant (unlike wild type snail1) is not able to promote resistance to γ radiation-induced apoptosis. MDCK control, MDCK-snail1 and MDCK-snail S246A were challenged to a 20Gy γ radiation dose and the percentage of viable cells of the three different subpopulations was analyzed by tripan blue staining. The figure shows the results of a representative experiment.

Yang and co-workers have proposed Ser246 as a key residue responsible for snail1 targeting to the nucleus in MCF-7. Phosphorylation of this residue by PAK results in snail1 enrichment in the nucleus where it is able to repress its target genes. They propose that snail1 S246A cannot be phosphorylated in this residue and therefore, remains mostly cytoplasmic, no being able to repress its target genes. However, our results are in disagreement with this statement. Unlike in MCF-7 cells, the subcellular localization of snail1 (S246A) in

MDCK cells is absolutely nuclear and indistinguishable from that of the wild type protein (**FIGURE R-12**).

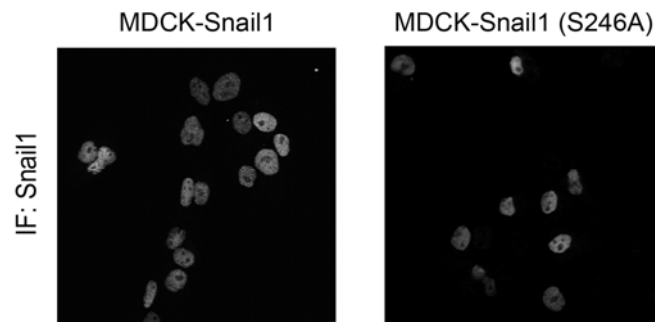


FIGURE R-12. Snail1 S246A is located in the nucleus of MDCK. The localization of snail1 (S246A) is the same of the wild type snail1 protein in MDCK cells. The immunofluorescence was performed as described in Materials & Methods.

This observation opened a new question. Yang et. al propose that snail1-(S246A) is incapable of repressing genes because of its subcellular localization, however, we wondered whether snail-1 (S246A) would still be able not to repress its target genes in our MDCK cells, where its subcellular localization is nuclear. We hypothesize that, unlike its localization, the mutation in Ser246 residue could affect the structure of the C-terminus domain of snail1, affecting the fourth zinc finger present in the wild type protein, and disrupting the binding of this transcription factor to its DNA targets. To prove so, we performed “in vitro” binding assays with a probe bearing the two E-boxes present in *PTEN* promoter and the wild-type or the snail1 (S246)-GST mutant. As **FIGURE R-13** shows, unlike wild-type snail1, the mutant is unable to bind the probe, suggesting that, at least “in vitro”, the snail1 (S246A) mutant cannot bind the *PTEN* probe.

Results

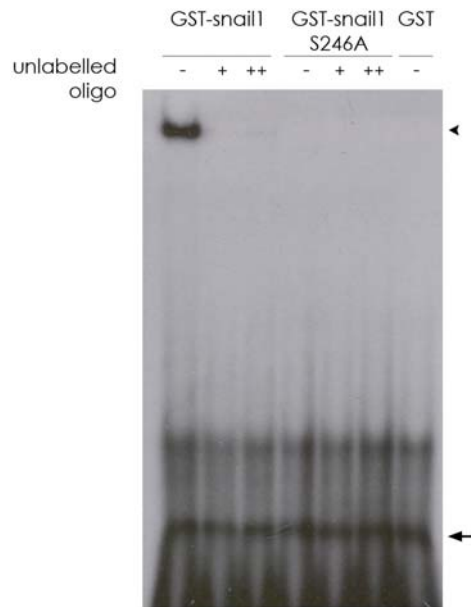


FIGURE R-13. Snail1 S246A cannot bind *PTEN* probe in vitro. Either GST-snail1 or GST-snail1 S246A fusion protein or the GST protein alone were incubated with a double-stranded ³²P-radiolabeled probe corresponding to a DNA fragment within which the two E-boxes of *PTEN* promoter are present. Binding experiments were carried out with 150ng of recombinant protein without competitor probe (-) or competing with an excess of unlabeled wild-type oligonucleotide at 10x fold (+) or 100x fold (++). Arrow, free probe; arrowhead, specific shifted band.

Besides the “in vitro” evidences and in accordance to them, our western blot experiments also show that snail1 (S246A) is unable to repress E-cadherin to the same extent than the wild type protein (**FIGURE R-14**). These results match with those published by Yang and co-workers in MCF-7 cells, however, the molecular mechanism proposed by them seems not to apply, at least, for our MDCK cell model.

The experiments above seem to discard S246 as the residue responsible for snail1 stabilization in response to γ radiation. In fact, snail1 (S246A) mutant behaves, in terms of the observed stabilization, as the wild type protein (**FIGURE R-14**). Moreover, our experiments point to the existence of other residues within

snail1 responsible for that observation. Our current “in vitro” phosphorylation assays with Chk1 kinase and wild-type snail1, coupled to mass spectrometry, should provide us with new candidate residues within snail1 and responsible for the stabilization. Note, however, the possibility that snail1 stabilization responds to the participation of more than one residues, among which, S246 cannot be discarded.

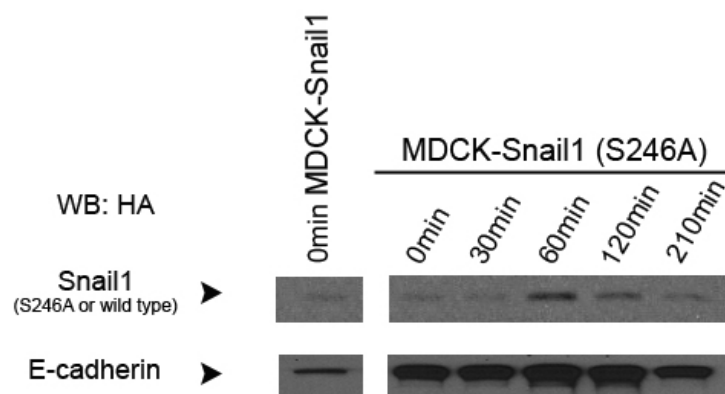


FIGURE R-14. Snail1 S246A protein is stabilized in response to γ radiation in MDCK-snail1 (S246A) cells but is unable to repress E-Cadherin. (A) Microscopy image of the MDCK control (left), MDCK-snail1 (middle) and MDCK-snail1 (S246A) (right). Note the characteristic epithelial phenotype of control cells, disrupted by snail1 or snail1 S246A transfection, conferring a more scattered phenotype. (B) Protein levels of wild type snail1 or S246A mutant and E-cadherin were determined at the indicated times after γ irradiation in MDCK-snail1 or MDCK-snail1 (S246A) cells.

R.2.4. Summary to Chapter 2.

Note that this is a summary of current work. Many issues remain still unclear and need to be addressed into more detail. So far, we can conclude that snail1 protein is stabilized in the nucleus in response to γ radiation, where it binds to its target gene *PTEN* to promote resistance to apoptosis. The mechanism responsible for this stabilization might relay in snail1 phosphorylation by Chk1, most likely out of the Pro-Ser-rich domain.

RESULTS 3. SNAIL1 BINDS TO ITS OWN PROMOTER AND GENERATES A NEGATIVE FEED-BACK LOOP THAT CONTROLS ITS EXPRESSION IN EPITHELIAL CELLS

The identification of *PTEN* as a transcriptional target of snail1 allows us to establish a link between this transcription factor and the PI3K pathway. The relevance of this signaling pathway for EMT has been reported before [138]. In fact, *SNAIL1* transcription has been shown to be dependent on this pathway. The combination of the results above and our snail1 background could give an explanation to this observation and prompted us to study the elements modulating *SNAIL1* gene expression.

R.3.1. *SNAIL1* expression is stimulated by serum.

Snail1 expression is not constitutive. Apart from the low expression of this protein in epithelial cells, snail1 mRNA is not expressed in all mesenchymal cells tested (not shown). This observation suggests the existence of a tight transcriptional regulation of the snail1 gene expression (*SNAIL1*) that prompted us to study if the cellular amount of snail1 protein can be somehow modulated. To address this question, we chose the NIH-3T3 fibroblasts (a cell line with a high expression of endogenous snail1 that can be detected by western blot), synchronized the cells by a 24h serum depletion and analyzed the response of these fibroblasts at different times after serum re-exposure.

As shown in **FIGURE R-15**, snail1 protein levels are up-regulated when serum-depleted NIH-3T3 fibroblasts are stimulated with serum. The kinetic of this stimulation displays a maximal amount of protein accumulation three hours after serum stimulation, followed by a snail1 protein levels decrease that equals that of the non-depleted fibroblast 12h after serum stimulation (**FIGURE R-15A** and **FIGURE R-15B**). To our surprise, snail1 protein levels do not remain constant at later time-points, but keep oscillating with a regular and

Results

reproducible pattern (FIGURE R-15A and FIGURE R-15B). These changes in snail1 protein are also found for snail1 mRNA by RT-PCR (FIGURE R-15C).

Such an oscillatory pattern is characteristic of genes that present auto-regulation [139] and suggests that *SNAIL1* is subjected to a tight and complex transcriptional regulation that prompted us to deepen into the study of the elements controlling *SNAIL1* gene.

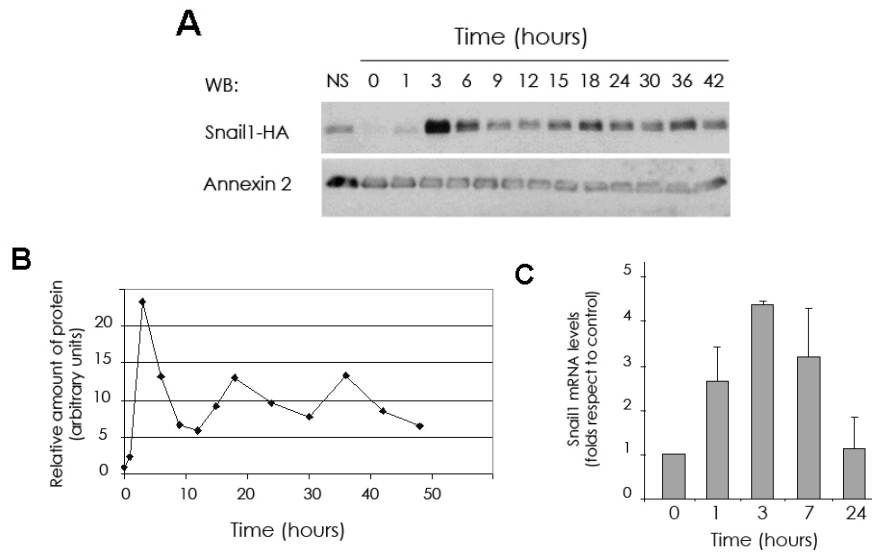


FIGURE R-15. Snail1 expression is stimulated by serum. NIH-3T3 fibroblasts were incubated in the absence of serum for 24 hours and treated with 10% FBS during the indicated times. Protein cell extracts or mRNA were obtained and analyzed by western blot (A and B) or quantitative RT-PCR (C) as indicated in Methods. Analysis of annexin 2 was used to verify that equal amounts of protein were loaded. NS, not synchronized (serum-starved) cells. (A) Shows the results of a representative experiment of three performed; (B) shows the density values obtained after scanning the blot in panel A, referred to that obtained in serum starved cells. (C) Shows the average \pm SD of three experiments performed.

R.3.2. Characterization of three E-boxes within *SNAIL1* promoter.

To study the elements controlling *SNAIL1* gene expression, we took advantage of the human *SNAIL1* promoter fragments (**FIGURE R-16**) cloned in our laboratory [85].

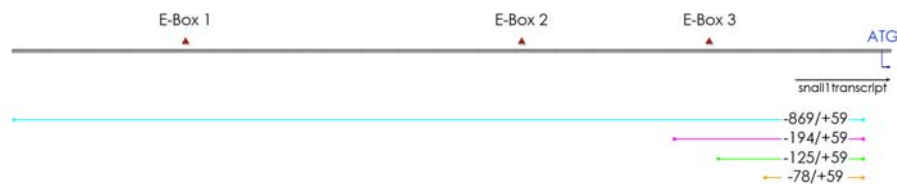


FIGURE R-16. Scheme of the different *SNAIL1* promoters used in this study. The sizes of the different fragments are shown in between of the different color arrows. The snail1 transcript is labeled in black and the beginning of the open reading frame and the ATG start codon are labeled in dark blue. Note the presence of three 5'-CAGCTG-3' E-boxes, in red.

This promoter is active in all cell lines analyzed by luciferase reporter assay, although its greater activity is achieved in those cells where EMT has been induced by expression of integrin-linked kinase (ILK) or oncogenes such as Ha-ras or v-Akt [85].

The analysis of *SNAIL1* promoter revealed the existence of an inhibitory sequence located between nucleotides -194 and -125, the deletion of which increased the activity of the promoter in almost all the cell lines studied (compare values for -194/+59 and -125/+59 promoters (bars 3rd and 5th, when available) in (**FIGURE R-17B**).

A closer look at this region revealed a 5'-CACCTG-3' E-box located between nucleotides -144 and -139 (both included). This box is a well established sequence motif known to be bound by snail1 protein in many snail1-targeted promoters, such as *CDH1* [31]. To check the relevance of this element in the transcriptional regulation of *SNAIL1* promoter, the 5'-CACCTG-3' was mutated to 5'-AACCTA-3', an already reported sequence unable to be bound by snail1 [31]. This two point mutations within the 5'-CACCTG-3' E-

Results

box resulted in a significantly increased activity of the -869/+59 promoter in RWP-1, SW-480, SW-620, NIH-3T3 (FIGURE R-17B) and MiaPaca-2 (not shown) cells (compare 1st and 2nd bars). Furthermore, we obtained similar results to those observed for the -869/+59 promoter when the two same point mutations in the E-box were tested in the -194/+59 *SNAIL1* promoter (compare 3rd and 4th bars). Not surprisingly, those cells with very low levels of endogenous snail1 protein, such as HT-29 M6 [31], display a minimal change in the activity of the -194/+59 promoter after being mutated (FIGURE R-17).

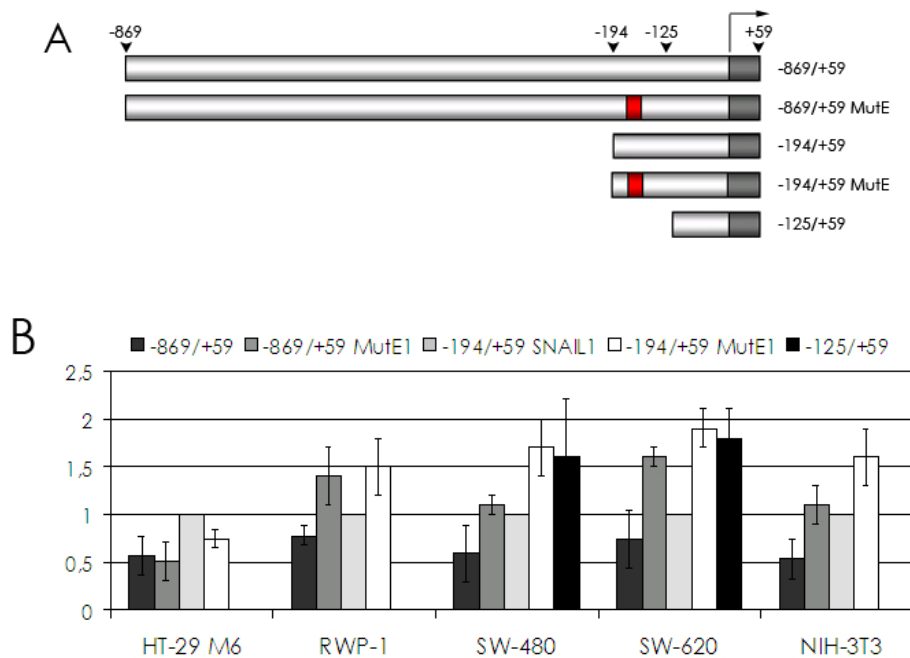
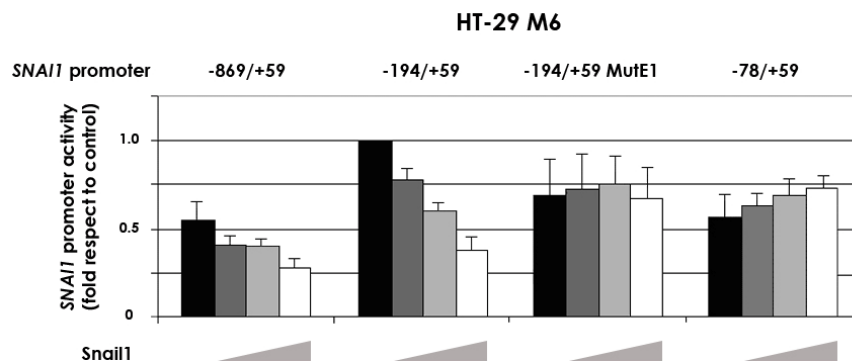


FIGURE R-17. *SNAIL1* promoter contains an E-box that binds a repressor. The activity of the indicated *SNAIL1* promoters was determined as described in Methods. Previous analysis of E-cadherin and snail1 mRNAs in these cells have shown that HT-29 M6 and RWP-1 present low levels of snail1, SW-480, intermediate; and SW-620 and NIH3T3, high. (A) This scheme shows the different *SNAIL1* promoters tested. (B) Graphical representation of the luciferase reporter assays. The graphic shows the average of 3 independent experiments.

R.3.3. Ectopic snail1 represses *SNAI1* promoter and down-regulates snail1 mRNA levels.

The results above made us think of the possibility that snail1 protein could be modulating its own promoter. Therefore, we analyzed the capability of ectopic snail1 protein to inhibit different constructs of the *SNAI1* promoter transfected in cells with low endogenous levels of the protein.

As observed in **FIGURE R-18A**, snail1 transfection to HT-29 M6 cells represses the basal activity of -869/+59 and -194/+59 *SNAI1* promoter constructs, but is inactive on the -194/+59 fragment once the E-box mentioned above is mutated (-194/+59 Mut E1), or on the *SNAI1* promoter fragment lacking the 5'-CACCTG-3' box (-78/+59). This same dependence on the E-box integrity for the inhibition of *SNAI1* promoter mediated by snail1 is also observed in RWP-1 cells (**FIGURE R-18B**).



Results

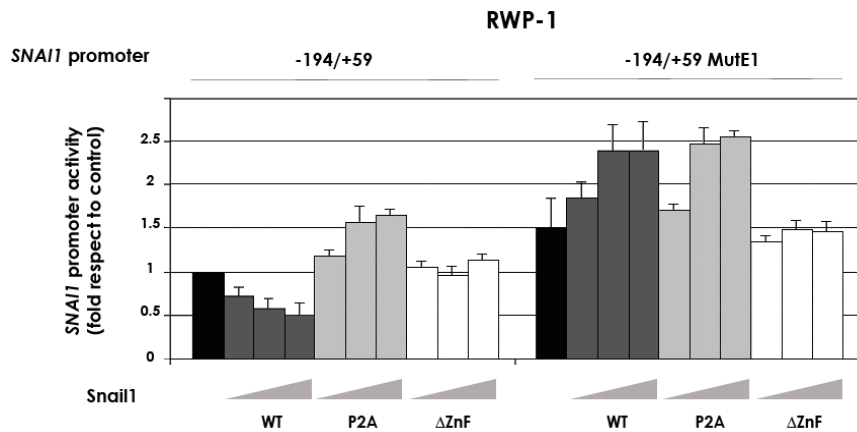


FIGURE R-18. Ectopic snail1 represses the activity of *SNAIL1* promoter. (A and B) Activity of the different promoter fragments was determined in HT-29 M6 and RWP-1 cells by transient transfection; when indicated, wild-type snail1 or P2A or Δ ZnF mutant cDNAs were cotransfected at several concentrations. The three mutants were expressed at similar levels (not shown). Black bars correspond to the activity of each promoter in the absence of snail1. The average \pm SD of three different experiments is shown.

Next, we analyzed the effect of two different snail1 mutants on *SNAIL1* promoter. Either the Δ ZnF mutant, in which the entire C-terminus of the snail1 protein has been deleted, or the P2A mutant, bearing a substitution of Pro2 to Ala within the N-terminus of snail1 protein, were tested. Both mutants have been reported to be inactive on *CDH1* promoter [31] and our results show that they behave the same on *SNAIL1* promoter (**FIGURE R-18B**).

To address the question of whether the snail1 repression of its own promoter correlated with a decrease of endogenous snail1 RNA levels, we took advantage of the fact that murine snail1 mRNA can be easily distinguished from the human snail1 mRNA. We then studied the effect of ectopic snail1 murine protein expression on endogenous (human) snail1 mRNA by RT-PCR. Results are displayed in **FIGURE R-19A**, where murine snail1 transfection to HT-29 M6 cells clearly down-regulates human endogenous snail1 mRNA. This down-regulation of endogenous snail1 mRNA by stable

ectopic expression of murine snail1 cDNA was determined to be between 40 to 60% by quantitative RT-PCR (qRT-PCR) depending on the HT-29 M6 clone analyzed (**FIGURE R-19B**). A pool of RWP-1 cells transfected with the murine snail1 cDNA also showed a similar decrease in human endogenous snail1 mRNA (**FIGURE R-19B**).

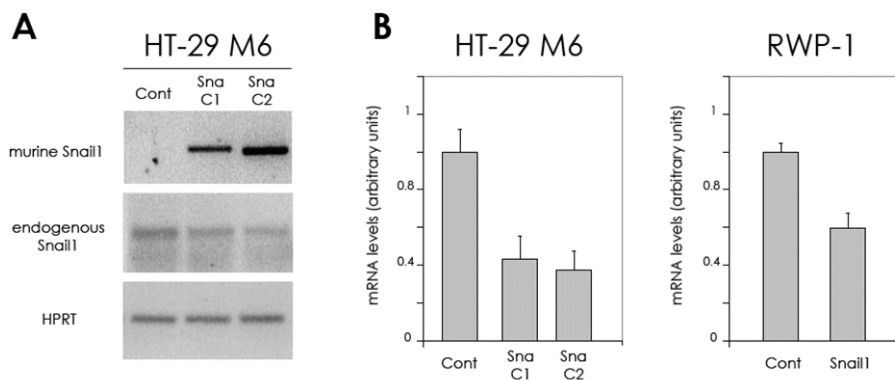


FIGURE R-19. Ectopic snail1 murine protein down-regulates human endogenous snail1 mRNA. (A and B) mRNA was obtained from control HT-29 M6 cells or clones expressing murine snail1-HA, or from a pool of RWP-1 cells stably transfected with pcDNA3-snail1-HA or with empty plasmid. Levels of endogenous human snail1 mRNA were determined as indicated by semi-quantitative (A) or quantitative RT-PCR (qRT-PCR) (B). The analysis of murine snail1 (*snail1*) and an internal control (*HPRT*) is also shown.

R.3.4. Snail1 protein binds to *SNAIL1* promoter.

After showing that the murine form of snail1 is able to modulate the activity of its human homologue, we wondered about the mechanism responsible for this observation. So far, snail1-mediated repression of target promoters has been shown to be dependent on direct binding to E-boxes present within these promoter regions. Therefore, we performed Gel-shift and Chromatin-Immunoprecipitation (ChIP) assays to confirm that binding of snail1 to *SNAIL1* promoter was indeed happening.

Gel-shift assays indicate that recombinant snail1 fused to glutathione-S-transferase (GST-snail1) binds efficiently to an oligonucleotide including the E-

Results

box sequence (FIGURE R-20). The presence of the specific shifted band is competed in the presence of a 100-fold excess of unlabelled oligonucleotide, as expected, but not in the presence of a 100-fold excess of unlabelled mutant oligonucleotide where the existing E-box described above has been modified not to bind snail1. This result evidences the fact that snail1 has the same requirements for binding to this region of the *SNAIL1* promoter than those previously described for E-cadherin (*CDH1*) promoter [31].

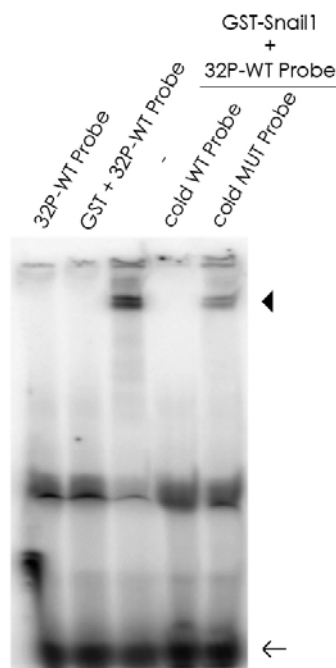


FIGURE R-20. Snail1 binds to *SNAIL1* promoter in vitro. Affinity-purified GST-snail1 fusion protein or GST protein alone was incubated with double-stranded ³²P-labelled oligonucleotides corresponding to the E-box of *SNAIL1* promoter. Binding experiments were carried out with 150ng of GST-snail1 without competitor, or competing with a 100-fold excess of unlabelled wild-type or mutant oligonucleotide. Arrow, free probe; arrowhead, specific shifted band.

The observation that snail1 could bind a 20bp *SNAIL1* oligonucleotide bearing the E-Box “in vitro” prompted us to determine if this association also existed “in vivo”. To do so, we performed ChIP experiments and again, we were able to detect binding of snail1 protein to *SNAIL1* promoter. In this case, HA-tagged snail1 was immunoprecipitated with an HA mab from HT-29 M6 cell clones stably expressing snail1. The presence of *SNAIL1* or *CDH1* (a target of snail1 used as positive control) promoter sequences was determined by PCR. Our results confirm that ectopic snail1 protein binds to the native *SNAIL1* promoter of HT-29 M6 cells “in vivo” (**FIGURE R-21**).

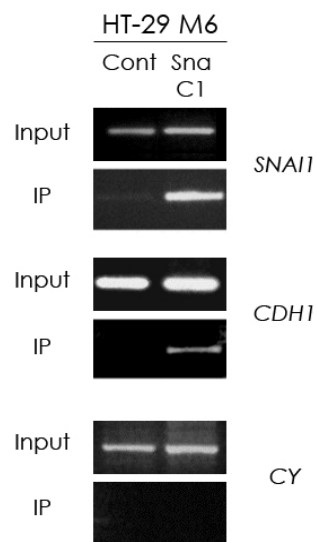


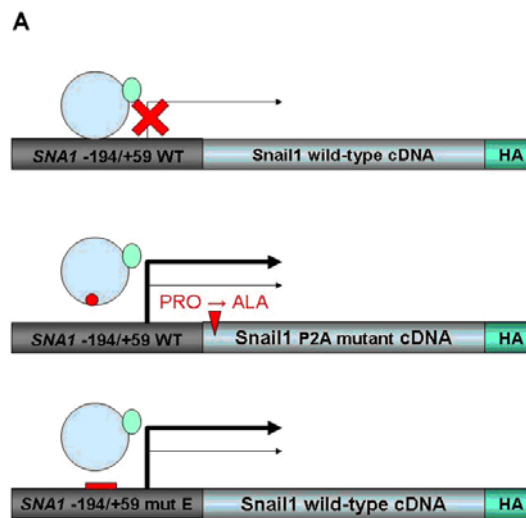
FIGURE R-21. Snail1 binds to *SNAIL1* promoter “in vivo”. ChIP analysis was performed as indicated in Materials & Methods using control or snail1-HA transfected HT-29 M6 clones. Analysis of E-cadherin (CDH1) and Cyclophilin (CY) was performed as positive and negative controls respectively.

R.3.5. A snail1 inhibitory feed-back loop is active in cell culture.

The results shown above popped the question about the physiological relevance of *SNAIL1* inhibition by snail1. We speculated with the existence of a negative feed-back loop responsible for the maintenance of snail1 protein

Results

levels within a tight range. To check if this negative feed-back loop exists in our cell models, snail1-HA cDNA was expressed in HT-29 M6 or RWP-1 cells under the control of a fragment of its own promoter (-194/+59). The constructions used in this experiment are shown in **FIGURE R-22A**. We reasoned that, if existing, this inhibitory loop should be interrupted either by using a snail1 mutant unable to repress *SNAI1* promoter (P2A mutant) or the mutated promoter (-194/+59 Mut E1) described above, leading to higher levels of ectopic snail1-HA protein expression. As observed in **FIGURE R-22B**, the amount of snail1-HA protein is evidently higher in both conditions if compared with our control condition, that is, the wild-type *SNAI1* promoter controls the transcription of the snail1-HA cDNA. This increase in snail1-HA protein, detected by western blot against the HA-tag, cannot be attributed to differences in the transfection efficiency or by a higher stability of snail1-HA P2A protein, as **FIGURE R-22B** shows.



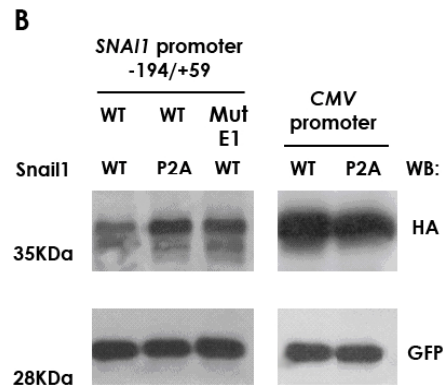


FIGURE R-22. Snail1 represses its own expression generating a negative feed-back loop. (A) Scheme of three DNA constructs used for the experiment in B. (B) Wild-type or P2A snail1-HA mutant cDNAs were inserted in pGL3 reporter plasmid, where *SNAI1* (-194/+59) promoter or (-194/+59 Mut E1) promoter had been previously cloned. The luciferase gene and the CMV promoter within pGL3 were deleted, leaving the expression of wild type snail1-HA or P2A mutant under the control of wild type *SNAI1* or *SNAI1*-Mut E1 promoter. The resulting three plasmids were transfected to RWP-1 cells and expression of ectopic snail1-HA was analyzed 48h later by western blot using the HA antibody. GFP was cotransfected in a ratio of 1:10 to check that differences in the HA expression were not due to distinct efficiency of transfection. As a control, wild type or P2A snail1-mutant were expressed under the control of CMV promoter, to check that the two proteins present a similar stability in these cells. The panel shows the result of a representative experiment of three performed. The estimated sizes of snail1-HA and GFP are shown.

The same results are observed in RWP-1 and HT-29 M6 (not shown) although in this latter cell line the protein expression levels are lower, reflecting the lesser activity of the *SNAI1* promoter in the cells.

R.3.6. Summary to Chapter 3.

We describe the existence of an inhibitory feed-back mechanism that controls *SNAI1* expression in epithelial cells. This mechanism is dependent on the repressive activity of snail1 protein and on the integrity of a 5'-CACCTG-3' element located within the *SNAI1* promoter.

RESULTS 4. SNAIL1 EFFECTS ON *SNAI1* TRANSCRIPTION ARE CELL DEPENDENT**R.4.1. Snail1 activates in its own promoter independently of the E-box.**

As it will be shown below, the inhibitory loop previously described is functional in all cell lines studied. However, and to our surprise, the predominant effect of snail1 expression on *SNAI1* promoter is significantly different in those cell lines with a more mesenchymal phenotype.

To try to elucidate the transcriptional mechanism leading to this different behavior of *SNAI1* promoter in these so called "mesenchymal" cells, we used one of the first approaches that had been useful in the past. We took profit again of the fact that by RT-PCR we can differentiate the endogenous snail1 levels in a pool of SW-480 cells (human) from the ectopically transfected murine snail1-HA.

In contrast with our previous results in epithelial cells (HT-29 M6 or RWP-1 cells), in SW-480 cells, ectopic snail1 increases the levels of endogenous snail1 mRNA two-fold, detected by qRT-PCR (**FIGURE R-23**). The same results were observed when two populations of MiaPaca-2 cells, transfected with control or murine snail1-HA plasmids were analyzed. In this latter case the presence of ectopic snail1-HA increases endogenous snail1 mRNA more than five-fold (**FIGURE R-23**).

Results

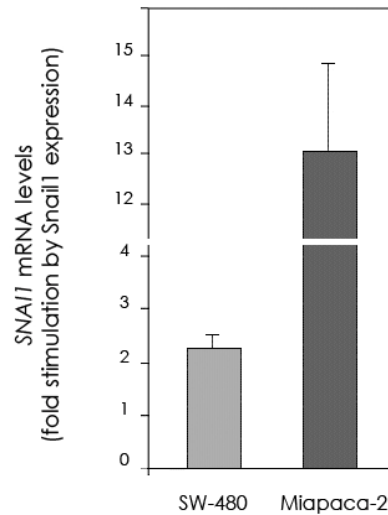


FIGURE R-23. Ectopic murine snail1 protein up-regulates human endogenous snail1 mRNA in mesenchymal cells. Endogenous snail1 mRNA levels were analyzed by qRT-PCR (as described before) in SW-480 or MiaPaca-2 cells transfected with murine -HA or with control plasmid. The figure shows the relative values of endogenous human snail1 mRNA in murine snail1-transfected cells respect to the control.

Again, as for the case of epithelial cells, *SNAIL1* promoter activity in mesenchymal cells correlated with the mRNA levels observed. As shown in **FIGURE R-24**, the activity of the -869/+59 and -194/+59 *SNAIL1* promoter fragments is higher in SW-480 snail cells than in SW-480 control cells. Furthermore, the mutation of the E-box does not prevent this effect, but, on the contrary, leads to an even larger stimulation. The results obtained for the shorter *SNAIL1* promoter (-125/+59) also lacking the E-box, reinforced our conclusion that this stimulation is not dependent on snail1 binding to its promoter.

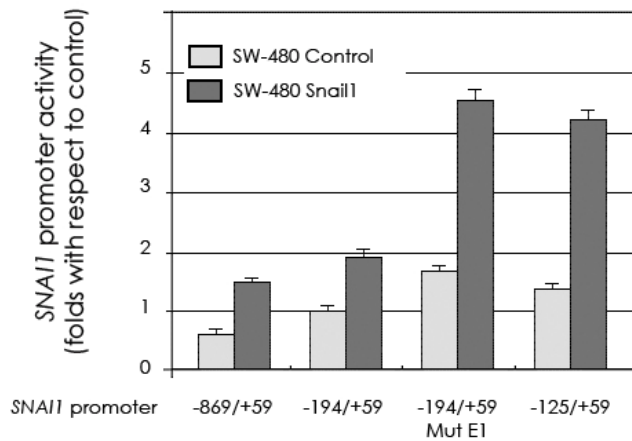


FIGURE R-24. Ectopic snail1 activates the activity of *SNAI1* promoter. The relative activity of the indicated *SNAI1* promoters was analyzed in SW-480 control or ectopic snail1 expressing clones. The results are average \pm SD of three experiments performed.

Additional reporter assays analyzing the effect of transient snail1 expression on *SNAI1* promoter activity in mesenchymal cells also agree with this conclusion. Snail1 activates the expression of its promoter independently of the presence of the E-box (**FIGURE R-25**). Both in SW-480 and NIH-3T3 cells, snail1 stimulation of the -194/+59 *SNAI1* promoter is not dependent on the integrity of the E-box. On top of that, the *SNAI1* -125/+59 promoter fragment (lacking the E-box sequence) also responds to snail1 (**FIGURE R-25**), reinforcing our idea that the activation of *SNAI1* promoter is not dependent on the E-box.

Results

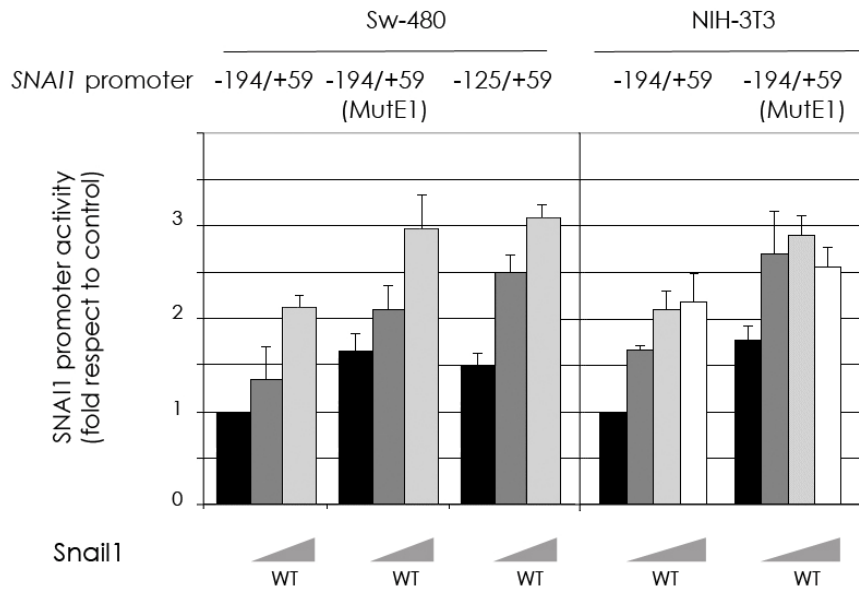


FIGURE R-25. Ectopic snail1 activates the activity of *SNAIL1* promoter. SW-480 or NIH-3T3 cells were transiently cotransfected with increasing amounts of wild-type snail1 DNA, together with the indicated *SNAIL1* promoters. The activities of these promoters were calculated taking as a reference the value obtained for the -194/+59 promoter in the absence of ectopic snail1.

Although the overall effect of snail1 expression in these mesenchymal cell lines was the stimulation of *SNAIL1* promoter, we observed that the *SNAIL1* promoter bearing the mutation in the E-box displayed an increased activity when compared with the wild type *SNAIL1* promoter. This observation was suggesting us that maybe snail1 binding to *SNAIL1* promoter and the subsequent repression was also happening in mesenchymal cells.

A ChIP assay verified our suspicions. Snail1 co-immunoprecipitated *SNAIL1* promoter as well as *CDH1* promoter in SW-480 cells (**FIGURE R-26**), confirming the binding of snail1 to *SNAIL1* not only in epithelial cells (where the overall effect of snail1 expression is *SNAIL1* repression, see **FIGURE R-21**), but also, at least, in the SW-480 cell model (where the overall effect is activation).

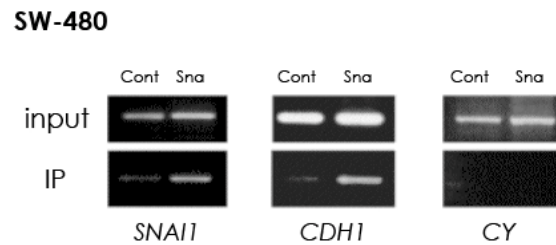


FIGURE R-26. ChIP analysis confirms snail1 binding to *SNAI1* in SW-480 cells. ChIP was performed as in FIGURE R-21 from two different populations of SW-480 cells either expressing snail1-HA or control plasmid. *CDH1* and *CY* were used as positive and negative controls respectively.

We then investigated whether the inhibitory loop that had been described in epithelial cells is functional in a cell line like the NIH-3T3 fibroblasts, which we have shown to respond to snail1 expression with a stimulation of *SNAI1* promoter.

As observed previously in the epithelial RWP-1 cells, snail1 P2A mutant protein accumulates to higher levels than the wild-type snail1 protein when expressed under the control of the -194/+59 *SNAI1* promoter, but not when expressed under the control of the constitutively active *CMV* promoter (**FIGURE R-27**).

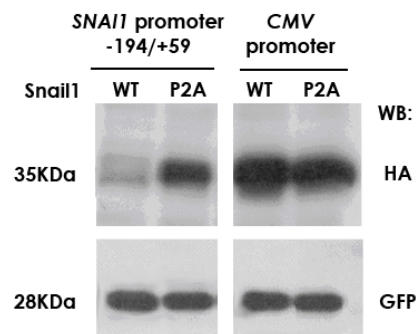


FIGURE R-27. The negative feed-back loop is functional in mesenchymal cells. NIH-3T3 cells were transfected with wild-type or P2A snail1 cDNAs under the control of *SNAI1* (-194/+59) promoter, or

Results

CMV promoter. Similar efficiencies of transfection were verified analyzing the levels of cotransfected GFP.

R.4.2. E-cadherin controls the activation of *SNAIL1* promoter by snail1.

Up-regulated expression of *SNAIL1* has been detected in several experimental conditions in which cells are forced to adopt a mesenchymal phenotype [80-85]. At this point of our study, we had realized that epithelial cells respond to snail1 transfection with a repression of its promoter, whereas a stimulatory loop is detected in cells with a more mesenchymal phenotype. In order to study this switch, we checked the effect of snail1 expression in our IEC-18 cell clones. We compared the control clone (epithelial phenotype) with an IEC-ILK clone (forced to undergo EMT by the expression of the integrin-linked kinase (ILK) cDNA). As a result of this ILK expression, and compared to IEC-18 control cells, IEC-ILK clones express lower levels of E-cadherin and higher levels of mesenchymal markers [85].

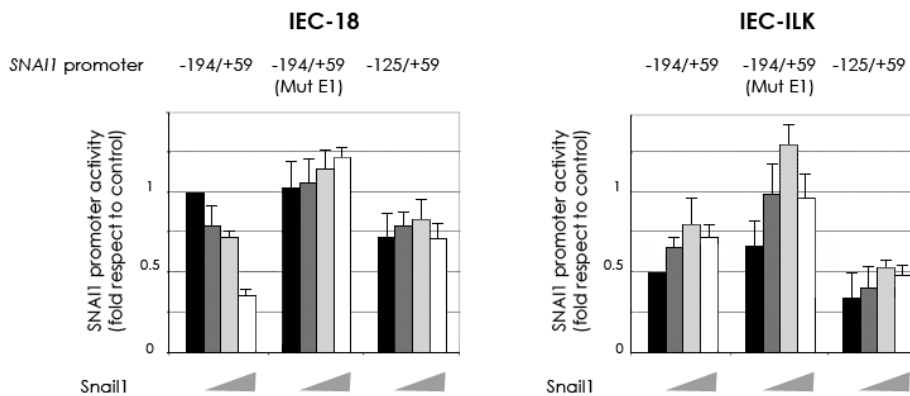


FIGURE R-28. ILK promotes EMT in IEC cells and switches *SNAIL1* responsiveness from repression to activation. The effects of snail1 cDNA transfection on the activity of the indicated promoters was analyzed by reporter assay either in IEC-18 (epithelial) or IEC-18-ILK (mesenchymal) cells. Though not shown, -194/+59 *SNAIL1* promoter showed a 2.5-fold higher activity in IEC-ILK than in IEC cells (as previously reported by Barberà et al. [85]).

As is shown in **FIGURE R-28**, the transfection of increasing amounts of snail1 cDNA to IEC-18 cells leads, as expected for epithelial cells (**FIGURE R-17** and **FIGURE R-18**), to a repression of -194/+59 *SNAI1* promoter, being this repression, again, dependent on the presence of the E-box. On the contrary, the performance of the experiment above in IEC-ILK cells, turns into an activation of -194/+59 *SNAI1* promoter which is, as described before (**FIGURE R-24** and **FIGURE R-25**), independent of the presence of the E-box. We conclude from this experiment that EMT is associated with a switch of the -194/+59 *SNAI1* promoter responsiveness that goes from an overall inhibition to an overall activation.

Because transcriptional repression of E-cadherin is the hallmark of EMT, we wondered whether the activation of the -194/+59 *SNAI1* promoter in mesenchymal cells could be reverted to the repression observed in epithelial cells by E-cadherin over-expression. To do so, reporter assays were performed in SW-480 cells. As shown in **FIGURE R-29A**, over-expression of E-cadherin slightly affects the basal activity of the -194/+59 *SNAI1* promoter, but totally prevents the activation triggered by snail1. In addition, mutation of the E-box only makes more evident the stimulatory effect induced by snail1 transfection and the subsequent blockage induced by E-cadherin. As a control, western blot analysis evidenced that, in our experimental conditions, E-cadherin expression does not affect the ectopic expression of snail1-HA (**FIGURE R-29B**).

Results

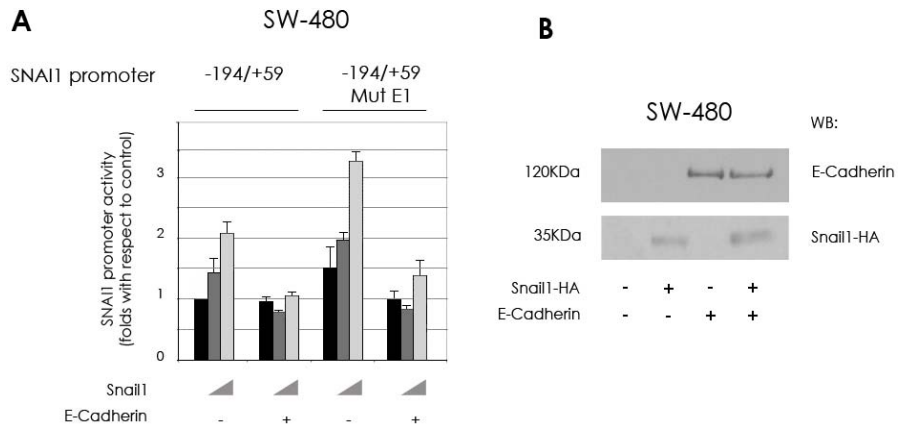


FIGURE R-29. Over-expression of E-cadherin blocks snail1 activation of -194/+59 *SNAIL1* promoter. (A) Snail1 induced stimulation of the -194/+58 *SNAIL1* promoter was determined by reporter assay in SW-480. Co-transfection with E-cadherin cDNA was performed when indicated. The figure shows the average \pm SD of three experiments performed. (B) Western blot analysis of the expression of E-cadherin and snail1-HA proteins in some of the samples from the reporter assay in (A) to show that E-cadherin over-expression does not affect snail1-HA over-expression and vice versa.

The relevance of E-cadherin in *SNAIL1* promoter regulation was also studied using stable transfectants. For this goal, we stably over-expressed E-cadherin and snail1-HA in SW-480 cells and checked the levels of the endogenous snail1 mRNA (taking advantage again of the fact that we can distinguish the ectopic snail1-HA (murine) from the endogenous human mRNA).

As shown in **FIGURE R-30A**, E-cadherin over-expression greatly reduced the levels of endogenous snail1 mRNA, either in control cells or in cells transfected with murine snail1-HA. By western blot, we also determined that E-cadherin over-expression does not modify the levels of ectopic snail1-HA. Similar results were obtained in the mesenchymal MiaPaca-2 cells although the effect of E-cadherin over-expression on snail1 mRNA was weaker; it prevented the stimulatory effect promoted by the ectopic expression of wild type snail1-HA (**FIGURE R-30B**).

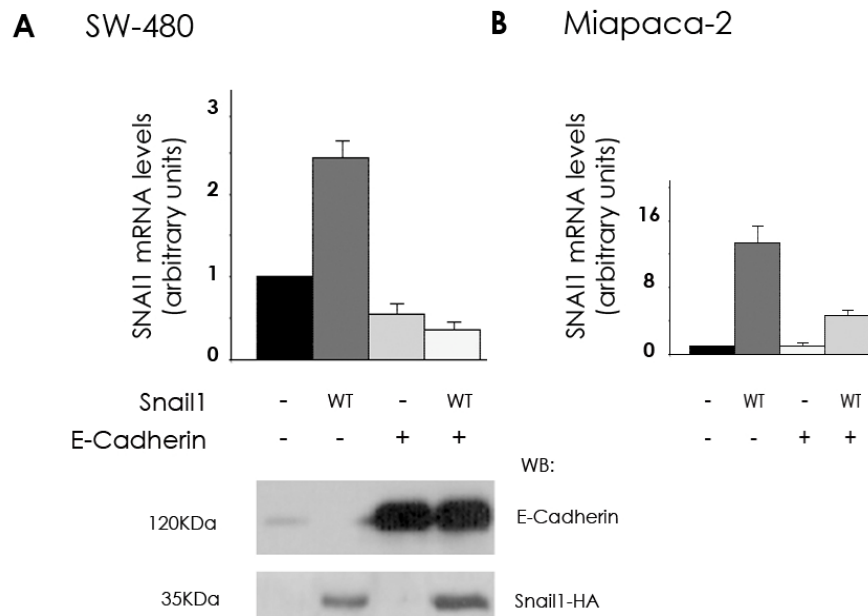


FIGURE R-30. Over-expression of E-cadherin blocks snail1 mRNA transcription. (A) Human endogenous snail1 mRNA was determined by qRT-PCR in SW-480 cells stably transfected either with murine snail1-HA cDNA, E-cadherin cDNA or both. The levels of E-cadherin and snail1-HA proteins are shown by western blot. (B) Same analysis that in (A) but performed in MiaPaca-2 cells.

R.4.3. Snail1 stimulation of *SNAIL1* promoter requires NF κ B transcriptional activity.

The activity of *SNAIL1* promoter has been reported to be modulated by ERK2 [59] and PI3K/NF κ B pathways [85]. Actually our results on *PTEN* repression by snail1 suggest a role for snail1 in the modulation of the PI3K pathway and therefore, in its own regulation through the Akt/NF κ B pathway. It is known that these signaling elements exert their function on different fragments within *SNAIL1* promoter. The ERK2-responsive element is located in the minimal -78/+59 *SNAIL1* promoter, whereas NF κ B requires additional upstream sequences [85]. Our experiments show that snail1 stimulation of *SNAIL1*

Results

promoter is maximal when the reporter assays are performed with the -125/+59 *SNAI1* promoter (FIGURE R-17). This suggests an important role for NFκB signaling in the transcriptional stimulation of *SNAI1* promoter that prompted us to study it into more detail. We checked the status of the NFκB signaling pathway by reporter assay in our SW-480 and Miapaca-2 mesenchymal cell models because in both of them (unlike our epithelial cell models) we had been able to prove the existence of a snail1-dependent positive feed-back loop on *SNAI1* promoter. As shown in FIGURE R-31, snail1 expressing cells (either SW-480 snail1 stable clones or Miapaca-2 cells transiently transfected with snail1 cDNA) display higher activity of the NFκB sensitive promoter (see Material & methods) than the respective control cells. Furthermore, the stimulation is totally (in the case of SW-480 cells) or partially (for MiaPaca-2 cells) abolished by co-expression of E-cadherin, mimicking the effects detected on *SNAI1* promoter.

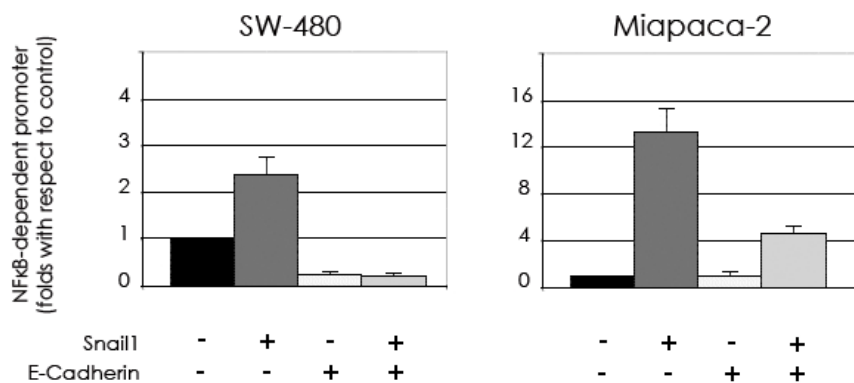


FIGURE R-31. NFκB signaling is increased in snail1 expressing cells and can be blocked by E-cadherin over-expression. The NF3 NFκB reporter plasmid was transfected to SW-480 cells stably transfected with snail1-HA cDNA, E-cadherin CDNA, or both. Miapaca-2 cells were transiently transfected with the NF3 NFκB reporter plasmid, together with the above indicated cDNAs.

To deepen into the relevance of NFκB signaling in the stimulation of the -194/+59 *SNAI1* promoter, we transfected a dominant negative form of RelA

(p65) lacking the transactivation domain (Δ RelA), that is, consisting only of the DNA-binding domain and performed reporter assays with the -194/+59 *SNAIL1* promoter and increasing amounts of *snail1*. As shown in **FIGURE R-32**, the transfection of this dominant negative form of Δ RelA (labeled Δ Rel in the figure) abrogated the stimulation of *SNAIL1* promoter by *snail1*, indicating that NF κ B signaling is relevant for activation of *SNAIL1* promoter triggered by *snail1*, that is for the existence of what we have called a “self-activation loop”.

SW-480

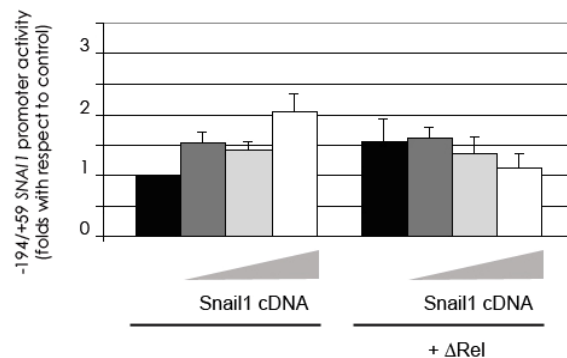


FIGURE R-32. *SNAIL1* induction by *snail1* requires NF κ B signaling. The stimulation of -194/+59 *SNAIL1* promoter by increasing amounts of pcDNA3-*snail1*-HA was determined in SW-480 cells in the presence of pcDNA3- Δ Rel (when indicated) or empty plasmid. The results are average \pm SD of three experiments performed.

R.4.4. Summary to Chapter 4.

We describe the existence of a stimulatory feed-back mechanism that controls *SNAIL1* expression in mesenchymal cells. This mechanism is not dependent on the integrity of a 5'-CACCTG-3' element located within the *SNAIL1* promoter, requires NF κ B signaling and can be blocked by E-cadherin.

MATERIALS & METHODS

MM.1. Cell culture.

Unless otherwise specified, all cells were grown in Dulbecco's modified Eagle's medium (DMEM) (Invitrogen) supplemented with 10% fetal bovine serum (FBS) (Biological Industries), 4.5 g/l glucose (Life Technologies), 2mM de glutamine, 56U/ml penicillin and 56µg/l streptomycin. The incubator atmosphere was 5% CO₂ and 95% air, and the temperature was held constant at 37°C.

- The generation and properties of **HT-29 M6 clones** stably transfected with snail1-HA has been previously described [31].
- To obtain **SW-480** double transfectants, pcDNA3 and pBATEM2 [140] (kindly provided by Dr. M. Takeichi, Kyoto University, Kyoto, Japan) plasmids were transfected to SW-480-ADH cells using Lipofectamine Plus (Invitrogen). Stable transfectants were obtained after selection with 2mg/ml G418 and screened by western blot and immunofluorescence. Those with higher E-cadherin expression were selected. Next, cells were retrovirally-transduced with the mouse snail1 cDNA tagged at the 3'-end with the sequence encoding the influenza hemagglutinin twelve-aminoacid peptide cloned into the pRV-IRES/gfp retroviral vector (ECADH-snail1-HA cells) or with the empty pRV-IRES/gfp vector (ECADH cells). Retroviral infection was performed as described [68]. Transduced (GFP+) cells were sorted using an Epics Altra HSS (Beckman-Coulter) and the pool of infected cells was used for further studies.
- The human pancreatic cancer cell line **RWP-1** was transfected with pcDNA3 or pcDNA3-snail1-HA using Lipofectamine Plus (Invitrogen) and stable clones were obtained after selection with 1mg/ml of G418. The isolated clones were screened by their characteristic morphological features and by western blot. **RWP-1 snail1-PTEN** clones were established

Materials & methods

as follows. The parental cell line was transfected with the DNA plasmids encoding the human PTEN or murine snail1-HA in pcDNA3 plasmid using the Lipofectamine Plus reagent. Cell transfectants were selected by treatment with 1mg/ml of G418 (for PTEN insertion) and hygromycin 250µg/ml for (snail1 insertion) as previously reported. The selected clones were analyzed by western blot.

- Use of other cell lines (**MiaPaca-2, RWP-1, SW-620, NIH-3T3, IEC-18, IEC-ILK**) has been previously reported [85].
- Madin Darby Canine Kidney (**MDCK**) is a well-established model of epithelial cells expressing wild-type PTEN. Ectopic expression of snail1 in this cell line has been reported to increase resistance to apoptosis induced by tumor necrosis factor α [63] as well as cause a complete EMT [30,31]. **MDCK-snail1(Ser → Ala)** and **MDCK-snail1 (S246A)** were established as previously reported for MDCK-snail1 [31]. **MDCK cells stably transfected with a short hairpin RNA (shRNA)** specific for snail1 (shsnail1), PTEN (shPTEN), or the corresponding control (shCtl) were established as follows. DNA from each of the five mission snail1 shRNA, PTEN short hairpin RNA (shRNA), or non-target control vectors (Sigma) was obtained, and 2 ng of an equimolar mix was transfected to control or snail1-expressing MDCK cells. Selection was performed for 5 days with puromycin (4µg/ml). PTEN or snail1-HA protein levels were analyzed by Western blotting as described below. Clones showing the lowest levels of ectopic snail1-HA or endogenous PTEN proteins were selected for further studies.

MM.2. DNA constructs and transfection.

- The cloning of the human **SNAIL1 promoter (-869/+59)** in pGL3 basic (Promega), had been previously described [85]. Note that a putative

snail1 binding site within the pGL3 plasmid was eliminated, and therefore re-named pGL3*.

- The human *SNAIL1* promoter constructs -194/+59, -125/+59 and -78/+59 have also been reported [85].
- The *SNAIL1* mutant promoters in the E-box3 (-869/+59 Mut E1 and -194/+59 Mut E1) had been reported [85] and were obtained using the QuickChange™ site-directed mutagenesis kit (Stratagene). The sense and antisense oligonucleotides used were, respectively:

5'-CCAGCAGCCGGCGAACCTACTCGGGGAGTG-3' and
5'-CACTCCCCGAGTAGGTCGCCGGCTGCTGG-3',
where the mutated oligonucleotides are displayed in bold.

- The cloning strategy for **pcDNA3 snail1**, **pcDNA3 snail1-P2A** and **pcDNA3 snail1 ΔZnF** mutants has been reported [31]. To confer pcDNA3 snail1 plasmid with the hygromycin resistance, the G418 cassette was deleted with SmaI/XbaI sites and a hygromycin cassette was cloned instead. The **pcDNA3 snail1 (Ser → Ala)** mutant has been reported before by our group [73]. The **pcDNA3 snail1-HA S246A** point mutant was obtained using the QuikChange site-directed mutagenesis kit (Stratagene) and pcDNA3-snail1 as the template. The sense primer used for the generation of the mutation was 5'-CGAACCTC**GCCCG**CATGTCC-3', where modified nucleotides with respect to the *SNAIL1* sequence (GenBank accession number gi: 6755586) are indicated in bold. All mutants were verified by sequencing.
- The preparation and use of **pcDNA3 snail2 (slug)** and **pcDNA3 zeb1** have previously been reported [66,73].

Materials & methods

- **pcDNA3 PTEN** was a kind gift of Dr. Puig and Dr. Larue, (Institut Curie, Paris, France).
- For GFP expression, **peGFP plasmid** (Clontech) was co-transfected in a ratio of 1 (peGFP) : 10 (cDNA of interest). Total amount of DNA transfected was decided following the Lipofectamine Plus reagent guidelines.
- **E-cadherin** over-expression was achieved by transfection of **pBATEM2** plasmid kindly provided by Dr. M. Takeichi (Kyoto University, Kyoto, Japan). Total amount of DNA transfected was decided following the Lipofectamine Plus reagent guidelines.
- **snail1-HA** or **snail1-P2A-HA** were also cloned in **pGL3* -194/+59 SNAIL1 promoter** or in **pGL3* -194/+59 (MUT E1) SNAIL1 promoter** vectors using the XbaI/HindIII sites present in pGL3* and removing the luciferase gene from the vector.
- **pcDNA3-ΔRelA** plasmid, where the DNA binding of RelA has been deleted, and NF3 reporter plasmid, consisting of three tandem RelA consensus binding elements cloned in pGL3 plasmid, were both kind gifts of Dr. M. Fresno (Universidad Autónoma de Madrid, Madrid, Spain) and used according to Lipofectamine Plus reagent guidelines.
- The **human PTEN promoter** (position numbers -883/+305; GeneCards database, NCBI: chromosome 10; positions 89612292 to 89613480) was cloned by PCR from HT-29 cell genomic DNA using high-fidelity polymerase (Pfx; Invitrogen) in pGL3* basic (Promega) (a putative snail1 binding site of the plasmid was eliminated). The sense oligonucleotide sequence was 5'-CGAGCTCCCGACGCCGCGAACC-3', and the antisense sequence was 5'-GGAAGATCTGAGAGGGGCTCCGGGC-3'.

- The **E1E2mut PTEN promoter** was obtained using the QuikChange site-directed mutagenesis kit (Stratagene). The sense oligonucleotide sequences used for performing the mutations in the two E-boxes present in the human -883/+305 *PTEN* promoter were '5-TACACTGAGCAGCGTGGT**AACCTAGTCCTTTT**CACCTGTGCACA-3' and '5-AGCGTGGTCACCTGGTCCTTT**AACCTATGCACAGGTAACCTCAGACTC**-3' for E-box1 and E-box2, respectively, where the mutated nucleotides are displayed in bold.

- **Interference of murine snail1 and human PTEN** was achieved by equimolar transfection of 5 MISSION shRNA (SHGLY-NM_011427 or SHGLY-NM_000314 respectively, Sigma). Total DNA transfected was used according to Lipofectamine Plus reagent guidelines.

MM.3. Fluorescence Activated Cell Sorter (FACS) analysis and determination of cell cycle and cell death.

1. **Irradiation:** cells were irradiated in a Schering (IBL 473C) ¹³⁷cesium irradiator. An initial dose-response study determined that a 20Gy γ radiation dose was required to induce apoptosis in 30 to 40% of control MDCK cells 48h after irradiation. RWP-1 cells were subjected to the same dose, but they were analyzed 24h after the irradiation since these cells are more sensitive to γ radiation.

2. **Trypsinization:** after the indicated times, the cells were trypsinized and counted. $1-3 \times 10^6$ cells were washed twice with ice-cold phosphate-buffered saline (PBS) and transferred to a 10ml tube.

Materials & methods

- 3. Centrifugation and cell pellet resuspension:** the 10ml tube was centrifuged (1000 rpm) for 5 minutes and the cellular pellet resuspended in 0,9ml of cold PBS.
- 4. Fixation:** cells were fixed by adding 2,1ml of ice-cold 100% ethanol (70% final percentage of ethanol) drop-wise. At this point, cells could be stored at 4°C or alternatively, stained for cytometry.
- 5. Washes:** before staining with propidium iodide, the cells were washed twice with PBS to remove the ethanol.
- 6. Staining:** after being washed, the fixed cells were treated with 1ml of solution PI (5µg/ml RNase A and 50µg/ml propidium iodide, in PBS) for 30min at 37°C or alternatively, for 48h at 4°C.
- 7. FACS analysis:** after the staining, the cells were analyzed with a FACScan flow cytometer and the results analyzed and discussed.

When indicated, instead of propidium iodide and FACS analysis, **tripan blue** staining was used after trypsinization and the percentage of blue (dieing) cells calculated. Note that n=200 cells were counted for each condition.

MM.4. Analysis of protein expression by Western Blot.

Analysis of endogenous snail1 and annexin 2 in NIH-3T3 cells (FIGURE R-15).

1. **Cell synchronization:** cells were grown in standard conditions for 24h and later on, deprived from serum (0.01% FBS) for 24h to synchronize them. To confirm the achievement of synchronization, an aliquot of cells was analyzed by flow cytometry (FACScan, Becton Dickinson) as previously described.
2. **Cell extract preparation:** at the indicated times after the addition of fresh medium (10% FBS), cells would be washed twice with PBS and total cell extracts obtained in SDS buffer (25mM Tris-HCl pH=7.6, 10mM KCl, 1mM EDTA, 1% SDS). Cell lysates were then centrifuged at 13,200 rpm during 15min and 60µg of the supernatant were used for Western Blot analysis.
3. **Electrophoresis and gel transfer:** samples were separated by 15% polyacrylamide gel electrophoresis (PAGE). After transference to a nitrocellulose membrane, the samples were analyzed by western blot.
4. **Western Blot:** before incubating with the primary antibodies, the nitrocellulose membranes were blocked with 5% non-fat milk in TBS-Tween for 1 hour at room temperature. Then, the membranes were incubated over-night at 4°C with, either a mouse anti-snail1 monoclonal antibody (mab) [94] diluted 1:40 in blocking solution. This antibody was prepared using as antigen a GST- murine-snail1 fusion protein and recognizes the N-regulatory domain of the protein (data not shown). As a loading control, the same samples were incubated for 30 minutes at room temperature with a polyclonal antiserum anti-annexin 2 (a kind gift of Dr. Navarro, IMIM, Barcelona, Spain). After three washes with TBS-Tween, the membranes were incubated for 1 hour with secondary antibodies (DAKO): anti-mouse-

Materials & methods

HRP for snail1 detection and anti-rabbit-HRP for annexin 2 detection. Both were used according to manufactures instructions. Next, the excess of secondary antibody was removed washing three times with TBS-Tween and then, the membranes were incubated for 1 minute with ECL solution (Pierce), containing a HRP substrate and the quimio-luminescence signal developed in a radiography film.

From now on, the details of the western blot technique will only be explained if different from those described above

Determination of the exogenous snail1 protein in transfected cells (FIGURE R-22B and FIGURE R-27):

1. **Transfection of DNA constructs:** for the determination of exogenous snail1 the following constructs:

pGL3* -194/+59 *SNAIL1* prom-snail1-HA
pGL3* -194/+59 (Mut E1) *SNAIL1* prom-snail1-HA
pGL3* -194/+59 *SNAIL1* prom-snail1-P2A-HA
pcDNA3-snail1-HA
pcDNA3-snail1-P2A-HA

were transfected together with 70ng of peGFP plasmid as internal control for transfection efficiency and according to Lipofectamine-Plus Reagent (Invitrogen) guidelines for 10mm plates.

2. **Protein expression analysis by western blot:** cell extracts were prepared and equal amounts of total cellular extracts were subjected to 15% polyacrylamide-SDS-PAGE and transferred to a nitrocellulose membrane. The blots were analyzed with the following primary antibodies diluted in TBS-T 5% non-fat milk: anti HA (rat mab, Roche 1:1000) or anti GFP (mouse

mab JL-8, Clontech 1:1000). Goat anti-rat-HRP and rabbit anti-mouse-HRP (DAKO) were used as secondary antibodies and blots were developed as described before.

Determination of exogenous E-cadherin protein in transfected cells (FIGURE R-14, FIGURE R-29 and FIGURE R-30).

20µg of each protein sample would be separated by 7% polyacrylamide-SDS-PAGE. Western blot against E-cadherin was performed with murine mabs (Transduction Laboratories, 1:1000) diluted in TBS-Tween 5% non-fat milk for 1 hour at room temperature. Rabbit anti-mouse (DAKO) was used as secondary antibody.

Determination of endogenous proteins in transfected cells (FIGURE R-1, FIGURE R-3, FIGURE R-5, FIGURE R-8 and FIGURE R-15).

1. **Cell extracts** were prepared as already indicated except for those for PTEN detection. Alternatively, cells would be lysed in cytosol buffer (10 mM Tris-HCl [pH 6.5], 150 mM NaCl, 0.01% saponin, 2 mM EDTA, 5 mM EGTA, supplemented with protease inhibitors). In the latter case, the lysing lasted 20 min on ice, to obtain the cytosolic fraction. Lysates were clarified by centrifugation, and supernatants were collected and quantified. 40µg of protein would be loaded for detection with the different antibodies.
2. **Western blot** analyses for detection of endogenous PTEN, P-Akt (Thr308), Akt, p21, P-p53 (Ser15) and caspase 3 (all of them rabbit immunoglobulins from Cell Signaling, 1:1000 in TBS-Tween 3% BSA, over-night at 4°C), α -actin (mouse, Sigma, 1:1000, 1 hour at room temperature), and annexin 2 (1:10000) 30 minutes at room temperature).

MM.5. Phosphorylated protein purification and western blot analysis (FIGURE R-8C).

1. **Purification of phosphorylated proteins:** the purification of phosphorylated proteins was performed using the PhosphoProtein purification kit (Qiagen) according to the manufacturer's instructions. Previous to purification, an aliquot of each sample (input) was collected as a control.
2. **Western blot:** input samples and samples eluted from the columns were separated by 15% polyacrylamide-SDS-PAGE and western blot against the HA epitope or P-p53 (Ser15) performed as described above.

MM.6. Immunofluorescence protocol (FIGURE R-8B, FIGURE R-9 and FIGURE R-12).

Immunofluorescence was basically performed as previously described in [73].

1. **Seeding:** cells were plated on sterile glass coverslips to achieve 70% confluence 24h later.
2. **Irradiation:** when needed, the coverslips would be irradiated as explained above and fixed at the indicated time-points.
3. **Fixation:** cells would be washed twice with PBS and then fixed with 4% paraformaldehyde for 10 minutes.
4. **Permeabilization:** this step was done by incubation with 1% sodium dodecyl sulfate (SDS) in PBS for 10 minutes.
5. **Blocking:** the coverslips were incubated for 1h at room temperature with PBS (0.1% saponin and 1% BSA).

6. **Primary antibody hybridization**: affinity-purified mouse monoclonal anti-smail1 antibody [94] was diluted 1:10 in PBS (1% BSA, 0.1% saponin) and incubated for 1h at room temperature.
7. **Washes**: three times with PBS.
8. **Secondary antibody hybridization**: the binding of the primary antibody was detected with anti-mouse Alexa 488 (Molecular Probes, 1:5000) immunoglobulins, incubated for 1 hour at room temperature and in the dark.
9. **Washes**: three times with PBS.
10. **Mounting**: the coverslips would then be mounted on slides and on top of a Fluoromount-G (SouthernBiotech) drop and allowed to dry in the dark.
11. **Confocal microscopy**: fluorescence was detected with a TCS-SP2 Leica confocal microscope.

MM.7. Luciferase reporter assays (FIGURE R-6A, FIGURE R-17, FIGURE R-18, FIGURE R-24, FIGURE R-25, FIGURE R-28, FIGURE R-29, FIGURE R-31 and FIGURE R-32).

1. **Cell seeding**: 6×10^4 cells per well would be seeded in a 24-well plate. Each transfection condition would be duplicated.
2. **Transfection**: 24 hours after seeding, the cells would be transfected with 100ng of the indicated human *SMAIL1* promoter, NF3 NFkB reporter or empty PGL3* vector. Alternatively, 25ng of *PTEN* promoters or empty PGL3* would be transfected. When indicated, co-transfection was performed with either:

- (a). 50ng of pBATEM2 (mouse E-cadherin) or
- (b). increasing amounts (0.1, 1 and 10ng) of pcDNA3-snail1 (wild type), snail1 mutant constructs (pcDNA3-snail1-P2A or pcDNA3-snail1 Δ ZnF), pcDNA3snail2 (slug), pcDNA3-zeb1) or
- (c). 50ng of pcDNA3 Δ RelA

1ng of SV40-Renilla luciferase plasmid was always co-transfected as a control for transfection efficiency.

3. **Firefly and renilla readouts:** the expression of *Firefly* and *Renilla* luciferases was analyzed 48 hours post-transfection, according to manufacturer's instructions. All experimental results would then be corrected by transfection efficiency (*Renilla* readouts) and by empty PGL* readouts.

MM.8. Chromatin immunoprecipitation assay (ChIP).

1. **Cell culture:** cells would be seeded in 150mm plates and allowed to grow for 48 hours. Before achieving confluence, the plates, with approximately $10e^6$ cells, were used for the ChIP experiment.
2. **Cross-linking:** the plates would first be washed twice with cold PBS and then treated for 4 minutes with 1% formaldehyde in DMEM without FBS. After this time, the cross-linking would be stopped by addition of 250 μ l of glycine 2,5M at room temperature.
3. **Washes and lysing:** the plates would then be washed twice with cold PBS and initially lysed in buffer IP2 (50mM Tris [pH 8], 2mM EDTA, 10% glycerol supplemented with protease inhibitors), transferred to an eppendorf tube and centrifuged for 15 min at maximum speed. The pellet (containing the

nuclei) was resuspended in buffer IP1 (50mM Tris [pH 8], 10mM EDTA, 1% SDS) for 10 min at room temperature.

4. **Sonication:** the cell lysates would then be sonicated (40%, 10 pulses, Branson) to generate 200 to 1500bp DNA fragments.
5. **Pre-clearing:** a 3hours pre-clearing with 50µl of protein G-agarose (Boehringer) would be done to remove unspecific binding of proteins to the resin. This step was performed at 4°C and the samples were all the time agitated.
6. **Immunoprecipitation:** the protein G used in the pre-clearing would be removed centrifuging the samples for 1 minute at 2000 rpm. The supernatant would then be recovered and transferred to a new tube, where the immunoprecipitation took place. This step was carried out over-night in IP1 buffer with either:
 - (a). antibodies against the HA epitope (Roche, 1:100) or
 - (b). monoclonal antibody (MAb) anti-snail1 (1:100) [94] or
 - (c). anti-p53 (catalog no. sc-126X; Santa Cruz, 1:60)

Note that, in parallel, the same samples were always immunoprecipitated with an irrelevant immunoglobulin G (IgG) (Sigma) in IP-dilution buffer (16.7mM Tris [pH 8], 167mM NaCl, 1.2mM EDTA, 1.1% Triton X-100, 0.01% SDS).

The following morning, 50µl of protein G-agarose would be added to each sample and left in agitation for 1 hour at 4°C. Later, the content of each tube would be transferred to a column to perform the washes.

7. **Washes:** subsequent washes of the columns would be performed with ice-cold buffers. First, three washes with low salt buffer (0,1% SDS, 1% Triton X-100, 2mM EDTA, 20mM Tris pH 8, 150mM NaCl), the, three washes with high salt buffer (0,1% SDS, 1% Triton X-100, 2mM EDTA, 20mM Tris pH 8, 500mM NaCl) and finally, three washes with LiCl buffer (250mM LiCl, 1% NP-40, 1% sodium deoxycholate, 1mM EDTA, 10mM tris pH 8).

After this step, the columns would be spined at 1000rpm to be dried and quickly prepared for elution.

8. **Elution:** the samples in the columns would then be treated with elution buffer (100mM Na₂CO₃, 1% SDS) and incubated at 65°C over-night to reverse formaldehyde cross-linking.
9. **DNA sequences purification:** the following morning, the columns were centrifuge for 1min at maximum speed and the eluted samples purified using the GFX PCR DNA and Gel Band Purification Kit (Amersham).
10. **Quantitative or alternatively, semi-quantitative PCR amplification of the DNA sequences:** the presence of promoter regions in the eluted DNA was detected as follows:

Semi-quantitative PCR amplification (FIGURE R-21 and FIGURE R-26): the presence of *SNAIL1*, *CDH1* and *CY* promoters among snail1 immunoprecipitated sequences was performed with the following specific primers:

- **Human SNAIL1 promoter (GI: 9650757):**
5'GGCGCACCTGCTCGGGGAGTG-3' and
5'-GCCGATTCGCGCAGCA-3',
corresponding to sequences 20603-20623 and 20811-20796,
respectively.

- **Human CDH1 (E-Cadherin) promoter (GI: 29568028):**
5'-ACTCCAGGCTAGAGGGTCAC-3' and
5'-CCGCAAGCTCACAGGTGCTTGCAGTTCC-3'
corresponding to sequences 80636-80655 and 80853-80825,
respectively.
- **Human Cy (Cyclophilin A), (GI:5882164):**
5'-ATGGTCAACCCCACCGTG-3' and
5'-TGCAATCCAGCTAGGCATG-3',
corresponding to sequences 137-154 and 800-782, respectively.

Quantitative PCR SYBR green (Qiagen) amplification (FIGURE R-7): PCR and data collection were performed on an ABI Prism 7900HT system. Binding of snail1 to the promoters of interest was calculated as a percentage of input. Where indicated, the data are presented as enrichment levels of snail1 at *PTEN* promoter [141]. These values correspond to changes in input percentage over that of the control (percentage obtained with the irrelevant IgG). The PCR was performed with the following specific primers:

- ***PTEN* promoter** (GeneCards database, NCBI36:10):
5'-CCGTGCATTCCTCTACAC-3' and
5'-GAGGCGAGGATAACGAGCTA-3'
corresponding to positions 89612787 to 89612807 and 89612979 to 89612959, respectively.

These two oligonucleotides, corresponding to the human sequence, also amplify the *Canis familiaris PTEN* gene, (determined by sequencing the amplified fragment).

- ***Human CDH1 promoter*** (GeneCards database, NCBI: 16) primers, 5'-ACTCCAGGCTAGAGGGTCAC-3' and 5'-GTCGGGCCGGGCTGGAGC-3', corresponding to positions 67328516 to 67328536 and 67328774 to 67328756, respectively.
- **irrelevant sequence**, the amplification of this sequence corresponding to the genomic sequence (GeneCards database, NCBI36:17) was performed with the following primers:

5'-ACTCCAGGCTAGAGGGTCAC-3' and
5'-CCGCAAGCTCACAGGTGCTTGCAGTTCC-3',
corresponding to positions 7328681 to 7328700 and 7328744
to 7328724, respectively.

MM.9. Gel retardation assays (FIGURE R-6, FIGURE R-13 and FIGURE R-20).

Assays were performed essentially as previously described in [31].

- 1. Generation of the recombinant proteins:** BL21 bacterial strain was transformed with either pGEX-snail1, PGEX-snail1 (S246A) or PGEX-GST. 3-5h later, the bacteria were induced to generate recombinant protein according to manufacturer's instruction (Pharmacia). Lysates were tested for protein expression in a polyacrylamide gel stained with coomassie blue.
- 2. Oligonucleotide annealing:** double stranded oligonucleotide corresponding to the -173/-125 sequence of *SNAIL1* promoter or, alternatively, to the -533/-557 sequence of the human *PTEN* promoter were used for these experiments. Sense and antisense oligonucleotides were annealed in TEN buffer (10mM Tris pH 7.5, 50mM NaCl, EDTA 1mM) for 5 minutes at 95°C, and then left alone to achieve room temperature over-night.
- 3. Probe radiolabeling:** annealed probes were next labeled with ³²P. T4 Polynucleotide Kinase (Gibco) was used according to manufacturer's instructions and the excess of unlabeled probe was removed with the use of "MicroSpin™ G-25 Columns" (Amersham Pharmacia Biotech Inc). One microliter was used for cpm counting quantification.
- 4. Gel retardation assays:** 200ng of recombinant protein were incubated at 4°C for 30min with the radiolabeled oligonucleotide (50e³ cpm) in Binding Buffer (20mM HEPES [pH 7.6], 150mM KCl, 3mM MgCl₂, 10% glycerol, 0.2mM

ZnSO₄, 0.3 mg/ml BSA and 500ng Poli-(dl-dC), (as a negative competitor for unspecific binding).

5. **Competition:** when indicated, competition with 10-fold or 100-fold of not radiolabeled probe (cold) was performed. Competition was either performed with wild type probe or with mutant cold probes where the snail1 binding sites (CACCTG) were mutated to AACCTA.
6. **Polyacrylamide-SDS-PAGE:** samples were run in a 4% gel (19:1, acrilamye : bisacrilamye in Tris-Borat 22mM) for 1 hour at 35 mV in TBX1 buffer and developed by autoradiography.

MM.10. Semi quantitative and quantitative RT-PCR analysis.

1. **Cell culture:** cells would be seeded in 10mm plates and allowed to grow for 48 hours. Before achieving confluence, the plates were lysed for mRNA extraction.
2. **Total mRNA extraction:** mRNA was extracted using the Gen Elute Mammalian total RNA kit (Sigma) according to manufacturer's instructions. Samples would then be quantified.

Semi-quantitative analysis (FIGURE R-19):

- **exogenous murine** or **endogenous human snail1** mRNA analysis was performed as previously described [66] using 28 and 29 cycles respectively. Annealing temperature: 55°C.
- **Hypoxanthine-Guanine Phosphoribosyl Transferase (HPRT)** was analyzed using oligonucleotides 5'-GGCCAGACTTTGTTGGATTG-3'

and 5'-TGCGCTCATCTTAGGCTTTGT-3' for 29 cycles. Annealing temperature: 55°C.

Quantitative determination of mRNA levels was performed in triplicate using QuantiTect SYBR Green RT-PCR (Qiagen).

- **exogenous murine *snail1* (FIGURE R-15) or endogenous human *SNAIL1* (FIGURE R-19, FIGURE R-23 and FIGURE R-30)** RNA analysis was performed with the same oligonucleotides that those used for semi-quantitative analysis. RT-PCR and data collection were performed on ABI PRISM 7900HT. All quantization were normalized to an endogenous control. Annealing temperature: 55°C.
- ***Canis familiaris PTEN mRNA (FIGURE R-1)***, (Gene-Cards database, BROADD1: 26) was analyzed with the following primers: 5'-CTTTGAGTCCCTCAGCCAT-3' and 5'-GGTTCCTCTGGCCTGGTA-3' (positions 39919229 to 39919249 and 39922770 to 39922750, respectively). Annealing temperature: 58°C.
- ***Homo sapiens PTEN mRNA (FIGURE R-3)*** was analyzed with 5'-AATCCTCAGTTTGTGGTCT-3' and 5'-GGTAACGGCTGAGGGA-3' (chromosome 10; positions 89707598 to 89707614 and 89707699 to 89707675, respectively). Annealing temperature: 58°C.
- ***Canis familiaris PUMA mRNA (FIGURE R-7)*** was analyzed with 5'-AGTGAGGGCTGAGGACCTG-3' and 5'-TGA CTGGAGGGAGGAAGAGA-3' (chromosome 1, positions 111631415 to 111631434 and 111633041 to 111633022, respectively). Annealing temperature: 55°C.
- **Hypoxanthine-guanine phosphoribosyl transferase (HPRT) mRNA** (GeneCards database, NCBI36:X) was analyzed as an internal control by using oligonucleotides 5'-GGCCAGACTTTGTTGGATTG-3' and 5'-TGCGCTCATCTTAGGCTTTGT-3' (133460124 to 133460316 and 133461784 to 133461763, respectively). Annealing temperature: 55°C.

The relative quantization value for each target gene compared to the calibrator for that target is expressed as $2^{-(Ct-Cc)}$ (Ct and Cc are the mean threshold cycle differences after normalizing to HPTR).

MM.11. Immunohistochemistry (FIGURE R-4).

1. **Paraffin sections re-hydration:** paraffin sections obtained from wild-type or snail1-deficient murine embryos (7.5 days postcoitum [dpc]), [49] were deparaffined with three subsequent washes in xylene and then re-hydrated by subsequent washes (5 minutes each) in 100% ethanol, 90% ethanol, 70% ethanol and finally, distilled water.
2. **Antigenic recovery:** the step of antigenic recovery was carried out in a pressure cooker for 15min in Tris-EDTA buffer pH 9.
3. **Endogenous peroxidase blocking:** after the antigenic recovery, the sections were treatment with 4% H₂O₂ in PBS for 15 minutes to remove the endogenous peroxidase.
4. **Washes and blocking:** after washing twice with PBS, the sections were blocked for 1 hour in PBS 3% BSA.
5. **Primary antibody:** the incubation with the primary antibodies was performed over-night at 4°C. The following MAbs were diluted in PBS 1% BSA: anti-phospho-Thr308 Akt (1:50), anti-PTEN (1:50), both from Cell Signaling, and anti-snail1 [94] (1:50).
6. **Washes:** six washes (5 minutes each) with PBS were done to remove the excess of primary antibody.

Materials & methods

7. **Secondary antibody:** immunohistochemical staining was performed using the EnVision system (DakoCytomation) following the manufacturer's instructions. The EnVision System employs goat anti-mouse and goat anti-rabbit immunoglobulins conjugated to a horseradish peroxidase (HRP) and were incubated for 1 hour at 27°C.
8. **Washes:** six washes (5 minutes each) with PBS were done to remove the excess of secondary antibody.
9. **Development:** the sections were finally developed adding DAB (EnVision) substrate for 5 minutes.
10. **Hematoxylin staining:** to be able to distinguish certain tissue structures, the sections were treated for 5 minutes with hematoxylin solution (20% hematoxylin in PBS). Next, the sections were washed with water to remove the excess of hematoxylin.
11. **Sections de-hydration:** the sections were finally de-hydrated by subsequent washes (5 minutes each) with 50% ethanol, 70% ethanol, 100% ethanol and finally, xylene.
12. **Section mounting:** last, the sections were covered with coverslips and sealed with DPX (BDH Chemicals).

MM.12.

“In vitro” phosphorylation assays (FIGURE R-10).

Alternatively, 1µg of snail1-GST or snail1(S246A)-GST was incubated for the indicated times in Kinase Buffer (20mM HEPES ph 8.0, 5mM MgCl₂, 1mM DTT) in the presence of 75 U of recombinant active Chk1 (stressgen, PPK-418), 0,5µl of ³²P-ATP (Amersham, 300µCi/ml) and 100µM cold ATP in a final volume of 20µl. The samples were resolved in a 12% polyacrylamide gel and developed by autoradiography. In parallel, coomassie staining of the gel was performed to show the presence of equal amounts of recombinant protein in each condition.

DISCUSSION

The PI3K/Akt/PTEN interplay and how snail1 fits in between to promote cell survival.

Before the beginning of our work, the role of snail family members in the acquisition of resistance against several types of programmed cell death had been already reported (see introduction, p51). In this work, we show that snail1 over-expression preserves epithelial MDCK cells from γ radiation induced apoptosis. Our results show that, 48h after irradiation, the percentage of MDCK-snail1 cells displaying characteristics of programmed cell death is significantly lower than in control cells.

This observation is in accordance with the results published by other authors using the same MDCK cellular model, in which snail1 protects from induced apoptosis, in this case, by the withdrawal of survival factors or by other pro-apoptotic signals [63]. Furthermore, these authors have also shown that snail1 induces the activation of PI3K and Akt, a pathway that confers resistance to apoptosis. Our results are in agreement with these observations and locate signaling through the PI3K/Akt as a central element in EMT, as it will be discussed. The main components of this pathway have been mentioned in the introduction and are summarized in **FIGURE D-1**. Note that signaling through this pathway is triggered by extrinsic signals, leading to the activation of receptor tyrosine kinases (RTKs) and PI3K that results in the generation of phosphatidylinositol 3,4,5-triphosphate (PIP3) generation, a membrane bound second messenger that recruits Akt/PKB.

The Akt family consists of three highly homologous serine/threonine kinases (Akt 1, Akt 2, and Akt 3), which, in unstimulated cells, reside mainly in the cytosol [142]. Once recruited to the cell membrane by PIP3, Akt is phosphorylated at Thr308 by 3-phosphoinositide-dependent protein kinase 1 (PDK1) [143]. Although Thr308 phosphorylation partially activates Akt, full activation requires additional phosphorylation at Ser473 by PDK2, a kinase for

Discussion

which the molecular identity remains to be established. After activation, Akt translocates to the cytosol and nucleus to phosphorylate its substrates [144], (FIGURE D-1).

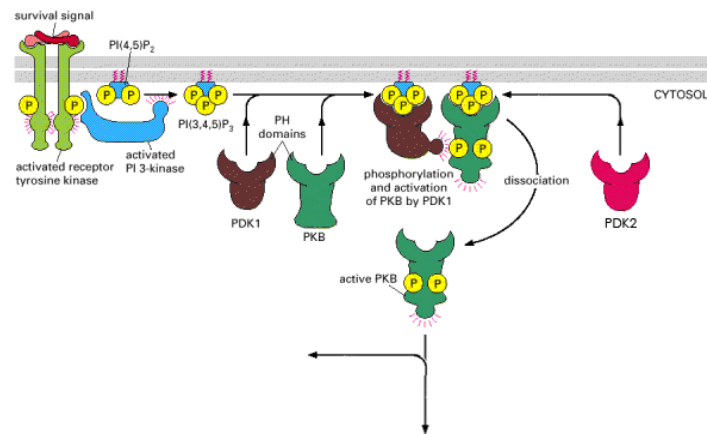


FIGURE D-1. PI3K pathway: Akt activation. Upon extracellular binding of a survival signal, RTK recruits and activates PI3K, which generates PI(3,4,5)P₃ (not shown), that serves as docking sites for Akt/PKB and PDK1. The binding of Akt/PKB to the inositol lipid alters its conformation so that the protein can be phosphorylated and activated by PDK1. The activated Akt/PKB dissociates from the plasma membrane and elicits downstream effects either in the cytoplasm or in the nucleus. Adapted from: www.ncbi.nlm.nih.gov/books/bv.fcgi?highlight=apoptosis&rid=mboc4.figgrp.2865

Once activated, Akt functions as a molecular switch that has been shown to target many different proteins and cellular pathways. Among those, and directly related to the matter of our work, Akt is extremely relevant for the suppression of apoptosis [145] and cell survival [146-148], a fact that converts its negative modulator, PTEN, in its gatekeeper. Apoptosis can be suppressed by Akt in three different ways:

- i. Akt can directly cause the inhibition of factors that are involved in the execution of apoptosis, such as BAD [149,150], caspases 9 [151] or ASK1 [152].

- ii. Akt can influence the transcriptional control needed during apoptosis. Akt promotes the activity of NF κ B facilitating the degradation of its inhibitor, I κ B [153]. Thus, NF κ B target genes (among them and as our results confirm, *SNAIL1*) result up-regulated. Akt also prevents p53 nuclear localization [154], inactivating its pro-apoptotic transcriptional function. Although we never tested p53 localization in our experiments, this, together with snail1 expression, could explain the repression of PTEN in our cells. Note, however, that no significant changes in p53-classical-target gene p21^{WAF1/CIP1} have been detected, suggesting that p53 function is not affected in our cells.
- iii. Akt can indirectly influence apoptosis impacting on cellular signaling relating to metabolic regulation [147].

In addition to promoting cell survival, Akt also targets p27^{KIP1} and p21^{WAF1/CIP1}, two well characterized inhibitors of the cell cycle (by cdk2/cyclin inhibition), that upon Akt phosphorylation are inactivated. In accordance to that, Akt also prevents cell cycle arrest by the phosphorylation of GSK3 β , which results in snail1 stabilization, suggesting the existence of a snail1 positive feed-back loop in which snail1 repression of *PTEN* would result in increased snail1 expression through GSK3 β inhibition.

Remains to be clarified, however, that Akt activation depends on growth factors binding to membrane RTK receptors and PI3K signaling [155]. This activation mechanism itself cannot explain the role for Akt in cell survival; however sustained PI3K/Akt signalling can occur as a result of PTEN function miss-regulation. PTEN, a lipid phosphatase that negatively modulates PI3K/Akt pathway arises then as the molecular switch for Akt function. Our results showing that snail1 down-regulates PTEN in response to DNA damage and promotes Akt activation, not only explain previous reported observations, but also open a whole new line of research that links snail1-promoted EMT with

Discussion

PI3K-promoted cell survival, cell proliferation and cell migration, the paradigm of cancer disease.

Our data show increased levels of active Akt in MDCK-snail1 and RWP-1-snail1 cells, with regard to the respective controls, and identify a critical effector of this pathway, *PTEN*, as a direct snail1 target gene. The relevance of this observation was straight forward clear to us. Though relatively recently discovered, PTEN is nowadays considered a key protein for the cell. As a matter of fact, PTEN was first identified as candidate tumor suppressor gene at chromosome 10q23 in a number of advanced tumors [156,157]. Shortly after its discovery, and to scientists surprise, PTEN was shown to demonstrate phosphatase activity against the phospholipid products of PI3K activity, namely phosphatidylinositol 3,4,5-triphosphate (PIP3) [158], although it was also shown to dephosphorylate protein substrates such as focal adhesion kinase (FAK) [159] and itself [160]. This dual capacity, intriguing as it is, is still a matter of study. Most of the PTEN-mediated effects are the result of its ability to dephosphorylate PIP3 and antagonize PI3K [161,162], although recent evidences indicate other functions beyond this lipid phosphatase activity, mainly related to cell migration restrain [160] or p53 stabilization [163].

Since it was first described to date, mutations and deletions in *PTEN* gene have been described for a wide variety of tumors, although in some advanced carcinomas, the silencing of this gene seems to be controlled epigenetically [164-166]. Furthermore, germline mutations result in Cowden Disease, Bannayan-Zonana syndrome, and Lhermitte-Duclos disease, all characterized by the development of hamartomas [167].

Such a relevance of PTEN as a tumor suppressor gene can be explained by four reasons [168]: (1) the existence of no other homologous family member that compensates the loss of PTEN, (2) the high potential of the

PI3K/Akt pathway for tumorigenesis, (3) the complex network of interactions with p53 and (4) the genomic instability derived from its loss.

No wonder the relevance of PTEN, it is obvious that it must be tightly regulated. At a transcriptional level, beyond the first idea of a constitutive expression, *PTEN* promoter has been shown to bind several transcription factors. Positive and negative modulators of *PTEN* transcription have been identified. Among them, p53 has been shown to be the most relevant activator of *PTEN* promoter and necessary for p53-mediated apoptosis [134]. Note that our *PTEN* promoter cloned fragment is 1188bp long (-883/+305) with respect to the transcription start point (see annex, p177). Within this promoter region and besides the snail1 binding site, we find the p53 responsive element. We have shown that snail1 binding to *PTEN* promoter not only represses its activity, but also impairs p53 binding and the subsequent transcriptional activation. The consequences could go beyond this observation if one takes into account the existence of a PTEN-p53 positive feed back loop. Several studies in MEFs have shown that, besides p53-mediated increase of PTEN, the latter is necessary for p53-mediated apoptosis. Conversely, PTEN forms a complex with p53 and protects p53 from MDM2-induced ubiquitinylation and degradation [163,169,170]. Moreover, the binding of PTEN to p53 increases DNA binding of p53 [163]. In conclusion, PTEN and p53 generate a positive feed back loop in which the loss of any of them results in the secondary loss of the other. As a result, snail1-impaired binding of p53 to *PTEN* promoter could result, in the end, in both PTEN and p53 loss, and in turn, in no induction of apoptosis, that is, in cell survival. However, in the early phases of MDCK response to γ radiation, such a positive feed-back loop seem not to be operating because in contrast to PTEN, no significant differences in p53 or its transcriptional target p21^{WAF1/CIP1} have been observed. It could then be that such a mechanism requires more time than we reflect in our experiments (48h) or that such a mechanism does not apply for MDCK cells.

Discussion

Moreover, *PTEN* transcription has been shown to be inhibited through NF κ B binding to a site in *PTEN* promoter [171], resulting in cell survival. In this report, they show mitogen-activated protein kinase kinase-4 (MKK-4) to modulate NF κ B activity; however the mechanism for repression remains unclear. It will then be worth studying the interplay between NF κ B and snail1 in *PTEN* promoter. Our results provide a possible explanation in which NF κ B negative effects on *PTEN* would not be a consequence of NF κ B binding to *PTEN* promoter, but the result of snail1 expression in response to NF κ B [84].

In accordance to this hypothesis, and regarding sequences upstream from the -1188 position (remember that our cloned promoter fragment goes from the -1188 to the +305 position with respect to the transcription start point), TGF β has also been reported to repress *PTEN* in cancer cells. The underlying mechanism, however, remains unclear. In some pancreatic cellular models, TGF β positively modulates *PTEN* promoter in a SMAD dependent manner and negatively modulates *PTEN* promoter in a SMAD independent manner [172]. Furthermore, in a mesangial cell model for diabetic disease, *PTEN* down-regulation has been proven to be TGF β -dependent.

TGF β has also been shown to induce *SNAIL1*. It could be then possible that TGF β inhibitory effects on *PTEN* are the result of snail1 induction. In fact, we hypothesized that this mechanism would not necessarily be specific for snail1, but that other EMT-promoting-E-box-binding transcription factors could be modulating *PTEN* as well. However, here we show that snail1 repression of *PTEN* promoter is somehow specific. Other members of the snail family of transcription factors, such as snail2 (slug) or zeb1, are not able to repress *PTEN* promoter, at least with the same specificity than snail1. In this regard, some other E-box binding transcription factors remain to be studied. In fact, the role of other bHLH factors such as E47 is worth being studied in the context of *PTEN* promoter regulation.

Taken together, it seems as though two signaling pathways involved in *SNAIL1* transcription (NF κ B and TGF β) could converge in snail1 and result in the direct repression of *PTEN* [173], allowing the cell to by-pass apoptosis in response to DNA damage.

Regarding the mechanism underlying *PTEN* transcriptional regulation by snail1, the requirements are not different from other snail1 target genes such as *CDH1* or *VDR*. The inhibitory effect is dependent on the integrity of two 5'-CACCTG-3' boxes present in the proximal human promoter and mutation of these two elements precludes the association of recombinant snail1 to this sequence and the snail1-mediated repression of *PTEN* promoter transcription. Note however, that only one of the boxes is present in every mammal *PTEN* promoter studied (mouse, rat, rabbit, dog), suggesting that, probably, only one of these elements within *PTEN* promoter is involved in repression. In accordance with this observation, our reporter assays show that snail1 effect on *PTEN* promoter is lower than that observed for *CDH1* promoter (bearing three functional E-boxes) [31], but comparable to the effect of snail1 on other target genes such as the vitamin D receptor [68].

The overview of *PTEN* transcriptional control can be summarized as follows. The role of *PTEN* transcriptional activators is strongly linked to cell response to cell damage. In this sense, it is not surprising that, upon radiation or other apoptotic stimulus, the cell response to this insult requires *PTEN* transcription to trigger apoptosis. The fact that p53 activates this promoter suggests a critical role for *PTEN* in the cell response to DNA damage beyond that exerted by p53 itself. On the contrary, the role of *PTEN* transcriptional repressors is not so obvious. Mostly, their necessity responds to the existence of negative feed-back loops than somehow restrict *PTEN* transcription, and to the importance of cell survival promotion in certain cells that are, for instance, migrating through hostile tissues to reach their target. The potential danger of *PTEN* miss-regulation is therefore evident. *PTEN* activators loss of function or,

Discussion

alternatively, PTEN repressors gain of function can results in inappropriate cell resistance to apoptosis, one of the classical hallmarks of cancer disease.

In the context of this study, our results show that snail1 prevents the up-regulation of PTEN phosphatase, abrogating PTEN modulation of apoptosis. In accordance to this, restoration of PTEN protein in several carcinoma cell lines can induce apoptosis directly or in cooperation with apoptotic stimuli [174]. In our MDCK cells, the ectopic manipulation of PTEN levels affects the capability of the cells to undergo apoptosis. Depletion of PTEN by interferent RNA increases the resistance of MDCK cells to γ radiation-induced apoptosis, indicating the role of PTEN and, therefore, of snail1 in the control of cell death (**FIGURE R-5A**). However, in the absence of PTEN, snail1 expression is still able to promote resistance to apoptosis (**FIGURE R-5B**). These results indicate that snail1's role in promoting cell survival are not only limited to *PTEN* repression, but are very likely dependent on an unknown cellular element. Chances are this additional mechanism to be dependent on snail1 transcriptional repression of target genes. In this direction, the search for novel snail1 target genes within the apoptotic pathway could undercover new functions for snail1 in the control of cell survival and apoptosis.

Taken together, it is the tempting to hypothesize that snail1 expression in advanced tumors could be responsible for *PTEN* silencing and cancer progression in those tumors where PTEN loss of function is the result of epigenetic events. However, snail1 limited expression in specific areas of epithelial tumors [94] suggests that snail1 might be involved in the down-regulation of *PTEN* in cells that are undergoing EMT, more than in the permanent silencing of this gene. However, snail1 has been proposed to be an EMT initiator whereas other transcription factors, for instance zeb1, have been proposed to maintain the mesenchymal phenotype. It could be then possible that this same mechanism applies to PTEN down-regulation so that, along a temporal sequence, different repressors bind *PTEN* promoter through

the two E-boxes and maintain its expression shut or even promote *PTEN* promoter silencing. Although terminal silencing of E-cadherin by DNA methylation has been reported [175,176], we have not been able to show that snail1 promotes DNA methylation of E-cadherin promoter. Moreover, we have shown that snail recruits polycomb to either E-cadherin or *PTEN* promoter. The consequence of polycomb recruitment to target genes is gene repression. In addition to that, note that, in some cases, polycomb recruitment is required, prior to DNA methylation [177]. It could be then possible that, as shown for E-cadherin (N.Herranz and S.Peiró, unpublished data), snail1 recruitment of polycomb to *PTEN* promoter could not only repress its transcription, but promote long-term gene silencing by DNA methylation. This issue should be addressed by DNA methylation experiments on *PTEN* promoter to check if snail1 or other EMT-related transcription factors somehow change the DNA methylation pattern of this gene.

Though not addressed in this work, note that PTEN can also be modulated at a post-translational level. Among the proteins that modulate PTEN function we find GSK3 β [178]. The phosphorylation of PTEN by GSK3 β within the C-terminal tail is thought to decrease membrane association and protein activity [179]. This provides us with an additional molecular mechanism by which once snail1 has repressed *PTEN*, the subsequent activation of Akt could result in GSK3 β inhibition and increased stabilization of snail1. That is, a positive feed-back loop by which PTEN protein activity would be abolished not only at a transcriptional level, but also at a post-translational level.

The importance of snail1-induced resistance to apoptosis.

The importance of apoptosis in tissue homeostasis and tumor progression has been already discussed in the introduction and above. To test the snail1-induced resistance to apoptosis in our MDCK cells, we chose γ radiation as a highly reproducible elicitor of the intrinsic apoptotic pathway (FIGURE I-17). The

Discussion

ability of γ radiation to induce apoptosis is obvious if we take into account the fact that cells exposed to ionizing radiation develop double-strand breaks (DSB) that can result in chromosomal rearrangements and in the worst case scenario, in cancer.

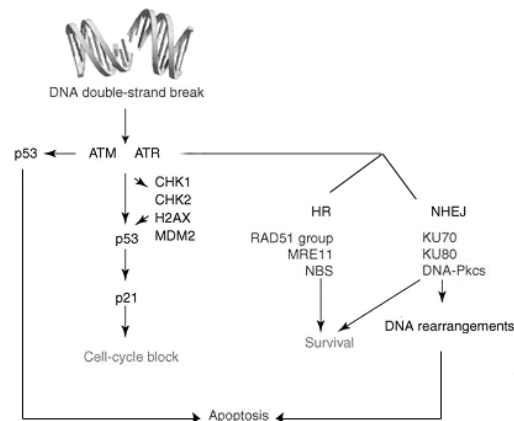


FIGURE D-2. Cell response to ionizing radiation. Downstream effectors of ATM/ATR in response to double-strand breaks, adapted from [180].

Under these conditions, the machinery of the cell activates the DNA damage response (DDR) that mediates cell cycle arrest, DNA repair and, if the damage is severe, apoptosis. The first sensor to be activated in response to ionizing radiation is the MRN complex (MRE11, Rad50 and NBS1) [181]. Next, the central players of DDR (ATM, ATR and DNA-PK) are recruited to the DNA lesions where they promote DNA repair (**FIGURE D-2**). Among these three kinases, ATM and DNA-PK seem to respond to DSB whereas ATR responds to single strand damage and stalled replication forks [182]. Upon MRN complex recruitment of ATM to the DSB [183], ATM is activated by a still ambiguous mechanism. Downstream effects of ATM are (1) the phosphorylation of histone H2AX, (2) DNA repair and (3) the activation of the effector kinases Chk1 and Chk2, that are responsible for the activation of the cell cycle DNA-damage checkpoint [184,185] and for p53 tumor suppressor gene activation.

In our assays, MDCK-snail1 cells respond normally to γ radiation, with an arrest in cell proliferation, and accumulate in G₂ phase (**FIGURE R-2**). This arrest is accompanied by an up-regulation of active p53 that is not affected by the expression of snail1 (**FIGURE R-1**). These results are in agreement with previous results showing that ectopic expression of snail1 in mouse embryo fibroblasts does not modify the expression of p53 after radiation [131] and similar to those observed for snail2 [186]. Consequently, as already discussed, the transfection of snail1 to our MDCK cells does not prevent the up-regulation of two p53 target genes, p21^{WAF1/CIP1} (**FIGURE R-1**) and PUMA (**FIGURE R-7D**) in response to γ radiation. Although p53 up-regulation in response to γ radiation is not impaired, our results demonstrate that snail1 binding to *PTEN* promoter precludes the binding of p53 (**FIGURE R-7C**), and the subsequent activation of *PTEN* during apoptosis. This observation suggests a specific role for snail1 in the modulation of *PTEN* that is not shared with other p53 target genes analyzed. Remains to be elucidated the potential role in the repression of other p53-target genes by snail1 and whether this mechanism could somehow go up against the effects of p53 in response to cell damage, as has been proven to be the case of PTEN. The consequences of this observation in the case of PTEN have already been described (p141). The existence of a positive p53-PTEN feed back loop could imply that snail1 binding to *PTEN* promoter results in the secondary loss of p53 by the breakage of the positive loop. This could explain the controversy generated with respect of snail1 effects on p53. Some authors have reported that snail1 can alter the response of MCF-7 cells to the genotoxic stress induced by doxorubicin, preventing the increase in p53 [70]. They show that the observed reduction in p53 protein levels after expression of snail1 or snail2 results from the combinatorial effects of three distinct mechanisms: a decline in p53 mRNA levels, increased MDM2-mediated turnover, and the loss of stabilizing modifications from the ATM kinase. It is then possible that the discrepancy between their results and those of others relays in the effect of doxorubicin on this p53-PTEN positive feed-back loop and in the robustness of it in different cell types. p53 secondary loss by snail1-

Discussion

mediated *PTEN* repression could explain the decrease in p53 mRNA [187] and the increased MDM2-mediated turnover [188]. However, remains to be explained the effects of snail1 in the loss of ATM kinase stabilization. It is also possible that snail1 modulates doxorubicin export or, alternatively, that the factor responsible for p53 repression is not snail1 by itself, but another transcriptional repressor specifically induced by snail1 in MCF-7 and not in other cells. Finally it could also be possible that different apoptotic stimulus elicit different responses. Our experiments have been mainly performed in MDCK cells in response to γ radiation. Obviously, remains to be clarified whether our experiments can be reproduced in other cell lines or to the induction of apoptosis by stimulus different from γ radiation, such as UV radiation, doxorubicin, etoposide or TNF α .

However, our results have been recently backed by a report in which snail2 (slug) is shown to repress *PUMA* [128]. The similarities existent between the regulation of *PTEN* by snail1 and that of *PUMA* by snail2 during the process of cell death are noteworthy. As named above, neither they nor we have found interference between either snail1 or snail2 with p53 expression or stabilization after γ radiation. Moreover, p21^{WAF1/CIP1} p53-target gene is neither affected by the presence of snail1 or snail2, suggesting that their ability to affect survival does not entail impaired p53 activation. As a matter of fact, both *PTEN* and *PUMA* are normally induced by p53 after γ irradiation, and in both cases, this induction is prevented in cells expressing snail1 (in the case of *PTEN*) or expressing snail2 (in the case of *PUMA*). This observation is in both cases due to direct binding of snail1 or snail2 to *PTEN* and *PUMA* respectively. Therefore, we hypothesized that these two pathways could be somehow interconnected. Remarkably, both *PTEN* and *PUMA* genes show a high specificity for their corresponding repressors, since snail2 cannot repress *PTEN* promoter (**FIGURE R-6**) and snail1 does not affects *PUMA* mRNA up-regulation in response to irradiation (**FIGURE R-7D**). These findings predict that Snail

superfamily members may protect cells from programmed cell death through different mechanisms in different biological contexts.

In addition to that, it has also been shown that snail2 itself is a target of p53 [128]. Upon γ radiation of wild type MEF cells, snail2 protein levels increase, however, this increase is not observed in p53^{-/-} MEF cells, suggesting a role for p53 in snail2 induction. They show that such an increase in snail2 protein levels responds to p53 transactivation of snail2 transcription and locate two p53 responsive elements (RE1 and RE2) able to bind p53 "in vivo". The relevance of such an observation remains unclear and seems apparently contradictory, due to the fact that p53 is not expected to activate potentially dangerous genes, such as snail2 (slug). However, the authors claim this to be a negative feed-back loop, responsible for *PUMA* down-regulation once apoptosis needs to be abrogated. Indeed, the human *SNAI1* promoter also has three putative p53 responsive elements determined with p53MH software [189] (see p181 for more information). Their relevance remains to be elucidated, but they could be good candidates for p53 transcriptional regulation of snail1 in a similar manner to that observed for snail2 (slug). **FIGURE D-3** summarizes the parallelisms between snail1 effects on *PTEN* and snail2 effects on *PUMA* and the subsequent cell consequences.

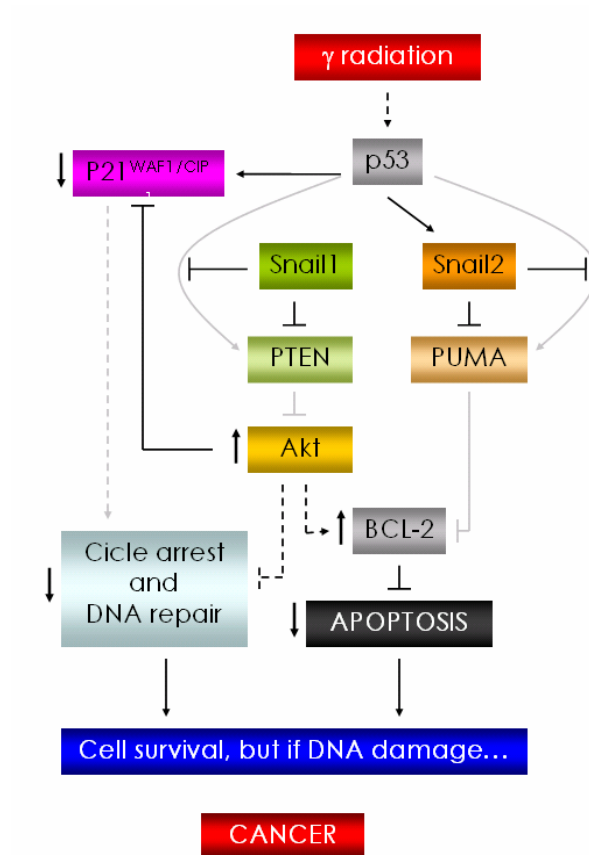


FIGURE D-3. Model of the conserved pathway by which snail1 and snail2 antagonize p53-mediated apoptosis. Direct effects are displayed with continuous lines whereas indirect effects are displayed with discontinuous lines. Light grey lines display down-regulated signaling due to upstream effects.

Besides the putative role of p53 in the transcriptional up-regulation of *SNAI1*, ectopic snail1 protein levels up-regulation was detected after γ radiation. Such observation can only respond to a post-translational effect in response to DNA damage, due to the absence of *SNAI1* promoter regions upstream of snail1 cDNA. Noteworthy, this increase in snail1 protein is transient; for instance, in our MDCK cells and 8h after γ irradiation, the total levels of snail1 protein are lower than those before the insult (FIGURE R-8A).

However, this down-regulation of snail1 is not reflected in a concomitant decrease in snail1-*PTEN* promoter association. This apparent discrepancy might be explained by the fact that the binding of snail1 to DNA stabilizes this protein, probably because it prevents its export from the nucleus. Therefore, we expect that *PTEN* promoter-bound snail1 is not an efficient target for the nuclear export machinery and therefore, the repression of this promoter is maintained even after the cellular levels of snail1 have returned to the basal levels.

The mechanism for this accumulation remains unclear. PAK1 has been reported to phosphorylate snail1 in S246, preventing its export from the nucleus and its subsequent degradation [78]. Moreover, this protein kinase (the γ isoform) is activated after DNA damage in fibroblasts [137] and has been shown to down-regulate several pro-apoptotic pathways (reviewed in [190]). However, unlike published data, here we report that S246A snail1 mutant is located in the nucleus, and not in the cytoplasm (**FIGURE R-12**). In response to γ radiation, this mutant also accumulates as the wild type protein (**FIGURE R-14**), suggesting that phosphorylation in S246 is not the mechanism leading to snail1 stabilization.

Although other molecular mechanisms different from phosphorylation have been considered, the fact that snail1 phosphorylation happens shortly after γ irradiation prompted us to study the role of DDR kinases in snail1 stabilization. The existence of a Chk1 putative site within the N-terminus of snail1 made Chk1 a good kinase candidate. Our results, however, show that Chk1 is able to phosphorylate snail1 within the C-terminus domain of snail1 and suggest more than one target residues. In vitro phosphorylation of the S246A snail1 mutant by Chk1 is much lower than that of the wild type, though still existent (**FIGURE R-10**). In the present, new experiments are being done in order to characterize what residues within snail1 might be phosphorylated by Chk1. With respect to S246A mutant and the discrepancies among our results

Discussion

and those of Yang et al, we show that the mutation in S246 impairs snail1 DNA binding (FIGURE R-13). This would explain the incapability of this mutant to repress its target genes in a mechanism different from its subcellular localization. Indeed, this incapability of S246A snail1 mutant to bind DNA makes it more accessible for the export machinery, resulting in a higher presence of snail1 in the cytoplasm and its subsequent degradation. In fact, *PTEN* repression and Akt activation by snail could, in turn, result into snail1 stabilization via inhibition of GSK3 β and the subsequent impairment of snail1 degradation by the proteasome, a mechanism worth studying in the future.

The complex network of *SNAIL1* transcriptional control.

In this work, we show that snail1 can directly repress its own expression. The molecular mechanism is based in the generation of a self-inhibitory loop by which snail1 protein binds to an E-box sequence present in *SNAIL1* promoter. It is worth indicating that this E-box is conserved in other *snail1* promoters sequenced (mouse, rat, macaque, bovine, *Drosophila melanogaster* and zebrafish). The existence of feed-back loops has been shown to be particularly relevant in several cell pathways involved in embryo development [191]. They provide the cell with the capability of buffering, allowing corrections of the cell system in response to perturbations. In the case of *SNAIL1*, the existence of a negative feed-back loop may be relevant for controlling snail1 expression in epithelial cells; avoiding transient increases in the pathways involved in *SNAIL1* transcription (ERK2 and PI3K), that could end up triggering a sustained activation of snail1 protein and the subsequent phenotypic changes. In this sense, the existence of the inhibitory loop would be responsible for the stability of *SNAIL1* transcription; preventing undesired effects such as those related to the inhibition of cell growth, a general effect observed when snail1 is over-expressed in several cell lines [63].

In any case, our results are in agreement with the existent evidence indicating that self-regulation of their own promoters might be a general property of the snail family members. Snail2 (slug) can also bind to an E-box present in its own promoter [192] but, unexpectedly, this binding results in *SNAI2* transcriptional activation. Note, however, that according to our results, snail2 does not affect *SNAI1* promoter activity (not shown).

The reported feed-back control, although being able to restrict *SNAI1* transcription, can be over-run by a potent stimulation of ERK2 and PI3K pathways, resulting in a substantial activation of *SNAI1* transcription and the subsequent EMT. Therefore, we hypothesize that this feed-back control of snail1 expression creates a threshold that, once overcome, generates a sustained expression of snail1. In any case, the existence of this feed-back pathway helps us understand the intrinsic cell networks controlling EMT during early embryo development and provide new insights to explain the induction of this transition during tumor invasion.

Besides the fact that snail1 can repress its own expression by direct binding to *SNAI1* promoter, here we have shown that snail can also activate its own promoter. This observation is restricted to those cell lines with fibroblastic characteristics and low levels of E-cadherin. However, we show that this positive feed-back loop would be coordinated with the negative self-regulation already described for this gene. In agreement with this, the mutation of the functional E-box in *SNAI1* promoter increases the activity of this promoter not only in epithelial cells (where the negative loop is active), but also in these fibroblastic cells with low levels of E-cadherin (**FIGURE R-24**) (where the positive feed-back loop is active), indicating that the negative feed-back control is somehow still active under these conditions.

As it has been mentioned before, negative feed-back loops protect the system against slight perturbation. Opposite to that, positive feed-back loops

Discussion

allow a small initial change or cellular stimulus to be amplified and become irreversible [191], such as is EMT. In accordance to this, we propose a role for *SNAI1* promoter in the integration of upstream signals promoted by the FGF and TGF β families, shown to be required for the induction of snail1 expression during development [27,54]. Unfortunately, in the context of tumor progression, we believe that this positive feed-back loop and its subsequent amplification can be related to the snail1 over-expression in the latest stages of tumorigenesis.

So far we have shown that *SNAI1* is subjected to context-dependent negative and positive feed-back regulation. A possible consequence of this situation is the appearance of *SNAI1* oscillatory patterns of expression [191]. In accordance with our results, note that positive and negative feed-back mechanisms have been involved in the establishment of left-right asymmetry, a process that requires snail1 [193,194]. In this respect, snail1 mRNA levels (in mouse) and snail2 mRNA levels (in chick) have been shown to display an oscillatory pattern within the presomitic mesoderm (PSM), that requires Wnt and FGF signaling [195]. Both genes are rhythmically transcribed with a periodicity (120 minutes) that matches the budding off of epithelial somites and miss-regulation of the endogenous transcription by ectopic over-expression results in the disruption of the segmentation clock.

Our results also suggest a central role for E-cadherin in the switch from *SNAI1* negative to positive transcriptional responsiveness. We show that E-cadherin loss of function is necessary for the existence of the self-activation loop. E-cadherin over-expression disrupts the positive loop (**FIGURE R-29**) and results in *SNAI1* transcriptional repression (**FIGURE R-30**). This implies an important consequence, the assumption that the flow of information from snail1 towards E-cadherin is bi-directional, in other words, (1) snail1 blocks *CDH1* transcription but (2) E-cadherin also modifies *SNAI1* expression. Snail1 down-regulation of *CDH1* is a good characterized molecular mechanism in which snail1 direct

binding to *CDH1* promotes its transcriptional repression [30,31]. On the other hand, E-cadherin effects on *SNAI1* remain to be elucidated. Our results are in agreement with the evidences showing that E-cadherin negatively controls the activity of NF κ B [196], in fact, we have recently published that E-cadherin and other cell adhesion components, associate with NF κ B p65 subunit and abrogate NF κ B transcriptional activity (G. Solanas and J. Baulida, unpublished data). As a matter of fact, this novel mechanism explains the transcriptional behavior of several mesenchymal genes such as fibronectin (FN) and lymphoid enhancer binding factor 1 (LEF1) and could also apply for the case of *SNAI1*. In accordance with this hypothesis, in mesenchymal cells, we show that E-cadherin over-expression blocks the snail1-induced positive feed-back loop concomitantly with the low activity of NF3 NF κ B reporter (**FIGURE R-31**). Moreover, we show the requirement of NF κ B signaling for the existence of the positive feed-back. Transfection of a dominant negative RelA construct lacking the transactivation domain (Δ p65) completely blocks *SNAI1* transcriptional activation by snail1 (**FIGURE R-32B**).

Although NF κ B signaling arises as a pivotal event in the modulation of *SNAI1*, other elements different from it, might also be relevant for *SNAI1* transcription. For instance, in keratinocytes, snail1 has been shown to activate ERK2, whereas reintroduction of E-cadherin in these cells restores the activity of this kinase to basal levels [197]. The molecular link, however, remains unclear and worth being studied.

Moreover, in the last years several reports have evidenced new factors, other than snail1, also capable to down-regulate E-cadherin. These can act, either by direct repression of gene expression, as is the case of snail2 (slug), zeb1 and zeb2, E12/E47 and twist [37,41,49,198,199]; or inducing E-cadherin degradation, as is the case of Hakai [200]. Our results suggest that these factors cooperate somehow with snail in the modulation of *SNAI1* and, therefore, are involved in the maintenance of the negative feed-loop and

Discussion

the amplification of *SNAIL1* expression once the switch to the positive feedback loop occurs.

New strategies by which snail1 promotes EMT and cell migration.

The sequence of events leading to EMT has been already discussed in the introduction. In addition to that, the role of snail1 in promoting EMT has also been addressed. Here we show a novel mechanism involving PI3K pathway that links snail1 to EMT. As it has been discussed above, in spite of its important role in the modulation of apoptosis, not much is known about the mechanisms controlling the expression of PTEN. Other than p53 direct binding and activation of *PTEN* promoter, PTEN levels are negatively regulated by TGF β and NF κ B, two factors that stimulate *SNAIL1* transcription in MDCK and other epithelial cells [59,85]. As our results show, a consequence of *PTEN* repression by snail1 is the activation of Akt. Intriguingly, the over-expression of Akt has also been shown to induce EMT through the NF κ B-dependent activation of *SNAIL1* [84,201]. Therefore, a sustained stimulation of *SNAIL1* in tumor cells facilitates the creation of this positive loop up-regulating the activity of NF κ B transcriptional factor and thus, that of *SNAIL1*. Our results reinforce the existence of a positive feedback loop wherein snail1 induces its own transcription and links the acquisition of mesenchymal-like phenotypic changes during EMT with the ability of these cells to survive under conditions that otherwise would lead to cell death.

Moreover, in addition to its role in the modulation of apoptosis, PTEN reconstitution or over-expression inhibits cell migration [202] and prevents tumoral cell invasion [203]. PTEN-null mouse fibroblasts show increased rates of migration, a property that is reversed by the reintroduction of PTEN [204]. PTEN has also been related to chemotaxis in single-cell migration studies performed in *Dictyostelium discoideum*. This mechanism seems to be dependent on PI3K signaling. In fact, cells that lack PTEN are defective in chemotaxis, showing

increased, rapid and erratic protrusions [205,206]. It has been shown that GFP-tagged-PTEN localization changes in the presence of a chemoattractant gradient. Whereas PI3K localizes in the leading edge, towards the chemoattractant, PTEN accumulates in the rear. The complexity of these observations increases since the contribution of PTEN lipid and protein phosphatase activities to them remains to be elucidated. Several mechanisms by which PTEN reduces cell migration have been proposed. PTEN impairs cell migration in a PIP3-dependent manner through repression of Cdc42 and Rac1 signaling. In addition to that, the two most well characterized "in vitro" protein targets of PTEN, FAK and Shc, are also involved in cell migration. In the cellular context, both can be activated by integrins and other receptors and whereas FAK-p130^{Cas} signaling pathway is involved in directional migration and increase focal contacts, Shc and its downstream effectors are related to random motility (**FIGURE D-4**). However, the physiological role of FAK and Shc dephosphorylation by PTEN remains unclear. PTEN KO cells fail to show changes in FAK phosphorylation or ERK activity [204,207]. Interestingly, "in vivo" experiments point to a different behavior of PTEN (G129E) mutant, which abrogates most PTEN activity against PIP3 but keeps protein phosphatase activity [208], and that of catalytic inactive PTEN (C124A) mutant, suggesting an additional role for PTEN protein phosphatase activity in cell spreading [209].

Discussion

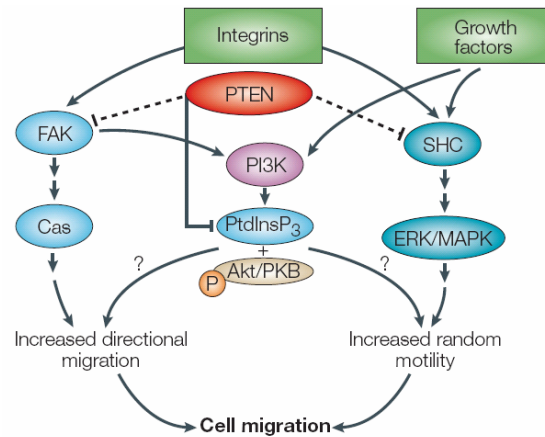
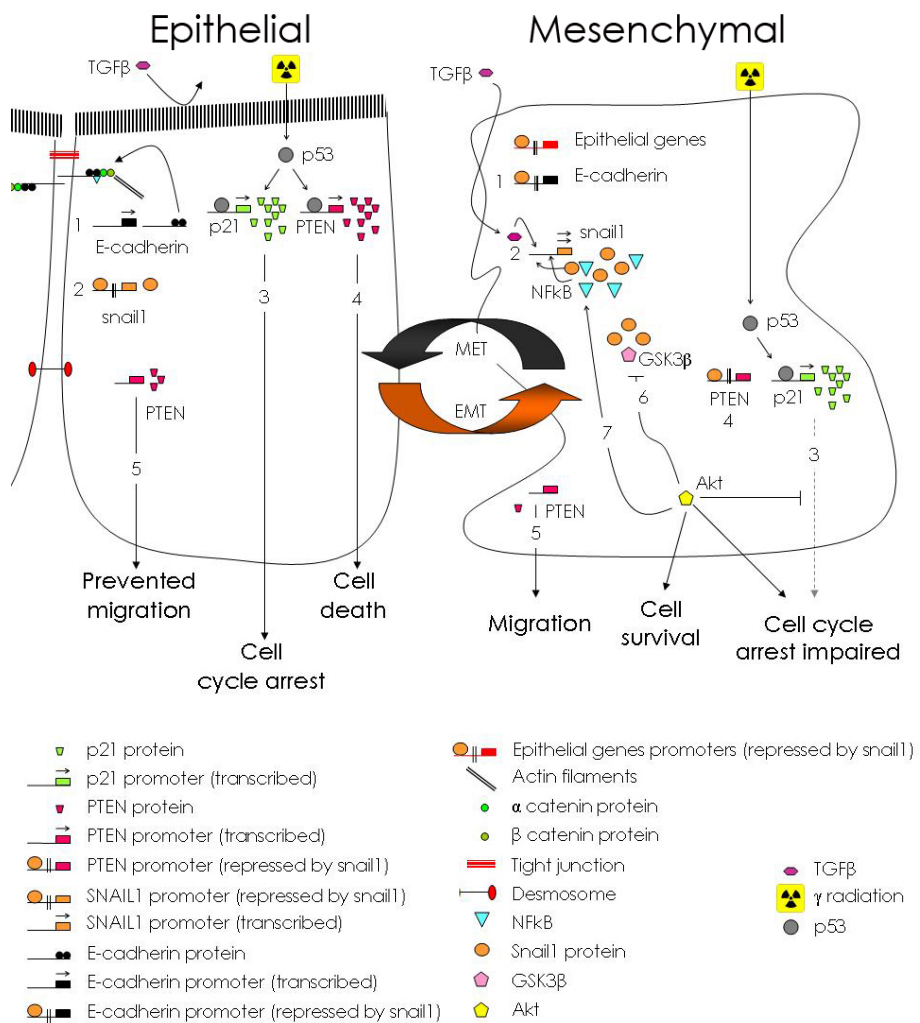


FIGURE D-4. Effects of PTEN on migration and motility. PTEN effects on cell migration relay in three different pathways: (1) the FAK-p130Cas pathway, (2) the SHC-MAPK pathway and (3) the Akt (Cdc42, Rac1) pathway.

Finally, increasing evidence suggest a role for several cellular phosphatases, not only in the regulation of matrix-cell adhesion, but also in the regulation of cell-cell adhesion. Prior to migration, cell-cell contacts need to be disrupted. During EMT, E-cadherin gets phosphorylated. This results in β -catenin release in the cytoplasm. Protein tyrosine phosphatase LAR (PTP-LAR) abolishes E-cadherin phosphorylation and promotes the stability of the epithelial phenotype [210]. Connected to this, PTEN promotes GSK3 β activation and the subsequent degradation of β -catenin [211] and snail1. It could be then possible that PTEN phosphatase activity affects E-cadherin phosphorylation status, abrogating β -catenin release and repressing EMT. On the contrary, snail1 repression of *PTEN* during EMT would by-pass these putative effects of PTEN on E-cadherin, and the subsequent activation of Akt would stabilize snail1 and β -catenin through the inactivation of GSK3 β and the activation of NF κ B signaling. Unfortunately, in the context of cancer disease, the combination of high levels of snail1 in the leading edges of tumors, together with PTEN-loss-derived increased motility and survival can result in tumor progression and secondary metastasis.

General overview of this thesis: our working model.

The following scheme and lines try to summarize our results in a simplified model. For the sake of a better understanding, the relationship between the different players is only shown as activation or repression, no matter what their relationship (direct or indirect) may be. Further information is given below for specific details.



Discussion

Note the indicated numbers that will guide the reader through the scheme.

1. EMT promotes the loss of the well-established cell-to-cell contacts. Tight junctions and desmosomes are represented in the epithelial cell in red, whereas E-cadherin adherens junctions are represented in black (●●) and green (●●). Note NFκB (▲) recruitment to the adherens junctions. Unlike the epithelial cell, the mesenchymal cell has lost cell-to-cell contacts because of the transcriptional repression of E-cadherin (by snail1) and other epithelial genes.
2. Snail1 (●) is slightly expressed in epithelial cells, where transient increases in TGFβ signaling are buffered by snail1 repression of its own promoter, remaining snail1 protein levels low and constant. As a result of EMT, *SNAIL1* expression increases. This results in E-cadherin and other epithelial genes transcriptional repression. As a result of E-cadherin repression, the adherens junctions disappear and the pool of intracellular NFκB, together with other signaling pathways, such as TGFβ (●), increase *SNAIL1* transcription. Under these conditions snail1 positive feed-back loop on its promoter is active and fosters not only *SNAIL1* transcription, but also that of other mesenchymal genes.
3. In the context of cell damage by γ radiation, the cell response differs according to snail1 protein levels. In cells with low levels of snail1 (epithelial), γ radiation promotes p53 (●) activation and the subsequent transcription of p53-targets: p21 (■) and PTEN (■), resulting in **cell cycle arrest (3)** and **apoptosis (4)** respectively. In contrast, mesenchymal cell with high levels of snail1 (●) respond alike. Although p53-p21 signaling seems to be working normally (3), snail1 repression of *PTEN* promoter (4) abrogates cell death and promotes Akt activation (●). Akt downstream effects result in NFκB (▲) activation and snail1 transcriptional activation (7), GSK3β (●) inhibition and snail1 stabilization (6), **cell cycle progression (3)** and **cell survival (4)**.

4. Finally, snail1 effects on PTEN and the consequences of *PTEN* repression in cell migration are also represented. In cells with low levels of snail and good cell-to-cell adhesion, PTEN expression contributes to prevent **cell migration (5)**. In the contrary, in mesenchymal cells with low or absent cell-to cell adhesion and high levels of snail1, *PTEN* repression results in **increased migration (5)**.

ANNEX

A.1. ChIP-on-CHIP.

- 1. Chromatin immunoprecipitation:** SW-480 control and SW-480 snail1 cells were subjected to regular ChIP (p124). Immunoprecipitation was carried out with antibodies against the HA epitope (Roche). The protocol followed was the "The Chromatin immunoprecipitation Protocol for Microarray Analysis" from the UHN Microarray Centre that can be consulted below.
- 2. CpG Rich array hybridization:** DNA fragments eluted from the SW-480 control would first be labeled in green and DNA fragments eluted from SW-480 snail1 would be labeled in red. Hybridization was performed in a Human CpG-island 12K Array (HCGI12K) containing 12,192 CpG-island clones from the Wellcome Trust Sanger Institute. The analysis of the hybridization results was performed taking into consideration the fact that any sequence located downstream of a CpG-island and followed by a gene was considered as a promoter (Note the potential error of this assumption). The whole protocol was performed twice. In the second row, DNA fragments eluted from the SW-480 control would first be labeled in red and DNA fragments eluted from SW-480 snail1 would be labeled in green (opposite from the first row), to avoid artifacts due to the different fluorescent dye. Those DNA sequences consistently enriched in SW-480 snail1 cells in the two experiments are listed below.

scaled I2ratio(M)_CpG_H1	scaled I2ratio(M)_CpG_H1	scaled I2ratio(M)_H12k_C1	scaled I2ratio(M)_H12k_C1	scaled I2ratio(M)_H12k_C1	scaled average aminocall	scaled average random pr	scaled average all	unscaled I2ratio(M)_CpG	unscaled I2ratio(M)_CpG	unscaled I2ratio(M)_H12k	unscaled I2ratio(M)_H12k	unscaled average aminocall	unscaled average random	unscaled average all	ID	Name	Conversion	gene (100% match)	definition (100% match)	probe type	Hartwell sequence file	Symbol SOURCE annotated	definition (Hartwell)	Acc No (Hartwell)	probe type	gene content annotation	#chr/prank	scaled Mean Fold_change	scaled B	scaled B rank	scaled N good spots	scaled N defect Cy5	scaled N defect Cy3
0	0	0	0	0	0	0	0	0	0	0	0	0	0	0	11_M_5	41_G_3	41g3			No	CPG41G3.FT1H	QSCN6	Homo sapiens c	NM_002826	genyes	5258	4.17	1.18	96.29	4	4	4	
0	0	0	0	0	0	0	0	0	0	0	0	0	0	0	17_T_13	65_E_7	65x7			No	CPG65E7.FT1A	HUMPPA	Homo sapiens f	NM_014603	genyes	955	4.08	1.96	97.27	4	4	4	
0	0	0	0	0	0	0	0	0	0	0	0	0	0	0	29_H_2	117_D_1	117d1			No	CPG117D1.RT1A	C1orf38	Homo sapiens c	NM_004848	genyes	1326	2.61	2.45	97.75	4	4	4	
0	0	0	0	0	0	0	0	0	0	0	0	0	0	0	20_H_4	80_D_2	80d2			No	CPG80D2.RT1B	UCP2	Homo sapiens t	NM_003355	genyes	3414	1.85	-0.42	93.42	4	4	2	
0	0	0	0	0	0	0	0	0	0	0	0	0	0	0	23_L_17	91_F_9	91f9			No	CPG91F9.FT1B	RPL18	Homo sapiens r	NM_000979	genyes	4539	1.77	-0.16	94.07	4	4	3	
0	0	0	0	0	0	0	0	0	0	0	0	0	0	0	5_T_23	17_E_12	17x12			No	CPG17E12.RT1B	GABPB2	Homo sapiens c	NM_002041	genyes	11739	1.74	-1.15	91.07	4	4	2	
0	0	0	0	0	0	0	0	0	0	0	0	0	0	0	21_D_8	84_B_4	84b4			No	CPG84B4.FT1B	HKR2	Homo sapiens c	NM_181846	genyes	7792	1.73	0.22	94.80	4	4	4	
0	0	0	0	0	0	0	0	0	0	0	0	0	0	0	21_D_4	84_B_2	84b2			No	CPG84B2.RT1A	EIF2B4	Homo sapiens e	NM_172195	genyes	3440	1.72	0.65	95.58	4	4	4	
0	0	0	0	0	0	0	0	0	0	0	0	0	0	0	25_N_9	99_G_5	99g5			No	CPG99G5.RT1A	MGC1136	Homo sapiens f	NM_024025	genyes	9450	1.71	-0.26	93.84	4	4	3	
0	0	0	0	0	0	0	0	0	0	0	0	0	0	0	20_H_3	79_D_2	79d2			No	CPG79D2.FT1A	UCP2	Homo sapiens t	NM_003355	genyes	2326	1.70	-1.26	90.59	4	4	3	
0	0	0	0	0	0	0	0	0	0	0	0	0	0	0	19_P_19	75_H_10	75h10			No	CPG75H10.RT1A	HRM11L1	Homo sapiens f	NM_001535	genyes	6681	1.69	0.38	95.05	4	4	3	
0	0	0	0	0	0	0	0	0	0	0	0	0	0	0	25_K_8	98_F_4	98f4			No	CPG98F4.RT1A	SON	Homo sapiens e	NM_003103	genyes	8092	1.68	0.05	94.53	4	4	3	
0	0	0	0	0	0	0	0	0	0	0	0	0	0	0	31_P_1	124_H_1	124h1			No	CPG124H1.FT1A	PTPDC1	Homo sapiens f	NM_177995	genyes	250	1.67	-1.27	90.53	4	4	4	
0	0	0	0	0	0	0	0	0	0	0	0	0	0	0	25_G_8	98_D_4	98d4			No	CPG98D4.RT1A	HOXC9	Homo sapiens f	NM_006897	genyes	8094	1.66	-0.70	92.59	4	4	3	
0	0	0	0	0	0	0	0	0	0	0	0	0	0	0	18_G_18	70_D_9	70d9			No	CPG70D9.FT1B	MGC14289	Homo sapiens s	NM_080660	genyes	5845	1.63	-0.58	92.98	4	4	4	
0	0	0	0	0	0	0	0	0	0	0	0	0	0	0	19_H_21	75_D_11	75d11			No	CPG75D11.FT1A	WIG1	Homo sapiens f	NM_022470	genyes	8861	1.62	-0.32	93.68	4	4	0	
0	0	0	0	0	0	0	0	0	0	0	0	0	0	0	13_H_14	52_D_7	52d7			No	CPG52D7.FT1A	TIGD1	Homo sapiens t	NM_145702	genyes	1197	1.62	-0.51	93.20	4	4	3	
0	0	0	0	0	0	0	0	0	0	0	0	0	0	0	9_M_4	34_G_2	34g2			No	CPG34G2.FT1A	MYST2	Homo sapiens m	NM_007067	genyes	4154	1.62	-1.16	91.05	4	4	3	
0	0	0	0	0	0	0	0	0	0	0	0	0	0	0	23_E_10	90_C_5	90c5			No	CPG90C5.FT1A	NOTCH2	Homo sapiens m	NM_024408	genyes	10798	1.61	-1.00	91.64	4	4	4	
0	0	0	0	0	0	0	0	0	0	0	0	0	0	0	23_F_9	91_C_5	91c5			No	CPG91C5.FT1A	TUSC4	Homo sapiens t	NM_006545	genyes	9438	1.59	-0.88	92.10	4	4	4	
0	0	0	0	0	0	0	0	0	0	0	0	0	0	0	23_C_20	90_B_10	90b10			No	CPG90B10.RT1A	LYZ	Homo sapiens b	NM_000239	genyes	8079	1.58	-0.59	92.95	4	4	4	
0	0	0	0	0	0	0	0	0	0	0	0	0	0	0	14_E_19	53_C_10	53c10			No	CPG53C10.RT1B	CCDC2	Homo sapiens c	NM_025103	genyes	7445	1.58	-1.16	91.01	4	4	4	
0	0	0	0	0	0	0	0	0	0	0	0	0	0	0	9_M_11	33_G_6	33g6			No	CPG33G6.FT1A	MRPL43	Homo sapiens r	NM_032112	genyes	11770	1.58	-0.46	93.31	4	4	4	
0	0	0	0	0	0	0	0	0	0	0	0	0	0	0	22_F_21	87_C_11	87c11			No	CPG87C11.FT1A	LOC126248	Homo sapiens f	NM_173479	genyes	9413	1.57	-1.13	91.15	4	4	4	
0	0	0	0	0	0	0	0	0	0	0	0	0	0	0	9_A_23	33_A_12	33a12			No	CPG33A12.RT1A	NXN	Homo sapiens r	NM_022463	genyes	11775	1.57	-1.31	90.36	4	4	4	
0	0	0	0	0	0	0	0	0	0	0	0	0	0	0	25_M_10	98_G_5	98g5			No	CPG98G5.RT1A	FLJ39660	Homo sapiens f	NM_173646	genyes	10810	1.57	-0.83	92.22	4	4	4	
0	0	0	0	0	0	0	0	0	0	0	0	0	0	0	22_O_6	86_H_3	86h3			No	CPG86H3.RT1B	RPS5	Homo sapiens r	NM_001009	genyes	5874	1.56	-0.46	93.28	4	4	2	
0	0	0	0	0	0	0	0	0	0	0	0	0	0	0	25_C_17	97_B_9	97b9			No	CPG97B9.FT1A	GSTK1	Homo sapiens c	NM_015917	genyes	4831	1.55	-1.07	91.40	4	4	4	
0	0	0	0	0	0	0	0	0	0	0	0	0	0	0	20_O_23	77_H_12	77h12			No	CPG77H12.RT1A	TSPYL1	Homo sapiens t	XM_371844	genyes	11297	1.54	-0.91	92.02	4	4	4	
0	0	0	0	0	0	0	0	0	0	0	0	0	0	0	21_D_22	84_B_11	84b11			No	CPG84B11.RT1A	ANKRD25	Homo sapiens e	NM_015493	genyes	9967	1.54	-0.65	92.71	4	4	4	
0	0	0	0	0	0	0	0	0	0	0	0	0	0	0	22_M_4	86_G_2	86g2			No	CPG86G2.RT1B	ZNF451	Homo sapiens z	NM_015555	genyes	4242	1.54	-1.16	91.03	4	4	4	
0	0	0	0	0	0	0	0	0	0	0	0	0	0	0	18_K_16	70_F_8	70f8			No	CPG70F8.RT1A	ZXDB	Homo sapiens z	NM_007157	genyes	3667	1.51	-0.97	91.75	4	4	4	
0	0	0	0	0	0	0	0	0	0	0	0	0	0	0	16_O_5	61_H_3	61h3			No	CPG61H3.RT1A	FLJ25179	Homo sapiens f	NM_144670	genyes	4738	1.51	-0.89	92.08	4	4	4	
0	0	0	0	0	0	0	0	0	0	0	0	0	0	0	20_G_13	77_D_7	77d7			No	CPG77D7.FT1A	MPP2	Homo sapiens r	NM_005374	genyes	421	1.51	-1.04	91.48	4	4	4	
0	0	0	0	0	0	0	0	0	0	0	0	0	0	0	14_L_7	55_F_4	55f4			No	CPG55F4.RT1A	ELMOD1	Homo sapiens f	NM_018712	genyes	6628	1.50	-0.89	92.10	4	4	4	
0	0	0	0	0	0	0	0	0	0	0	0	0	0	0	18_N_9	71_G_5	71g5			No	CPG71G5.FT1A	RPL28	Homo sapiens r	NM_000991	genyes	9378	1.50	-1.14	91.11	4	4	4	
0	0	0	0	0	0	0	0	0	0	0	0	0	0	0	20_I_4	78_E_2	78x2			No	CPG78E2.RT1A	C6orf122	Homo sapiens c	NM_207502	genyes	4228	1.50	-1.36	90.15	4	4	4	
0	0	0	0	0	0	0	0	0	0	0	0	0	0	0	14_F_17	55_C_9	55c9			No	CPG55C9.RT1A	OPA3	Homo sapiens c	NM_025136	genyes	4997	1.50	-1.38	90.04	4	4	4	
0	0	0	0	0	0	0	0	0	0	0	0	0	0	0	23_L_8	92_F_4	92f4			No	CPG92F4.RT1A	ZRANB3	Homo sapiens z	NM_032143	genyes	7804	1.49	-1.19	90.94	4	4	4	
0	0	0	0	0	0	0	0	0	0	0	0	0	0	0	19_M_7	73_G_4	73g4			No	CPG73G4.RT1A	PTEN	Homo sapiens f	NM_000314	genyes	7498	1.48	-1.19	90.92	4	4	4	
0	0	0	0	0	0	0	0	0	0	0	0	0	0	0	28_G_5	110_D_3	110d3			No	CPG110D3.RT1A	C6orf29	Homo sapiens c	NM_032794	genyes	4838	1.48	-1.36	90.14	4	4	4	
0	0	0	0	0	0	0	0	0	0	0	0	0	0	0	21_P_9	83_H_5	83h5			No	CPG83H5.FT1A	MAD2L1BP	Homo sapiens m	NM_014628	genyes	8874	1.48	-1.30	90.39	4	4	4	
0	0	0	0	0	0	0	0	0	0	0	0	0	0	0	9_M_8	34_G_4	34g4			No	CPG34G4.FT1A	C6orf96	Homo sapiens c	NM_017909	genyes	8506	1.46	-1.39	90.00	4	4	3	

Chromatin Immunoprecipitation Protocol for Microarray Analysis – Protein A/G Bead Method, Protocol From the UHN Microarray Centre.

Protocol modified from the Brown and Farnham labs by James Paris and Mark Takahashi

Day One:

Prepare Solutions

1. Prepare necessary volumes of 1x PBS + 0.5 mM EDTA and RIPA Lysis Buffer. Add 100x Protease Inhibitor Cocktail as required. The Protein A Sepharose/1x TE (pH 8.0)– 50% Slurry may also be prepared at this time. Each + or – antibody IP reaction will require the combined sonicated cell lysate from two 150 mm dishes, each dish having 5 – 15 x 10⁶ cells depending on confluence.

Cross-Linking Reaction

2. To reduce any variability in fixation, pool the medium from all like-treated dishes, mix, and re-aliquot so that each 150 mm dish has a final volume of 13 mL.
3. Cross link protein to DNA by adding formaldehyde directly to culture medium to a final concentration of 1% (351 μ L of 37% formaldehyde (Sigma, catalogue # F-8775)) into 13 mL growth medium). Incubate at 37°C for 10 min.
4. Stop the cross-linking reaction by adding glycine (Sigma, catalogue # G7126) to a 125 mM final concentration (650 μ L of 2.5 M stock in 15 mL medium). Incubate at 37°C for 5 min.
5. Aspirate away media and rinse twice with 13 mL of ice-cold 1x PBS + 0.5 mM EDTA. If collecting cells from a number of dishes at once, allow them to sit on ice in the second wash as you work through them.
6. Aspirate away PBS, wash, add 1.5 mL 1x PBS + 0.5 mM EDTA + protease inhibitors and scrape cells into 2 mL microfuge tube (Sarstedt, catalogue # 72.695). Pellet cells by centrifuging at 2000 rpm for 5 min at 4°C and carefully remove supernatant. **At this point cell pellets may be snap frozen in liquid nitrogen and stored at -70°C for subsequent processing.**

Sonication/Chromatin Shearing Efficiency

7. Resuspend the cell pellets in 200 μ L RIPA Lysis Buffer + protease inhibitors and transfer to a 1.5 mL microfuge tube (conical bottom improves sonication efficiency). Incubate samples on ice for 10 min.
8. Keeping samples ice cold, sonicate the cell lysates in order to shear chromatin into lengths of E1000 base pairs. (6 intervals of 25 s, 2 min 'rests' between intervals, power setting '3', Branson 150 cell disruptor).

9. Remove cell debris by centrifuging 20 min at 13 000 rpm at 4°C. Combine the cleared supernatants from the two sonicated cell pellets/condition to a fresh 2 mL Sarstedt tube (catalogue # 72.695).
10. Following sonication a 3 µL aliquot of lysate may be run on a 1% agarose gel to confirm shearing efficiency. To get a truly accurate determination of fragment size, samples should be de-crosslinked at 65°C for 5 hours and the DNA purified before electrophoresis.
11. Typical lysate volume for two sheared cell pellets should be about 600 µL. Bring IP reaction up to 2 mL by adding RIPA Lysis Buffer with protease inhibitors as required.

Preclearing/Immunoprecipitation with Antibody

12. Reduce nonspecific background by pre-clearing the 2 mL sample with 80 µL of Protein A Sepharose/1x TE (pH 8.0) – 50% Slurry. Allow samples to incubate 1 hr at 4°C with rocking.
13. Centrifuge samples at 2000 rpm for 2 min. to pellet the beads and carefully transfer supernatant to a new 2 mL Sarstedt tube avoiding any carry-over of beads. Add 20 µL (1% volume) of 10 mg/mL purified BSA (New England Biolabs, catalogue # B900IS) to each IP sample as a blocking agent.
14. Add 1 µg of antibody against the protein of interest to each '+ antibody' IP reaction and incubate overnight at 4°C with rocking. No-antibody negative control samples are also incubated overnight at 4°C with rocking before continuing with **Day Two** protocol.

Day Two:

Antibody – Protein – DNA Complex Recovery and Washing

1. Add 20 µL of 100 mg/mL yeast tRNA (Invitrogen, catalogue # 15401-029) to each 2 mL IP reaction (1000 µg/mL final concentration) as a blocking agent before adding 60 µL of Protein A Sepharose/1x TE (pH 8.0) – 50% slurry. Incubate at 4°C for 1 hr with rocking.
2. Pellet beads by centrifuging at 2000 rpm for 2 min. Discard the supernatant from the antibody treated samples as this contains unbound, non-specific DNA. A 100 µL aliquot of the supernatant from the 'no-antibody' samples may be taken as 'Total Input Chromatin' positive control for the PCR reaction. This sample is considered to be the input/starting material and needs to have the Protein – DNA crosslinks reversed by heating at 65°C for 5 hours.
3. Wash beads with 1 mL of each of the wash buffers listed below, rocking for 10 min at room temperature. Note: it is recommended that the pelleted beads be gently resuspended in the Low Salt wash buffer and carefully transferred to a conical bottom 1.5 mL microfuge tube as this greatly facilitates spinning the beads down during subsequent wash steps. Remove as much buffer as possible between washes without loss of beads.

- one wash: **Low Salt Immune Complex Wash Buffer**
- four washes: **High Salt Immune Complex Wash Buffer**
- one wash: **LiCl Immune Complex Wash Buffer**
- two washes: **1x TE (pH 8.0)**

Elution of bound Protein – DNA complex

4. Prepare fresh Elution Buffer (1% SDS, 0.1 M NaHCO₃).
 - For each IP reaction: 2x 250 µL elutions → prepare 510 µL:
NaHCO₃: 51 µL 1 M stock (Sigma, catalogue # S-6297)
SDS: 51 µL 10% stock (BioRad, catalogue # 161-0302)
H₂O: 408 µL (Sigma, catalogue # W-9502)
Total volume: 510 µL
5. Elute the Protein–DNA complex by adding 250 µL of elution buffer to the pelleted beads. Incubate 15 min at room temperature with rocking. Spin down and transfer supernatant to a fresh tube avoiding any bead carry-over. Repeat elution and combine the supernatants, centrifuging and transferring supernatant to a fresh tube if necessary to remove all beads. Add 200 µL elution buffer to 100 µL Total Input Chromatin control samples to bring volume up to 300 µL.

De-crosslinking Protein – DNA complex/RNA Digest

De-crosslinking, Proteinase K digest based on Farnham Lab Protocol:
<http://mcardle.oncology.wisc.edu/farnham/protocols/chips.html>

6. Add 20 µL of 5 M NaCl to the combined eluates (200 mM final concentration) and 1 µL of 10 mg/mL RNAse A (Qiagen, from DNeasy Tissue Kit, catalogue # 69504). Incubate at 65°C for 5 hours to reverse the formaldehyde crosslinks.
7. Add 1 mL 100% ethanol, mix by inversion, and allow samples to precipitate at – 20 °C overnight.

Day Three:

Proteinase K Digest

1. Centrifuge samples at maximum rpm for 15-20 min. at 4°C. Carefully remove supernatant and resuspend pellet in 70% ethanol. Spin again at maximum rpm 15-20 min. at 4°C. Remove supernatant and allow pellet to air dry completely.
2. Resuspend pellet in 100 µL 1x TE (pH 7.5). Add 25 µL 5x PK Buffer and 1.5 µL 22 mg/mL Proteinase K (Roche, catalogue # 745723). Incubate at 42°C for 2 hours.

DNA Recovery – QiaQuick PCR Purification Columns

3. DNA may be recovered from the 126.5 µL Proteinase K digested sample using QiaQuick PCR Purification columns following the manufacturer's protocol, but eluting with 100 µL Sigma water. Sample is then dried down to 7 µL using the SpeedVac.

Immunoprecipitated DNA Amplification

DNA amplification based on Brown Lab Protocol:
http://www.microarrays.org/pdfs/BeadBeat_IP.pdf

- wear gloves throughout protocol as you will amplify any DNA that is present/introduced
- enzyme is available from US Biochemical, Sequenase Kit Ver. 2.0 (USB cat # US 70770)
- **Primer A: GTT TCC CAG TCA CGA TCN NNN NNN NN**
- **Primer B: GTT TCC CAG TCA CGA TC**

Round A :

1. Prepare Round A Setup and Reaction Mix.

Arabidopsis Control DNA

During slide scanning, signals from the experimental (+antibody) and reference (– antibody) samples may be normalized using the Arabidopsis Control Spots printed on the array. To do this it is necessary to add a quantity of Arabidopsis Control DNA directly to the Round A Setup master mix for all samples to be amplified and labeled. A stock of Arabidopsis Control DNA is created by amplification of the Arabidopsis Chlorophyll Synthetase insert from a vector produced in-house. The product is size confirmed on an agarose gel, excised and purified using the GFX PCR DNA and Gel Band Purification Kit following manufacturer's protocol.

- **Arabidopsis Control Primer sense: GTT TCC CAG TCA CGA TCN NNN NNN NN**
- **Arabidopsis Control Primer antisense: GTT TCC CAG TCA CGA TC**

The amount of Arabidopsis Control DNA to be added to the Round A Setup master mix is determined by the number of amplification cycles needed to give a good signal from the experimental samples while avoiding saturating the Control Spots. Typically, for amplifications of 22 cycles or so, 1 ng of Arabidopsis Control DNA added to the Round A Setup mix was adequate.

Round A Setup: (per IP)	μL	Round A Reaction Mix	1 rxn (μL)	2.5 rxn (μL)
DNA (can dry down more)	7	5x Sequenase Buffer	1	2.5
5x Sequenase Buffer	2	DNTP's	1.5	3.75
Primer A (100 pmol/ μL)	0.6	DTT	0.75	1.875
Arabidopsis Control DNA (optional)	1 ng	BSA	1.5	3.75
Water (if necessary)		Sequenase	0.3	0.75
Total volume	10	Total volume	5.05	5.05 μL aliquots

- Incubate Round A Setup at 94°C for 2 min. Go to 10°C and hold for 5 min while adding Reaction Mix.
- After 10°C hold, ramp up to 37°C over 8 min.
- Hold at 37°C for 8 min; go to 94°C for 2 min.
- Go to 10°C and hold for 5 min while adding 1.2 μL of diluted Sequenase (dilute 4-fold with Sequenase Dilution Buffer).
- After 10°C hold, ramp up to 37°C over 8 min.
- Remove Round A and add 43.75 μL RNase/DNase-free water (Sigma, catalogue # W4502). This brings the template volume up to 60 μL .

Round B:

- Prepare Round B Setup in PCR tube.

Round B Setup:	1 rxn (μL)	2.5 rxn (μL)
Round A Template	15	--
MgCl ₂	8	20
10x PCR Buffer	10	25
50x aa-dUTP/dNTP's	2	5
Primer B (100 pm/ μL)	1	2.5
Taq	1	2.5 ⁶
Water	63	157.5
Total volume	100	85 μL aliquots + 15 μL sample

- Amplification/Nucleotide Incorporation Program: 92°C for 30 s → 40°C for 30 s → 50°C for 30 s → 72°C for 1 min x optimal cycle number determined by the researcher.

Round B Purification Using CyScribe GFX Purification Kit

PCR Amplified DNA is purified using the CyScribe GFX Purification Kit (Amersham, catalogue # 27-9602-02). 80% ethanol is substituted for the Wash Buffer provided with the kit as it contains Tris, as does the provided Elution Buffer. Tris contains primary amines that will interfere with the dye-coupling reaction. Purified DNA must be eluted with 0.1 M sodium bicarbonate (pH 9.0) NOT water!

- Place one GFX column in a collection tube for each purification to be performed.
- Add 500 μL Capture Buffer to the GFX column.

Annex

3. Transfer the 100 μ L PCR amplification reaction to the GFX column.
4. Mix thoroughly by pipetting sample 4 – 6 times.
5. Centrifuge at 13 000 rpm for 30 sec.
6. Discard flow-through by emptying collection tube. Place GFX column back into the collection tube.
7. Add 600 μ L of 80% ethanol to the column. Centrifuge at 13 000 rpm for 30 sec.
10. Repeat this wash step twice more. Empty the collection tube and spin column for an additional minute to remove all traces of 80% ethanol.
8. Discard the collection tube and transfer GFX column to a fresh 1.5 mL microfuge tube.
9. Apply 60 μ L of 0.1 M sodium bicarbonate (pH 9.0) directly to the top of the glass fiber matrix in the GFX column, ensuring that it is completely covered.
10. Incubate sample at room temperature for 5 min.
11. Centrifuge sample at full speed for 1 min. to recover the purified DNA.
12. Dry sample down to 8 μ L final volume for the labeling reaction. SpeedVac for \approx 20 min. at medium heat. **Should it be necessary the purified aa-dUTP labeled DNA may be frozen at – 20°C before concentration and the protocol continued the next day.**

Labeling Reaction with Alexa Fluor Reactive Dyes

1. Just prior to use resuspend one vial of Alexa 647 or Alexa 555 dye (Molecular Probes catalogue # A-32756) in 2 μ L 100% DMSO (Sigma, catalogue # D-5879). Vortex for 10 s to ensure that dye is completely dissolved.
2. Add the 8 μ L sample to the resuspended fluor and vortex briefly to ensure that reaction is well mixed. DO NOT spin sample down to bottom of tube, but let it settle by gravity instead.
3. Allow the reaction to incubate 1 hour at room temperature in the dark.

Purification of Fluorescently Labeled Probe Using CyScribe GFX Purification Kit

Following dye-coupling, samples are purified separately using the CyScribe GFX Purification Kit (Amersham catalogue # 27-9606-02)

1. Add 90 μ L RNase/DNAse-free water (Sigma, catalogue # W4502) to each labeling reaction to bring volume up to 100 μ L.
2. Place one GFX column in a collection tube for each purification to be performed.
3. Add 500 μ L Capture Buffer to the GFX column.
4. Transfer the 100 μ L labeled sample to the GFX column.
5. Mix thoroughly by pipetting sample 4 – 6 times.
6. Centrifuge at 13 000 rpm for 30 sec.
7. Discard flow-through by emptying collection tube. Place GFX column back into the collection tube.

8. Add 600 μ L of 80% ethanol to the column. Centrifuge at 13 000 rpm for 30 sec. Repeat this wash step twice more. Empty the collection tube and spin column for an additional minute to remove all traces of 80% ethanol.
9. Discard the collection tube and transfer GFX column to a fresh 1.5 mL microfuge tube.
10. Apply 60 μ L of 0.1 M sodium bicarbonate (pH 9.0) directly to the top of the glass fiber matrix in the GFX column, ensuring that it is completely covered.
11. Incubate the GFX column at room temperature for 5 min. Centrifuge at 13 000 rpm for 1 min to collect the purified labeled DNA. At this point paired reactions may be pooled together.
12. To reduce the 120 μ L combined eluent volume to 5 μ L for hybridization, SpeedVac for \approx 35 min at medium heat.

Hybridization Protocol

1. Prepare 100 μ L of hybridization solution per slide. To each 100 μ L of DIG Easy Hyb solution (Roche, catalogue # 1 603 558) add 5 μ L of 10 mg/mL calf thymus DNA (Sigma, catalogue # D8661) and 5 μ L of 10 mg/mL yeast tRNA (Invitrogen, catalogue # 15401-029). Mix thoroughly avoiding formation of bubbles and incubate mixture at 65 °C for two minutes. Cool to room temperature (at least 2 min).
2. Add 85 μ L of hyb solution to the pooled Alexa 647 and Alexa 555 labeled DNA. Mix and incubate the solution at 65 °C for two minutes. Cool to room temperature (at least 2 min).
3. Pipette the labeled probe onto an array. Place a 24 x 60 mm glass coverslip (Corning, catalogue # 48396-160) onto the droplet, angling it in such a way that any bubbles are pushed out from underneath as the coverslip settles. Place the loaded array into a hybridization chamber (microscope boxes using slides as rails to support the arrays). Hybridization chambers contain a small amount of DIG Easy Hyb solution in the bottom to maintain a humid environment.
4. Incubate on a level surface in a 37°C incubator for 8-18 hours.

Day Four:

Slide Washing – CpG Arrays

1. Preheat three slide staining boxes containing a wash solution of 1x SSC and 0.1% SDS (50 mL of 20x SSC stock, 10 mL of 10% SDS, bring to 1L with milliQ water) by allowing to incubate 15 min. in 50 °C water bath. Also, prepare one staining box containing a staining rack filled with 1x SSC, and two other boxes containing 0.1x SSC for the final rinses. These boxes are kept at room temperature.
2. Open the hybridization chamber and remove the coverslip by gently but quickly dipping the array into the slide box containing 1x SSC, allowing the coverslip to slide off on its own. Place slide into the staining rack (up to four slides) and agitate several times before transferring to box containing

Annex

incubating wash solution. Agitate briskly and allow to incubate 8 min. Agitate, incubate for an additional 8 min, agitate and transfer to the next wash box. Repeat with the next two wash boxes.

3. Transfer the staining rack into a staining box containing 0.1x SSC at room temperature. Rinse the slides by agitating briskly about 10x in each of the rinse boxes and quickly remove rack.
4. Remove slide from rack, tap off excess rinse solution and quickly transfer to a microscope box lined on the bottom with blotting paper. Spin slides dry at 640 rpm for 15 min. Arrays can be stored in the dark until scanned for several hours to days.

Chromatin Immunoprecipitation Protocol for Microarray Analysis - Reagents/Solutions

Protease Inhibitor Cocktail (100x):

50 mM AEBSF (Sigma, catalogue # A-8456)	dissolved in DMSO
100 µg/mL aprotinin (Sigma, catalogue # A-1153)	stored at - 20°C,
100 mM benzamidine (Sigma, catalogue # B-6506)	store at 4°C once thawed
1 mg/mL leupeptin (Sigma, catalogue # L-2884)	
1 mg/mL pepstatin (Sigma, catalogue # P-5318)	

1x PBS + 0.5 mM EDTA: 2 x 15 mL washes required per 150 mm dish:

→ add 500 µL 0.5M EDTA to 500 mL 1x PBS to yield ≈ 0.5 mM final concentration of stock for washing adherent cells.

1x PBS + 0.5 mM EDTA with protease inhibitors: 1.5 mL per dish to harvest cells:

→ add 15 µL 100x protease inhibitor cocktail to 1485 µL 1x PBS + 0.5 mM EDTA

RIPA Lysis Buffer:

0.1% SDS (Biorad, catalogue # 161-0302)
1% sodium deoxycholate (Sigma, catalogue # D-5670)
150 mM NaCl (Sigma, catalogue # S-7653)
10 mM NaPO₄ (pH 7.2) (Sigma, catalogue # S-9638)
2 mM EDTA
0.2 mM NaVO₃ (Sigma, catalogue # S-6508)
1% IGEPAL CA-630 (Sigma, catalogue # I-3021)

→ prepare 210 µL per dish/cell pellet by adding 2.1 µL 100x protease inhibitor cocktail to 207.9 µL RIPA Lysis Buffer

Protein A Sepharose/1x TE (pH 8.0) – 50% Slurry:

→ each IP reaction will require 40 µL (preclearing) + 30 µL (recovery) of Protein A Sepharose beads (Amersham, catalogue # 17-0974-01)

Determine total required amount and add a little extra to allow for pipetting error. Wash up to 1 mL of beads three times in 1 mL 1x TE (pH 8.0) by vortexing briefly and then spinning down at 2000 rpm for 2 min. Discard the supernatant. Following last wash add an equal volume of 1x TE to yield a 50% final slurry. Prepare fresh for each experiment as slurry lasts 4 days at 4 °C.

Low Salt Wash Buffer:

0.1% SDS
1% Triton X-100 (Sigma, catalogue # T-9284)
2 mM EDTA
150 mM NaCl
20 mM Tris-HCl (pH 8.0)

Annex

High Salt Wash Buffer:

0.1% SDS
1% Triton X-100
2 mM EDTA
500 mM NaCl
20 mM Tris-HCl (pH 8.0)

LiCl Wash Buffer:

0.25 M LiCl (Sigma, catalogue # L-4408)
1% IGEPAL CA-630
1% sodium deoxycholate
1 mM EDTA
10 mM Tris-HCl (pH 8.0)

Elution Buffer:

1% SDS
0.1 M NaHCO₃ (Sigma, catalogue # S-6297)

Round A Stocks:

dNTP's :

dATP, dGTP, dCTP, dTTP = 3 mM (Invitrogen, catalogue # 10297-018)

DTT:

0.1 M (Invitrogen, Part # Y00147)

BSA:

500 µg/mL (New England Biolabs, catalogue # B900IS)

Sequenase:

13 U/µL (USB, catalogue # 70775Z)

Round B Stocks:

10x PCR Buffer:

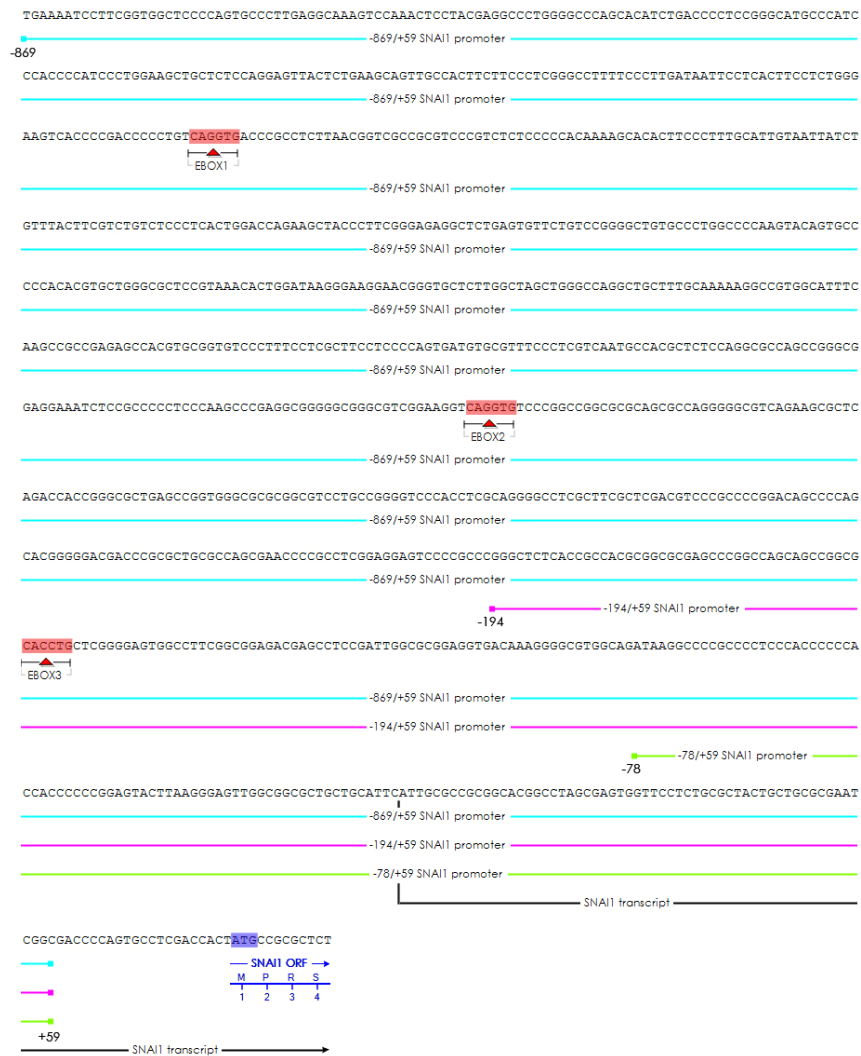
500 mM KCl (Sigma, catalogue # P-9333)
100 mM Tris (pH 8.3)
MgCl₂: 25 mM (Sigma, catalogue # M-2670)
Taq: 5 U/µL

50x aa-dUTP/dNTP:

dATP, dGTP, dCTP = 25 mM each
dTTP = 10 mM,
aa-dUTP = 15 mM (Sigma, catalogue # A-0410)

A.2. Sequence of the -883/+305 *PTEN* promoter and its representative motifs.

A.3. Sequence of the different SNAIL1 promoters used in this study and its representative motifs.



A.4. p53MH software analysis of mouse snail2 transcript and human snail1 transcript.

>16 dna:chromosome:NCBIM37:16:14705945:14709488:1 (mouse slug)

ATGCTATAGGACCGCCGCTGGACCGTATCCGCCCGCGCCCCGCCGAGCCACC
ATGCCGCGCTCCTCCTGGTCAAGAAACATTTCAACGCCTCCAAGAAGCCCAACTACA
GCGAACTGGACACACACACAGGtaaaaatcgctctgtaaatctgtgcgcgagtaaacccgggt
ctattgcttgactcagagaacacacccgggcccgttcccttfaatgctgtgccaaaactgtcctgcagictct
gattacttaggftaagtttaattcaaacctttgagatcttctgacaaaggaagcttccctccggctgggca
gtatagttcctgagcctgtgtacgcaaaaggagtcacggacgtgatgcaccctcccctgcctgag
cagcaatcctgaagccaagcactgggaaagcagctggattcgtgcatgccattaccgcgcaaggc
acggtacagctagaacagcccacgcataaaatgaaaagcaactttataaaaagtttaatatagtgctagt
tcttcttaaatgggacagcaaacctctcagcctgagcctgagcctgggcaactgtcagcctgcac
gaggacagtaagcccagggtgaaggggaagactttatgtgtctctgtgagtaaggctgtctcactagagagt
ctcctatggagctcctgcctgctgtgctcctcagactgtgtacatataatftaaaaatatttgccttaatttt
ttcttcttcttcttcttctccagTTATTATTTCCCATATCTCTATGAAAGTTACCCTATACCTGTCAT
ACCAAACCAGAGATCCTCACCTCGGGAGCATAACAGCCCTATTACTGTATGGACATCG
TCGGCAGCTCCACTCCACTCTCCTTACCCAGTGGCCTTCTCCTTACTGGATACTCCT
CATCCTTGGGGCGTGAAGTCCCCCGCCTTCTCTGACACTTCATCCAAGGATCACAGT
GGTTCAGAAAAGTCCCATTAGTGACGAAGAGGAGAGACTGCAGCCCAAGCTTTCAGAC
CCCCATGCCATCGAAGCTGAGAAGTTTCAGTGCAATTTATGCAATAAGACCTATTCTACGT
TCTCTGGGCTGGCCAAACACAAGCAGCTGCACTGTGATGCCAGTCTAGGAAATCGTT
CAGCTGCAAGTACTGTGACAAGGAATATGTGAGCCTGGGTGCCCTGAAGATGCACAT
CGAACCCACACATTGCCTTGTGTCTGCAAGATCTGTGGCAAGGCTTCTCCAGACCCTG
GCTGCTCAAGGACACATTAGAATCACACTGgtaagagaaatgtagaaaacctgctctcag
ctcaaacagtggtgtgacagagctgtctgcggggtgtcttaagggactgacagggggtgtttcataaggtg
aaccactgatagctgcttctgctctaagcttgttagaacagcaagtgtccttccagcctctgtccaggg
attgtaaacagcatttagactttggaagcacatgcaggagatttggctcaaatcagttagaagcaag
attgaggtatttgggtgtgttctgcagaactgatagtcagtaaatcaaatgtctggctcctagtgttattgat
aaacaggcagagggggttccctatagtttttggctatacttttgcctatgaatttccaactctgactaattag
taaatgaggctaaattggatctggcctgtgtgtttgtttcattttctgttgcctgattttaaaaaagcccaa
gcatgaaatcatatgcaggaagtcaggaattatccagcttagtcatcatacagaagaggagacatact
ggaaatggaggagctgctcatcattgtgcacctgttgaagcagaaacccttagcaagaaaaagcccc
aattctgaatgtgtgtctgtcggcagaacggaagctgttggctgatattttaaagttttgaaaggccaaa
taggaatagaattacataactgggggtgatgatcaagctatgataattctatttctaagctactgttgatg
ttcattaatattactgattttgtcctataaaaagctgactgtctttatftccctaccctaccctcaaacagGG
GAAAAGCCITTTCTTGCCCTCACTGCAATAGGGCTTTTGCAGACAGATCAAACCTGAG
GGCACATCTGCAGACCCACTCTGATGTAAAGAAATACCAGTGCAAAAACCTGCTCCAAA
ACCTTCTCCAGAATGTCGCTTCTGCATAAACATGAGGAGTCTGGCTGCTGTGTGGCACAC
TGA

>20 dna:chromosome:NCBI36:20:48032934:48038825:1 (human snail1)

ATGCCGCGCTCTTTCCTCGTCAGGAAGCCCTCCGACCCCAATCGGAAGCCTAACTAC
AGCGAGCTGCAGGACTCTAATCCAGgtgcgttgaggggtctgggctccaggagggtggggga
gacaggcgaaggctgcgtggggggcacctgagggaggcggcctgcctgagccaggatcgagtcacag
gatgtttgtggaccattgctgggctcgggagaccgggcaagtgggtcccagttccggggatctgtctgggt
ggttgggggagtgccgtgtagagggcaggggtctcagctggggggcctttgtagccggcagagggcgg
aggagctccgcaagagggaaggagaggaggcctgtgtcaggaggccctctggacgctgctgggga
gagtccggagtccagagggtgaggggaggggtggggagacgagatgtgtgaggagggggattggg
gcagggtgggtggctccggggctgggatgatgggtctggcctcaggctggagactggggactaggaga
gggagatcaggaaatgaccctcctcaactgggggtcctacgtgtgagagactcagattgggtgacctggg
cgaggaggcaggaacctggctgtcctgtggataatTTTTgatctaattatgtattgagaatcgcccccac
ccagccccggccagcgggtgggctcatgtttgtgattgagtgatgatttaacccctgactctgtctttct
ccctcagAGTTACCTCCAGCAGCCCTACGACCAGGCCACCTGCTGGCAGCCATCC
CACCTCCGGAGATCCTCAACCCACCCGCTCGCTGCCAATGCTCATCTGGGACTCTGT
CCTGGCGCCCCAAGCCCAGCCAATTGCCTGGGCCTCCCTTCGGCTCCAGGAGAGTC
CCAGGTGGCAGAGCTGACCTCCCTGTCAGATGAGGACAGTGGGAAAGGCTCCA
GCCCCCAGCCCACCCCTCACGGCTCCTTCGTCCTTCTCCTACTTCACTCTCTTCTT
GGAGGCCGAGGCCTATGCTGCCTTCCCAGGCTTGGGCCAAGTGCCCAAGCAGCTG
GCCAGCTCTCTGAGGCCAAGGATCTCCAGGCTCGAAAGGCCTTCAACTGCAAATAC
TGCAACAAGGAATACCTCAGCCTGGGTGCCCTCAAGATGCACATCCGAAGCCACAC
GCTGCCCTGCGTCTGCGGAACCTGCGGGAAGGCCCTTCTAGGCCCTGGCTGTACA
A**GGCCATGTCCGGACCCACACTGgtacgtgccc**ctccaggcgccccaccgttctctctctggc
agcttttgaatctgggcttctgttctcattcccaagctgtggacactgaggccccagctcttaacttcta
gctcaagttccaggccctggctctctggaacgtttggcagaaactttctcatcagctaagcagatgggca
aagcagcaacttcccaatcccctgcagcctgtttctcagccaaatgggtcggagctggatattggaaag
gtgcaaccaacaccttctgtggggccagggtgtgagggggcccaaccggccacaccctctccgggt
ccgccccctcctagccagacaggatgtgtcagaccctggctgtgactcttcttggagaacttct
tcaaaacttaggctgatgttctctctgtgagcctcatttctctatcttccagatgggcatgagaacagctttgg
ggttctatacaggctaaatgcaggaatgcatatgggaagcacctggcaaaagtccgggtacctgctaaact
ctcaaaaaatggctctggcattgtctgtctctctgtgtgactttggcaagcaacttaacctctctga
gcccttaggggaaactatgatagcctgttttagagagtggtctgtaaaagggtggctaatcactttatgtaatt
attataccgaacgggtctcaggtcggcttccccacccccactgaatcctagcacacagaccaggaaac
ggcatctttgggagagaaacacaatcacgtcttttgaaaatttactaatgtgtaaaaaactttctggacatg
gagaaaaggtagaaccttttagaacttgaatgggtggcagccactgtgctggagctgctctttggagagtga
cagttgagggagaagattccacagggtcaagctggccagggtctgccatttctggcctggcgcctgacct
ctgagcggtaggggttagtgagggtctgggaggactggcaattcgcgggctttattggcatctattcgacta
aggctaccatttctctctcgtgaccaattgctctgatttfaacatgtaagggtccaactgctggcctctct
gggtgctgcccagctcacagggtctattttgggacagttgaaccctcagggtgctgagctctgctgctgc
ctctctcacctcccactggacatttttaatgtaaggcatggctgagacacagaatccccctgaaatgta
tcattgggtcctcattgactcccattgtgtgccttaatgggtgggcccagtggtgggggctgggaggggtgg
agcaggtgcatggggcagcgggtgccagcactgttccagtcacagctgctggcccactgcatggcagc
cccccttaatcggggatcgcattgtacagtgccccctcggcgccccctttgtccccggcggctgggtgccg
attcacacttggcaggagtaccatgaaggcgtctggggggcaggggatccaaggagtgggggtctgtgc
ctctgctgtgacacagccccgccccagcccatcatgtcctagaatgtcctctccccctttgtttgggtt
caggtctcatcacacttgggcaacttactgtacaggagggtagtgcctcaggacttccaacacagccctggg
aaggaagggagggtgctgtcctaactctggtcttacaatggactccagcccctttccagatctccagagt
cagccccttagttcacaagggtgaacttacccttctcattcacatgaagacttagaatgcaatcaacaacc
ttcagggctggcgtgtggaggctgctgagtaatggcagagtggagtgtgctcaggcaccctcccccaat
cctctatgtccccaccctttggagtggcagtttccatttctgccccatgagactgagctcagctctcaggc
gctccataagttccctattgaatgcatgggtcccattggagccatcctctggactctctctaccctggtagct

agtgtggcaccctagcaccaggaggatggaatgaattcactctcagctctaaattccatccagcgt
 gggattcacagggggccctgacctgcgggcatatcagactgggcgtgaggggattggagaattgcat
 gttttfaaaagactattcagatattggaatagtgctagcacttagtaggagctcagtagattaaaaaaa
 aattatgacagggcttgccttgccttaggcttgcctcaactcctggctcaagcaatcctgcctcactg
 gcctccagagtgatgggattacaagcgtgagccaccacaccagcctcaatagattttggttaatgggta
 ctgtatgacctttattggaaaatgctgcatccccagaaaaaacaatcaacattattggtttttggaa
 ctatatgcttttggttggagcagggtttatgagggcatgagtgagggggcagactcctctgaggccttt
 aatfttaaacagactatttattcctaaagcctttagggatttacttaggacccagctcctgtgcaaga
 ctttcccaacacagccttgccaggcagatgggtgtcagggccacagggttccgtagcctctgggtgata
 gaaagggggccaggccctgggctggggctcagaagggactcaaggaggccctgccctatgggact
 cagcctgattggagaacagacaaggagattgggattacagcgcaggagggtgggtgaggaaagc
 aggtgctggccggggccaggagtgccctaacagcctggagggtgggggaggccttaaggc
 tgaactctggctttggcccaacagagtaaatcaaggaatgactccaggactgatggaaggacaccagt
 cacgtcctccctgactgaaggcagtaaggcagtaggtgaaatcagaggctttgggtcctgcccagggg
 aacctgaacatgctactctgggctcagttcactgtctctgaaatgagaccacagtaggatcaagtaca
 gtaggatgaatcagtaaagggttgatgactttgaccacttcgcacgtccctgcgggatgaggatgagta
 cctacctctgtcactatcaaccctatgagtggggggtgaaatagcccaatttacagggtgggaaaatggg
 gctcagagaagccagacaactgtcagagttgcacagtggaagcagcagagctccgtcaggtcccg
 gcctttggaccctggctgtgtgttgacggaggcctggcttccctgggatcatgggattcttcaggggtgggg
 atgcggggagggttcccatcactgccagccgttgcaccaggctcactggcctttctggcgttctctccc
 agGCGAGAAGCCCTTCTCCTGTCCCCACTGCAGCCGTGCCTTCGCTGACCGCTCCAA
 CCTGCGGGCCACCTCCAGACCCACTCAGATGTCAAGAAGTACCAGTGCCAGGCGT
 GTGCTCGGACCTTCTCCGAATGTCCCTGCTCCACAAGCACCAAGAGTCCGGCTGCT
 CAGGATGTCCCC

-
- **Introns** are displayed in blue lower case.
 - Exons are displayed in BLACK UPPER CASE.
 - **ATG** is displayed in underlined bold.
 - Color boxes are putative (in the case of snail1 human transcript) or confirmed (in the case of snail2 mouse transcript) p53 responsive elements.

Annex

Program p53MH
J. Hoh and J. Ott
Version of 01 Sep 2002

Treatment of "N" sites:
In filter: No filtering
Scoring: Give anti-consensus weight

current maximum sequence length: 30000000 bp
gap weights used: FALSE
smoothing factor for gap weights: 0.10
factor for core sites: 2.00
filtering applied: TRUE
smoothing constant s in ln(LR+s): -1 (automatic)
lik.ratio (vs probability) scoring: TRUE
sequence length: Whole gene
print flanking sequences: FALSE
gap lengths tested: -1 14 variable
max gap length: 14

=== snail human gene ===

Sequence length = 5892
Using s = 0.273414
Total sequence length = 5892
Maximum possible score (no gap weights): 25.911
171 out of 5873 sites have score calculated (not filtered)

Observed order statistics:

Order	Site	Score	%max	
1	3667	24.042	92.79	GGTCTTGCTT TATCGCCT AGGCTTGTCT (p53 RE2)
2	1341	19.469	75.14	GGCCATGTCC GGACCCACACTG GTACGTGCC (p53 RE1)
3	3984	19.450	75.06	GGGCTTGTGG AGGATTACTGGG CACCCAGCTC (p53 RE3)

=== slug mouse gene ===

Sequence length = 3544
Using s = 0.262229
Total sequence length = 3544
Maximum possible score (no gap weights): 26.009
103 out of 3525 sites have score calculated (not filtered)

Observed order statistics:

Order	Site	Score	%max	
1	1541	22.375	86.03	AAGCTTGTTA GAA CAGCAAGTGC (p53 RE2)
3	633	19.480	74.90	AGGCTAGTCC AGAATGA AGGTTAGTCA (p53 RE1)

BIBLIOGRAPHY

Bibliography

- [1] P. Savagner Leaving the neighborhood: molecular mechanisms involved during epithelial-mesenchymal transition, *Bioessays* 23 (2001) 912-923.
- [2] L. Larue, M. Ohsugi, J. Hirchenhain and R. Kemler E-cadherin null mutant embryos fail to form a trophoderm epithelium, *Proc Natl Acad Sci U S A* 91 (1994) 8263-8267.
- [3] C. Bierkamp, K.J. McLaughlin, H. Schwarz, O. Huber and R. Kemler Embryonic heart and skin defects in mice lacking plakoglobin, *Dev Biol* 180 (1996) 780-785.
- [4] H. Haegel, L. Larue, M. Ohsugi, L. Fedorov, K. Herrenknecht and R. Kemler Lack of beta-catenin affects mouse development at gastrulation, *Development* 121 (1995) 3529-3537.
- [5] E.D. Hay An overview of epithelio-mesenchymal transformation, *Acta Anat (Basel)* 154 (1995) 8-20.
- [6] P. Savagner, B. Boyer, A.M. Valles, J. Jouanneau and J.P. Thiery Modulations of the epithelial phenotype during embryogenesis and cancer progression, *Cancer Treat Res* 71 (1994) 229-249.
- [7] M.A. Nieto, M.G. Sargent, D.G. Wilkinson and J. Cooke Control of cell behavior during vertebrate development by Slug, a zinc finger gene, *Science* 264 (1994) 835-839.
- [8] C. Thisse, B. Thisse and J.H. Postlethwait Expression of snail2, a second member of the zebrafish snail family, in cephalic mesendoderm and presumptive neural crest of wild-type and spadetail mutant embryos, *Dev Biol* 172 (1995) 86-99.
- [9] S. Allard, P. Adin, L. Gouedard, N. di Clemente, N. Josso, M.C. Orgebin-Crist, J.Y. Picard and F. Xavier Molecular mechanisms of hormone-mediated Mullerian duct regression: involvement of beta-catenin, *Development* 127 (2000) 3349-3360.
- [10] J.M.W. Slack *From egg to embryo : determinative events in early development*, Cambridge University Press, Cambridge, 1983.
- [11] W.J. Larsen *Human embryology*, Churchill Livingstone, New York ; Edinburgh, 1993.
- [12] D. Sela-Donenfeld and C. Kalcheim Regulation of the onset of neural crest migration by coordinated activity of BMP4 and Noggin in the dorsal neural tube, *Development* 126 (1999) 4749-4762.
- [13] N.M. Le Douarin and M.E. Halpern Discussion point. Origin and specification of the neural tube floor plate: insights from the chick and zebrafish, *Curr Opin Neurobiol* 10 (2000) 23-30.
- [14] J.A. Weston A radioautographic analysis of the migration and localization of trunk neural crest cells in the chick, *Dev Biol* 6 (1963) 279-310.
- [15] R.J. Keynes and C.D. Stern Segmentation in the vertebrate nervous system, *Nature* 310 (1984) 786-789.
- [16] C.A. Erickson and R. Perris The role of cell-cell and cell-matrix interactions in the morphogenesis of the neural crest, *Dev Biol* 159 (1993) 60-74.
- [17] M. Bronner-Fraser Analysis of the early stages of trunk neural crest migration in avian embryos using monoclonal antibody HNK-1, *Dev Biol* 115 (1986) 44-55.

Bibliography

- [18] R.W. Raven *The theory and practice of oncology : historical evolution and present principles*, Parthenon, Camforth, 1990.
- [19] D. Hanahan and R.A. Weinberg *The hallmarks of cancer*, *Cell* 100 (2000) 57-70.
- [20] L. Foulds *The experimental study of tumor progression: a review*, *Cancer Res* 14 (1954) 327-339.
- [21] P.C. Nowell *The clonal evolution of tumor cell populations*, *Science* 194 (1976) 23-28.
- [22] M. Dean *Cancer as a complex developmental disorder--nineteenth* Cornelius P. Rhoads Memorial Award Lecture, *Cancer Res* 58 (1998) 5633-5636.
- [23] K. Vleminckx, L. Vakaet, Jr., M. Mareel, W. Fiers and F. van Roy *Genetic manipulation of E-cadherin expression by epithelial tumor cells reveals an invasion suppressor role*, *Cell* 66 (1991) 107-119.
- [24] A.K. Perl, P. Wilgenbus, U. Dahl, H. Semb and G. Christofori *A causal role for E-cadherin in the transition from adenoma to carcinoma*, *Nature* 392 (1998) 190-193.
- [25] J.J. Christiansen and A.K. Rajasekaran *Reassessing epithelial to mesenchymal transition as a prerequisite for carcinoma invasion and metastasis*, *Cancer Res* 66 (2006) 8319-8326.
- [26] M.A. Huber, N. Kraut and H. Beug *Molecular requirements for epithelial-mesenchymal transition during tumor progression*, *Curr Opin Cell Biol* 17 (2005) 548-558.
- [27] B. De Craene, F. van Roy and G. Berx *Unraveling signalling cascades for the Snail family of transcription factors*, *Cell Signal* 17 (2005) 535-547.
- [28] J.P. Thiery *Epithelial-mesenchymal transitions in development and pathologies*, *Curr Opin Cell Biol* 15 (2003) 740-746.
- [29] H. Peinado, D. Olmeda and A. Cano *Snail, Zeb and bHLH factors in tumour progression: an alliance against the epithelial phenotype?*, *Nat Rev Cancer* 7 (2007) 415-428.
- [30] A. Cano, M.A. Perez-Moreno, I. Rodrigo, A. Locascio, M.J. Blanco, M.G. del Barrio, F. Portillo and M.A. Nieto *The transcription factor snail controls epithelial-mesenchymal transitions by repressing E-cadherin expression*, *Nat Cell Biol* 2 (2000) 76-83.
- [31] E. Battle, E. Sancho, C. Franci, D. Dominguez, M. Monfar, J. Baulida and A. Garcia De Herreros *The transcription factor snail is a repressor of E-cadherin gene expression in epithelial tumour cells*, *Nat Cell Biol* 2 (2000) 84-89.
- [32] A. Eger, K. Aigner, S. Sonderegger, B. Dampier, S. Oehler, M. Schreiber, G. Berx, A. Cano, H. Beug and R. Foisner *DeltaEF1 is a transcriptional repressor of E-cadherin and regulates epithelial plasticity in breast cancer cells*, *Oncogene* 24 (2005) 2375-2385.
- [33] A.A. Postigo, J.L. Depp, J.J. Taylor and K.L. Kroll *Regulation of Smad signaling through a differential recruitment of coactivators and corepressors by ZEB proteins*, *Embo J* 22 (2003) 2453-2462.
- [34] J.E. Remacle, H. Kraff, W. Lerchner, G. Wuytens, C. Collart, K. Verschueren, J.C. Smith and D. Huylebroeck *New mode of DNA binding of multi-zinc finger transcription factors: deltaEF1 family members bind with two hands to two target sites*, *Embo J* 18 (1999) 5073-5084.

- [35] T. Van de Putte, M. Maruhashi, A. Francis, L. Nelles, H. Kondoh, D. Huylebroeck and Y. Higashi Mice lacking ZFX1B, the gene that codes for Smad-interacting protein-1, reveal a role for multiple neural crest cell defects in the etiology of Hirschsprung disease-mental retardation syndrome, *Am J Hum Genet* 72 (2003) 465-470.
- [36] T. Ellenberger, D. Fass, M. Arnaud and S.C. Harrison Crystal structure of transcription factor E47: E-box recognition by a basic region helix-loop-helix dimer, *Genes Dev* 8 (1994) 970-980.
- [37] M.A. Perez-Moreno, A. Locascio, I. Rodrigo, G. Dhondt, F. Portillo, M.A. Nieto and A. Cano A new role for E12/E47 in the repression of E-cadherin expression and epithelial-mesenchymal transitions, *J Biol Chem* 276 (2001) 27424-27431.
- [38] E. Takahashi, N. Funato, N. Higashihori, Y. Hata, T. Gridley and M. Nakamura Snail regulates p21(WAF/CIP1) expression in cooperation with E2A and Twist, *Biochem Biophys Res Commun* 325 (2004) 1136-1144.
- [39] W. Zheng, H. Wang, L. Xue, Z. Zhang and T. Tong Regulation of cellular senescence and p16(INK4a) expression by Id1 and E47 proteins in human diploid fibroblast, *J Biol Chem* 279 (2004) 31524-31532.
- [40] M.S. Kumar, J.A. Hendrix, A.D. Johnson and G.K. Owens Smooth muscle alpha-actin gene requires two E-boxes for proper expression in vivo and is a target of class I basic helix-loop-helix proteins, *Circ Res* 92 (2003) 840-847.
- [41] J. Yang, S.A. Mani, J.L. Donaher, S. Ramaswamy, R.A. Itzykson, C. Come, P. Savagner, I. Gitelman, A. Richardson and R.A. Weinberg Twist, a master regulator of morphogenesis, plays an essential role in tumor metastasis, *Cell* 117 (2004) 927-939.
- [42] A. Alberga, J.L. Boulay, E. Kempe, C. Dennefeld and M. Haenlin The snail gene required for mesoderm formation in *Drosophila* is expressed dynamically in derivatives of all three germ layers, *Development* 111 (1991) 983-992.
- [43] M.A. Nieto, M.F. Bennett, M.G. Sargent and D.G. Wilkinson Cloning and developmental expression of *Sna*, a murine homologue of the *Drosophila* snail gene, *Development* 116 (1992) 227-237.
- [44] D.E. Smith, F. Franco del Amo and T. Gridley Isolation of *Sna*, a mouse gene homologous to the *Drosophila* genes *snail* and *escargot*: its expression pattern suggests multiple roles during postimplantation development, *Development* 116 (1992) 1033-1039.
- [45] M. Hammerschmidt and C. Nusslein-Volhard The expression of a zebrafish gene homologous to *Drosophila* snail suggests a conserved function in invertebrate and vertebrate gastrulation, *Development* 119 (1993) 1107-1118.
- [46] J.A. Langeland, J.M. Tomsa, W.R. Jackman, Jr. and C.B. Kimmel An amphioxus snail gene: expression in paraxial mesoderm and neural plate suggests a conserved role in patterning the chordate embryo, *Dev Genes Evol* 208 (1998) 569-577.
- [47] S. Wada and H. Saiga Cloning and embryonic expression of *Hrsna*, a snail family gene of the ascidian *Halocynthia roretzi*: implication in the origins of mechanisms for mesoderm specification and body axis formation in chordates, *Dev Growth Differ* 41 (1999) 9-18.

Bibliography

- [48] R. Mayor, N. Guerrero, R.M. Young, J.L. Gomez-Skarmeta and C. Cuellar A novel function for the Xslug gene: control of dorsal mesendoderm development by repressing BMP-4, *Mech Dev* 97 (2000) 47-56.
- [49] E.A. Carver, R. Jiang, Y. Lan, K.F. Oram and T. Gridley The mouse snail gene encodes a key regulator of the epithelial-mesenchymal transition, *Mol Cell Biol* 21 (2001) 8184-8188.
- [50] A. Mancilla and R. Mayor Neural crest formation in *Xenopus laevis*: mechanisms of Xslug induction, *Dev Biol* 177 (1996) 580-589.
- [51] T.F. Carl, C. Duffon, J. Hanken and M.W. Klymkowsky Inhibition of neural crest migration in *Xenopus* using antisense slug RNA, *Dev Biol* 213 (1999) 101-115.
- [52] C. LaBonne and M. Bronner-Fraser Snail-related transcriptional repressors are required in *Xenopus* for both the induction of the neural crest and its subsequent migration, *Dev Biol* 221 (2000) 195-205.
- [53] Y. Grau, C. Carteret and P. Simpson Mutations and Chromosomal Rearrangements Affecting the Expression of Snail, a Gene Involved in Embryonic Patterning in *DROSOPHILA MELANOGASTER*, *Genetics* 108 (1984) 347-360.
- [54] M.A. Nieto The snail superfamily of zinc-finger transcription factors, *Nat Rev Mol Cell Biol* 3 (2002) 155-166.
- [55] V. Mauhin, Y. Lutz, C. Dennefeld and A. Alberga Definition of the DNA-binding site repertoire for the *Drosophila* transcription factor SNAIL, *Nucleic Acids Res* 21 (1993) 3951-3957.
- [56] N. Fuse, S. Hirose and S. Hayashi Diploidy of *Drosophila* imaginal cells is maintained by a transcriptional repressor encoded by *escargot*, *Genes Dev* 8 (1994) 2270-2281.
- [57] T. Inukai, A. Inoue, H. Kurosawa, K. Goi, T. Shinjyo, K. Ozawa, M. Mao, T. Inaba and A.T. Look SLUG, a *ces-1*-related zinc finger transcription factor gene with antiapoptotic activity, is a downstream target of the E2A-HLF oncoprotein, *Mol Cell* 4 (1999) 343-352.
- [58] H. Kataoka, T. Murayama, M. Yokode, S. Mori, H. Sano, H. Ozaki, Y. Yokota, S. Nishikawa and T. Kita A novel snail-related transcription factor *Smuc* regulates basic helix-loop-helix transcription factor activities via specific E-box motifs, *Nucleic Acids Res* 28 (2000) 626-633.
- [59] H. Peinado, M. Quintanilla and A. Cano Transforming growth factor beta-1 induces snail transcription factor in epithelial cell lines: mechanisms for epithelial mesenchymal transitions, *J Biol Chem* 278 (2003) 21113-21123.
- [60] J.P. Liu and T.M. Jessell A role for rhoB in the delamination of neural crest cells from the dorsal neural tube, *Development* 125 (1998) 5055-5067.
- [61] M.G. del Barrio and M.A. Nieto Overexpression of Snail family members highlights their ability to promote chick neural crest formation, *Development* 129 (2002) 1583-1593.
- [62] J. Grosshans and E. Wieschaus A genetic link between morphogenesis and cell division during formation of the ventral furrow in *Drosophila*, *Cell* 101 (2000) 523-531.
- [63] S. Vega, A.V. Morales, O.H. Ocana, F. Valdes, I. Fabregat and M.A. Nieto Snail blocks the cell cycle and confers resistance to cell death, *Genes Dev* 18 (2004) 1131-1143.

- [64] M.M. Metzstein and H.R. Horvitz The *C. elegans* cell death specification gene *ces-1* encodes a snail family zinc finger protein, *Mol Cell* 4 (1999) 309-319.
- [65] A. Barrallo-Gimeno and M.A. Nieto The Snail genes as inducers of cell movement and survival: implications in development and cancer, *Development* 132 (2005) 3151-3161.
- [66] S. Guaita, I. Puig, C. Franci, M. Garrido, D. Dominguez, E. Batlle, E. Sancho, S. Dedhar, A.G. De Herreros and J. Baulida Snail induction of epithelial to mesenchymal transition in tumor cells is accompanied by MUC1 repression and ZEB1 expression, *J Biol Chem* 277 (2002) 39209-39216.
- [67] J. Ikenouchi, M. Matsuda, M. Furuse and S. Tsukita Regulation of tight junctions during the epithelium-mesenchyme transition: direct repression of the gene expression of claudins/occludin by Snail, *J Cell Sci* 116 (2003) 1959-1967.
- [68] H.G. Palmer, M.J. Larriba, J.M. Garcia, P. Ordonez-Moran, C. Pena, S. Peiro, I. Puig, R. Rodriguez, R. de la Fuente, A. Bernad, M. Pollan, F. Bonilla, C. Gamallo, A.G. de Herreros and A. Munoz The transcription factor SNAIL represses vitamin D receptor expression and responsiveness in human colon cancer, *Nat Med* 10 (2004) 917-919.
- [69] C.E. Espineda, J.H. Chang, J. Twiss, S.A. Rajasekaran and A.K. Rajasekaran Repression of Na,K-ATPase beta1-subunit by the transcription factor snail in carcinoma, *Mol Biol Cell* 15 (2004) 1364-1373.
- [70] M. Kajita, K.N. McClinic and P.A. Wade Aberrant expression of the transcription factors snail and slug alters the response to genotoxic stress, *Mol Cell Biol* 24 (2004) 7559-7566.
- [71] A. Miyoshi, Y. Kitajima, S. Kido, T. Shimonishi, S. Matsuyama, K. Kitahara and K. Miyazaki Snail accelerates cancer invasion by upregulating MMP expression and is associated with poor prognosis of hepatocellular carcinoma, *Br J Cancer* 92 (2005) 252-258.
- [72] M. Taki, N. Kamata, K. Yokoyama, R. Fujimoto, S. Tsutsumi and M. Nagayama Down-regulation of Wnt-4 and up-regulation of Wnt-5a expression by epithelial-mesenchymal transition in human squamous carcinoma cells, *Cancer Sci* 94 (2003) 593-597.
- [73] D. Dominguez, B. Montserrat-Sentis, A. Virgos-Soler, S. Guaita, J. Grueso, M. Porta, I. Puig, J. Baulida, C. Franci and A. Garcia de Herreros Phosphorylation regulates the subcellular location and activity of the snail transcriptional repressor, *Mol Cell Biol* 23 (2003) 5078-5089.
- [74] H. Peinado, E. Ballestar, M. Esteller and A. Cano Snail mediates E-cadherin repression by the recruitment of the Sin3A/histone deacetylase 1 (HDAC1)/HDAC2 complex, *Mol Cell Biol* 24 (2004) 306-319.
- [75] B.P. Zhou, J. Deng, W. Xia, J. Xu, Y.M. Li, M. Gunduz and M.C. Hung Dual regulation of Snail by GSK-3beta-mediated phosphorylation in control of epithelial-mesenchymal transition, *Nat Cell Biol* 6 (2004) 931-940.
- [76] H. Peinado, M. Del Carmen Iglesias-de la Cruz, D. Olmeda, K. Csiszar, K.S. Fong, S. Vega, M.A. Nieto, A. Cano and F. Portillo A molecular role for lysyl oxidase-like 2 enzyme in snail regulation and tumor progression, *Embo J* 24 (2005) 3446-3458.
- [77] H. Peinado, F. Portillo and A. Cano Switching on-off Snail: LOXL2 versus GSK3beta, *Cell Cycle* 4 (2005) 1749-1752.

Bibliography

- [78] Z. Yang, S. Rayala, D. Nguyen, R.K. Vadlamudi, S. Chen and R. Kumar Pak1 phosphorylation of snail, a master regulator of epithelial-to-mesenchyme transition, modulates snail's subcellular localization and functions, *Cancer Res* 65 (2005) 3179-3184.
- [79] S. Yamashita, C. Miyagi, T. Fukada, N. Kagara, Y.S. Che and T. Hirano Zinc transporter LIV1 controls epithelial-mesenchymal transition in zebrafish gastrula organizer, *Nature* 429 (2004) 298-302.
- [80] F.M. Spagnoli, C. Cicchini, M. Tripodi and M.C. Weiss Inhibition of MMH (Met murine hepatocyte) cell differentiation by TGF(beta) is abrogated by pre-treatment with the heritable differentiation effector FGF1, *J Cell Sci* 113 (Pt 20) (2000) 3639-3647.
- [81] C. Tan, P. Costello, J. Sanghera, D. Dominguez, J. Baulida, A.G. de Herreros and S. Dedhar Inhibition of integrin linked kinase (ILK) suppresses beta-catenin-Lef/Tcf-dependent transcription and expression of the E-cadherin repressor, snail, in APC-/- human colon carcinoma cells, *Oncogene* 20 (2001) 133-140.
- [82] J. Gotzmann, H. Huber, C. Thallinger, M. Wolschek, B. Jansen, R. Schulte-Hermann, H. Beug and W. Mikulits Hepatocytes convert to a fibroblastoid phenotype through the cooperation of TGF-beta1 and Ha-Ras: steps towards invasiveness, *J Cell Sci* 115 (2002) 1189-1202.
- [83] M. Yanez-Mo, E. Lara-Pezzi, R. Selgas, M. Ramirez-Huesca, C. Dominguez-Jimenez, J.A. Jimenez-Heffernan, A. Aguilera, J.A. Sanchez-Tomero, M.A. Bajo, V. Alvarez, M.A. Castro, G. del Peso, A. Cirujeda, C. Gamallo, F. Sanchez-Madrid and M. Lopez-Cabrera Peritoneal dialysis and epithelial-to-mesenchymal transition of mesothelial cells, *N Engl J Med* 348 (2003) 403-413.
- [84] S.J. Grille, A. Bellacosa, J. Upson, A.J. Klein-Szanto, F. van Roy, W. Lee-Kwon, M. Donowitz, P.N. Tschlis and L. Larue The protein kinase Akt induces epithelial mesenchymal transition and promotes enhanced motility and invasiveness of squamous cell carcinoma lines, *Cancer Res* 63 (2003) 2172-2178.
- [85] M.J. Barbera, I. Puig, D. Dominguez, S. Julien-Grille, S. Guaita-Esteruelas, S. Peiro, J. Baulida, C. Franci, S. Dedhar, L. Larue and A. Garcia de Herreros Regulation of Snail transcription during epithelial to mesenchymal transition of tumor cells, *Oncogene* 23 (2004) 7345-7354.
- [86] M. Sefton, S. Sanchez and M.A. Nieto Conserved and divergent roles for members of the Snail family of transcription factors in the chick and mouse embryo, *Development* 125 (1998) 3111-3121.
- [87] K. Hemavathy, S.I. Ashraf and Y.T. Ip Snail/slug family of repressors: slowly going into the fast lane of development and cancer, *Gene* 257 (2000) 1-12.
- [88] M.J. Blanco, G. Moreno-Bueno, D. Sarrío, A. Locascio, A. Cano, J. Palacios and M.A. Nieto Correlation of Snail expression with histological grade and lymph node status in breast carcinomas, *Oncogene* 21 (2002) 3241-3246.
- [89] B. Ciruna and J. Rossant FGF signaling regulates mesoderm cell fate specification and morphogenetic movement at the primitive streak, *Dev Cell* 1 (2001) 37-49.
- [90] J.P. Thiery Epithelial-mesenchymal transitions in tumour progression, *Nat Rev Cancer* 2 (2002) 442-454.

- [91] A.F. Chambers, A.C. Groom and I.C. MacDonald Dissemination and growth of cancer cells in metastatic sites, *Nat Rev Cancer* 2 (2002) 563-572.
- [92] B. Alberts *Molecular biology of the cell*, Garland Science ; [London : Taylor & Francis, distributor], New York, 2008.
- [93] R.E. Bachelder, S.O. Yoon, C. Franci, A.G. de Herreros and A.M. Mercurio Glycogen synthase kinase-3 is an endogenous inhibitor of Snail transcription: implications for the epithelial-mesenchymal transition, *J Cell Biol* 168 (2005) 29-33.
- [94] C. Franci, M. Takkunen, N. Dave, F. Alameda, S. Gomez, R. Rodriguez, M. Escrava, B. Montserrat-Sentis, T. Baro, M. Garrido, F. Bonilla, I. Virtanen and A. Garcia de Herreros Expression of Snail protein in tumor-stroma interface, *Oncogene* 25 (2006) 5134-5144.
- [95] C.W. Cheng, P.E. Wu, J.C. Yu, C.S. Huang, C.T. Yue, C.W. Wu and C.Y. Shen Mechanisms of inactivation of E-cadherin in breast carcinoma: modification of the two-hit hypothesis of tumor suppressor gene, *Oncogene* 20 (2001) 3814-3823.
- [96] S.E. Moody, D. Perez, T.C. Pan, C.J. Sarkisian, C.P. Portocarrero, C.J. Sterner, K.L. Notorfrancesco, R.D. Cardiff and L.A. Chodosh The transcriptional repressor Snail promotes mammary tumor recurrence, *Cancer Cell* 8 (2005) 197-209.
- [97] S. Elloul, M.B. Elstrand, J.M. Nesland, C.G. Trope, G. Kvalheim, I. Goldberg, R. Reich and B. Davidson Snail, Slug, and Smad-interacting protein 1 as novel parameters of disease aggressiveness in metastatic ovarian and breast carcinoma, *Cancer* 103 (2005) 1631-1643.
- [98] K. Sugimachi, S. Tanaka, T. Kameyama, K. Taguchi, S. Aishima, M. Shimada, K. Sugimachi and M. Tsuneyoshi Transcriptional repressor snail and progression of human hepatocellular carcinoma, *Clin Cancer Res* 9 (2003) 2657-2664.
- [99] E. Rosivatz, I. Becker, K. Specht, E. Fricke, B. Luber, R. Busch, H. Hofler and K.F. Becker Differential expression of the epithelial-mesenchymal transition regulators snail, SIP1, and twist in gastric cancer, *Am J Pathol* 161 (2002) 1881-1891.
- [100] S. Takeno, T. Noguchi, S. Fumoto, Y. Kimura, T. Shibata and K. Kawahara E-cadherin expression in patients with esophageal squamous cell carcinoma: promoter hypermethylation, Snail overexpression, and clinicopathologic implications, *Am J Clin Pathol* 122 (2004) 78-84.
- [101] M.H. Yang, S.Y. Chang, S.H. Chiou, C.J. Liu, C.W. Chi, P.M. Chen, S.C. Teng and K.J. Wu Overexpression of NBS1 induces epithelial-mesenchymal transition and co-expression of NBS1 and Snail predicts metastasis of head and neck cancer, *Oncogene* 26 (2007) 1459-1467.
- [102] E. Rosivatz, K.F. Becker, E. Kremmer, C. Schott, K. Blechschmidt, H. Hofler and M. Sarbia Expression and nuclear localization of Snail, an E-cadherin repressor, in adenocarcinomas of the upper gastrointestinal tract, *Virchows Arch* 448 (2006) 277-287.
- [103] C. Pena, J.M. Garcia, J. Silva, V. Garcia, R. Rodriguez, I. Alonso, I. Millan, C. Salas, A.G. de Herreros, A. Munoz and F. Bonilla E-cadherin and vitamin D receptor regulation by SNAIL and ZEB1 in colon cancer: clinicopathological correlations, *Hum Mol Genet* 14 (2005) 3361-3370.
- [104] H.K. Roy, T.C. Smyrk, J. Koetsier, T.A. Victor and R.K. Wali The transcriptional repressor SNAIL is overexpressed in human colon cancer, *Dig Dis Sci* 50 (2005) 42-46.

Bibliography

- [105] W.Z. Gao, J.M. Li, F.D. Yang, J. Zhou and Y.Q. Ding [Expression of the zinc finger transcriptional factor Snail in colorectal carcinoma and its significance.], *Nan Fang Yi Ke Da Xue Xue Bao* 28 (2008) 162-165.
- [106] J. Lotem and L. Sachs Control of apoptosis in hematopoiesis and leukemia by cytokines, tumor suppressor and oncogenes, *Leukemia* 10 (1996) 925-931.
- [107] A. Ashkenazi and V.M. Dixit Apoptosis control by death and decoy receptors, *Curr Opin Cell Biol* 11 (1999) 255-260.
- [108] G. Evan and T. Littlewood A matter of life and cell death, *Science* 281 (1998) 1317-1322.
- [109] Y. Ishizaki, L. Cheng, A.W. Mudge and M.C. Raff Programmed cell death by default in embryonic cells, fibroblasts, and cancer cells, *Mol Biol Cell* 6 (1995) 1443-1458.
- [110] F.G. Giancotti and E. Ruoslahti Integrin signaling, *Science* 285 (1999) 1028-1032.
- [111] D.R. Green and J.C. Reed Mitochondria and apoptosis, *Science* 281 (1998) 1309-1312.
- [112] N.A. Thornberry and Y. Lazebnik Caspases: enemies within, *Science* 281 (1998) 1312-1316.
- [113] J.F. Kerr, A.H. Wyllie and A.R. Currie Apoptosis: a basic biological phenomenon with wide-ranging implications in tissue kinetics, *Br J Cancer* 26 (1972) 239-257.
- [114] C.C. Harris p53 tumor suppressor gene: from the basic research laboratory to the clinic--an abridged historical perspective, *Carcinogenesis* 17 (1996) 1187-1198.
- [115] S. Gupta, A. Agrawal, S. Agrawal, H. Su and S. Gollapudi A paradox of immunodeficiency and inflammation in human aging: lessons learned from apoptosis, *Immun Ageing* 3 (2006) 5.
- [116] S.Y. Shieh, M. Ikeda, Y. Taya and C. Prives DNA damage-induced phosphorylation of p53 alleviates inhibition by MDM2, *Cell* 91 (1997) 325-334.
- [117] R. Maya, M. Balass, S.T. Kim, D. Shkedy, J.F. Leal, O. Shifman, M. Moas, T. Buschmann, Z. Ronai, Y. Shiloh, M.B. Kastan, E. Katzir and M. Oren ATM-dependent phosphorylation of Mdm2 on serine 395: role in p53 activation by DNA damage, *Genes Dev* 15 (2001) 1067-1077.
- [118] M.F. Lavin and N. Gueven The complexity of p53 stabilization and activation, *Cell Death Differ* 13 (2006) 941-950.
- [119] A. Ashkenazi Targeting death and decoy receptors of the tumour-necrosis factor superfamily, *Nat Rev Cancer* 2 (2002) 420-430.
- [120] R. Yao and G.M. Cooper Growth factor-dependent survival of rodent fibroblasts requires phosphatidylinositol 3-kinase but is independent of pp70S6K activity, *Oncogene* 13 (1996) 343-351.
- [121] L.C. Cantley The phosphoinositide 3-kinase pathway, *Science* 296 (2002) 1655-1657.
- [122] B.M. Burgering and P.J. Coffe Protein kinase B (c-Akt) in phosphatidylinositol-3-OH kinase signal transduction, *Nature* 376 (1995) 599-602.

Bibliography

- [123] T.F. Franke, S.I. Yang, T.O. Chan, K. Datta, A. Kazlauskas, D.K. Morrison, D.R. Kaplan and P.N. Tsichlis The protein kinase encoded by the Akt proto-oncogene is a target of the PDGF-activated phosphatidylinositol 3-kinase, *Cell* 81 (1995) 727-736.
- [124] A.D. Kohn, K.S. Kovacina and R.A. Roth Insulin stimulates the kinase activity of RAC-PK, a pleckstrin homology domain containing ser/thr kinase, *Embo J* 14 (1995) 4288-4295.
- [125] G. Kulik, A. Klippel and M.J. Weber Antiapoptotic signalling by the insulin-like growth factor I receptor, phosphatidylinositol 3-kinase, and Akt, *Mol Cell Biol* 17 (1997) 1595-1606.
- [126] Z. Songyang, D. Baltimore, L.C. Cantley, D.R. Kaplan and T.F. Franke Interleukin 3-dependent survival by the Akt protein kinase, *Proc Natl Acad Sci U S A* 94 (1997) 11345-11350.
- [127] A. Inoue, M.G. Seidel, W. Wu, S. Kamizono, A.A. Ferrando, R.T. Bronson, H. Iwasaki, K. Akashi, A. Morimoto, J.K. Hitzler, T.J. Pestina, C.W. Jackson, R. Tanaka, M.J. Chong, P.J. McKinnon, T. Inukai, G.C. Grosveld and A.T. Look Slug, a highly conserved zinc finger transcriptional repressor, protects hematopoietic progenitor cells from radiation-induced apoptosis in vivo, *Cancer Cell* 2 (2002) 279-288.
- [128] W.S. Wu, S. Heinrichs, D. Xu, S.P. Garrison, G.P. Zambetti, J.M. Adams and A.T. Look Slug antagonizes p53-mediated apoptosis of hematopoietic progenitors by repressing puma, *Cell* 123 (2005) 641-653.
- [129] C. Martinez-Alvarez, M.J. Blanco, R. Perez, M.A. Rabadan, M. Aparicio, E. Resel, T. Martinez and M.A. Nieto Snail family members and cell survival in physiological and pathological cleft palates, *Dev Biol* 265 (2004) 207-218.
- [130] H.K. Roy, P. Iversen, J. Hart, Y. Liu, J.L. Koetsier, Y. Kim, D.P. Kunte, M. Madugula, V. Backman and R.K. Wali Down-regulation of SNAIL suppresses MIN mouse tumorigenesis: modulation of apoptosis, proliferation, and fractal dimension, *Mol Cancer Ther* 3 (2004) 1159-1165.
- [131] P.A. Perez-Mancera, M. Perez-Caro, I. Gonzalez-Herrero, T. Flores, A. Orfao, A.G. de Herreros, A. Gutierrez-Adan, B. Pintado, A. Sagrera, M. Sanchez-Martin and I. Sanchez-Garcia Cancer development induced by graded expression of Snail in mice, *Hum Mol Genet* 14 (2005) 3449-3461.
- [132] D.R. Alessi, M. Andjelkovic, B. Caudwell, P. Cron, N. Morrice, P. Cohen and B.A. Hemmings Mechanism of activation of protein kinase B by insulin and IGF-1, *Embo J* 15 (1996) 6541-6551.
- [133] V. Bolos, H. Peinado, M.A. Perez-Moreno, M.F. Fraga, M. Esteller and A. Cano The transcription factor Slug represses E-cadherin expression and induces epithelial to mesenchymal transitions: a comparison with Snail and E47 repressors, *J Cell Sci* 116 (2003) 499-511.
- [134] V. Stambolic, D. MacPherson, D. Sas, Y. Lin, B. Snow, Y. Jang, S. Benchimol and T.W. Mak Regulation of PTEN transcription by p53, *Mol Cell* 8 (2001) 317-325.
- [135] J.I. Yook, X.Y. Li, I. Ota, E.R. Fearon and S.J. Weiss Wnt-dependent regulation of the E-cadherin repressor snail, *J Biol Chem* 280 (2005) 11740-11748.
- [136] Y. Sanchez, C. Wong, R.S. Thoma, R. Richman, Z. Wu, H. Piwnicka-Worms and S.J. Elledge Conservation of the Chk1 checkpoint pathway in mammals: linkage of DNA damage to Cdk regulation through Cdc25, *Science* 277 (1997) 1497-1501.

Bibliography

- [137] J. Roig and J.A. Traugh p21-activated protein kinase gamma-PAK is activated by ionizing radiation and other DNA-damaging agents. Similarities and differences to alpha-PAK, *J Biol Chem* 274 (1999) 31119-31122.
- [138] S. Grille, A. Bellacosa and L. Larue [Regulation of E-cadherin by the Akt protein kinase B], *J Soc Biol* 198 (2004) 375-378.
- [139] J.R. Pomerening, E.D. Sontag and J.E. Ferrell, Jr. Building a cell cycle oscillator: hysteresis and bistability in the activation of Cdc2, *Nat Cell Biol* 5 (2003) 346-351.
- [140] A. Nose, A. Nagafuchi and M. Takeichi Expressed recombinant cadherins mediate cell sorting in model systems, *Cell* 54 (1988) 993-1001.
- [141] S.R. Frank, M. Schroeder, P. Fernandez, S. Taubert and B. Amati Binding of c-Myc to chromatin mediates mitogen-induced acetylation of histone H4 and gene activation, *Genes Dev* 15 (2001) 2069-2082.
- [142] S.R. Datta, A. Brunet and M.E. Greenberg Cellular survival: a play in three Akts, *Genes Dev* 13 (1999) 2905-2927.
- [143] B. Vanhaesebroeck and D.R. Alessi The PI3K-PDK1 connection: more than just a road to PKB, *Biochem J* 346 Pt 3 (2000) 561-576.
- [144] R. Wang and M.G. Brattain AKT can be activated in the nucleus, *Cell Signal* 18 (2006) 1722-1731.
- [145] R. Yao and G.M. Cooper Requirement for phosphatidylinositol-3 kinase in the prevention of apoptosis by nerve growth factor, *Science* 267 (1995) 2003-2006.
- [146] S. Bao, G. Ouyang, X. Bai, Z. Huang, C. Ma, M. Liu, R. Shao, R.M. Anderson, J.N. Rich and X.F. Wang Periostin potently promotes metastatic growth of colon cancer by augmenting cell survival via the Akt/PKB pathway, *Cancer Cell* 5 (2004) 329-339.
- [147] Q. Shi, S. Bao, J.A. Maxwell, E.D. Reese, H.S. Friedman, D.D. Bigner, X.F. Wang and J.N. Rich Secreted protein acidic, rich in cysteine (SPARC), mediates cellular survival of gliomas through AKT activation, *J Biol Chem* 279 (2004) 52200-52209.
- [148] H.G. Wendel, E. De Stanchina, J.S. Fridman, A. Malina, S. Ray, S. Kogan, C. Cordon-Cardo, J. Pelletier and S.W. Lowe Survival signalling by Akt and eIF4E in oncogenesis and cancer therapy, *Nature* 428 (2004) 332-337.
- [149] L. del Peso, M. Gonzalez-Garcia, C. Page, R. Herrera and G. Nunez Interleukin-3-induced phosphorylation of BAD through the protein kinase Akt, *Science* 278 (1997) 687-689.
- [150] S.R. Datta, H. Dudek, X. Tao, S. Masters, H. Fu, Y. Gotoh and M.E. Greenberg Akt phosphorylation of BAD couples survival signals to the cell-intrinsic death machinery, *Cell* 91 (1997) 231-241.
- [151] M.H. Cardone, N. Roy, H.R. Stennicke, G.S. Salvesen, T.F. Franke, E. Stanbridge, S. Frisch and J.C. Reed Regulation of cell death protease caspase-9 by phosphorylation, *Science* 282 (1998) 1318-1321.

- [152] A.H. Kim, G. Khursigara, X. Sun, T.F. Franke and M.V. Chao Akt phosphorylates and negatively regulates apoptosis signal-regulating kinase 1, *Mol Cell Biol* 21 (2001) 893-901.
- [153] L.P. Kane, V.S. Shapiro, D. Stokoe and A. Weiss Induction of NF-kappaB by the Akt/PKB kinase, *Curr Biol* 9 (1999) 601-604.
- [154] L.D. Mayo and D.B. Donner A phosphatidylinositol 3-kinase/Akt pathway promotes translocation of Mdm2 from the cytoplasm to the nucleus, *Proc Natl Acad Sci U S A* 98 (2001) 11598-11603.
- [155] T.F. Franke, C.P. Hornik, L. Segev, G.A. Shostak and C. Sugimoto PI3K/Akt and apoptosis: size matters, *Oncogene* 22 (2003) 8983-8998.
- [156] J. Li, C. Yen, D. Liaw, K. Podsypanina, S. Bose, S.I. Wang, J. Puc, C. Miliareis, L. Rodgers, R. McCombie, S.H. Bigner, B.C. Giovanella, M. Iftmann, B. Tycko, H. Hibshoosh, M.H. Wigler and R. Parsons PTEN, a putative protein tyrosine phosphatase gene mutated in human brain, breast, and prostate cancer, *Science* 275 (1997) 1943-1947.
- [157] P.A. Steck, M.A. Pershouse, S.A. Jasser, W.K. Yung, H. Lin, A.H. Ligon, L.A. Langford, M.L. Baumgard, T. Hattler, T. Davis, C. Frye, R. Hu, B. Swedlund, D.H. Teng and S.V. Tavtigian Identification of a candidate tumour suppressor gene, MMAC1, at chromosome 10q23.3 that is mutated in multiple advanced cancers, *Nat Genet* 15 (1997) 356-362.
- [158] T. Maehama, G.S. Taylor and J.E. Dixon PTEN and myotubularin: novel phosphoinositide phosphatases, *Annu Rev Biochem* 70 (2001) 247-279.
- [159] M. Tamura, J. Gu, E.H. Danen, T. Takino, S. Miyamoto and K.M. Yamada PTEN interactions with focal adhesion kinase and suppression of the extracellular matrix-dependent phosphatidylinositol 3-kinase/Akt cell survival pathway, *J Biol Chem* 274 (1999) 20693-20703.
- [160] M. Raptopoulou, S. Etienne-Manneville, A. Self, S. Nicholls and A. Hall Regulation of cell migration by the C2 domain of the tumor suppressor PTEN, *Science* 303 (2004) 1179-1181.
- [161] L.M. Chow and S.J. Baker PTEN function in normal and neoplastic growth, *Cancer Lett* 241 (2006) 184-196.
- [162] I. Sansal and W.R. Sellers The biology and clinical relevance of the PTEN tumor suppressor pathway, *J Clin Oncol* 22 (2004) 2954-2963.
- [163] D.J. Freeman, A.G. Li, G. Wei, H.H. Li, N. Kertesz, R. Lesche, A.D. Whale, H. Martinez-Diaz, N. Rozenfurt, R.D. Cardiff, X. Liu and H. Wu PTEN tumor suppressor regulates p53 protein levels and activity through phosphatase-dependent and -independent mechanisms, *Cancer Cell* 3 (2003) 117-130.
- [164] H.B. Salvesen, N. MacDonald, A. Ryan, I.J. Jacobs, E.D. Lynch, L.A. Akslen and S. Das PTEN methylation is associated with advanced stage and microsatellite instability in endometrial carcinoma, *Int J Cancer* 91 (2001) 22-26.
- [165] Y.E. Whang, X. Wu, H. Suzuki, R.E. Reiter, C. Tran, R.L. Vessella, J.W. Said, W.B. Isaacs and C.L. Sawyers Inactivation of the tumor suppressor PTEN/MMAC1 in advanced human prostate cancer through loss of expression, *Proc Natl Acad Sci U S A* 95 (1998) 5246-5250.

Bibliography

- [166] X.P. Zhou, O. Gimm, H. Hampel, T. Niemann, M.J. Walker and C. Eng Epigenetic PTEN silencing in malignant melanomas without PTEN mutation, *Am J Pathol* 157 (2000) 1123-1128.
- [167] D. Liaw, D.J. Marsh, J. Li, P.L. Dahia, S.J. Wang, Z. Zheng, S. Bose, K.M. Call, H.C. Tsou, M. Peacocke, C. Eng and R. Parsons Germline mutations of the PTEN gene in Cowden disease, an inherited breast and thyroid cancer syndrome, *Nat Genet* 16 (1997) 64-67.
- [168] L. Li and A.H. Ross Why is PTEN an important tumor suppressor?, *J Cell Biochem* 102 (2007) 1368-1374.
- [169] L.D. Mayo, J.E. Dixon, D.L. Durden, N.K. Tonks and D.B. Donner PTEN protects p53 from Mdm2 and sensitizes cancer cells to chemotherapy, *J Biol Chem* 277 (2002) 5484-5489.
- [170] M. Zhou, L. Gu, H.W. Findley, R. Jiang and W.G. Woods PTEN reverses MDM2-mediated chemotherapy resistance by interacting with p53 in acute lymphoblastic leukemia cells, *Cancer Res* 63 (2003) 6357-6362.
- [171] D. Xia, H. Srinivas, Y.H. Ahn, G. Sethi, X. Sheng, W.K. Yung, Q. Xia, P.J. Chiao, H. Kim, P.H. Brown, Wistuba, II, B.B. Aggarwal and J.M. Kurie Mitogen-activated protein kinase kinase-4 promotes cell survival by decreasing PTEN expression through an NF kappa B-dependent pathway, *J Biol Chem* 282 (2007) 3507-3519.
- [172] J.Y. Chow, K.T. Quach, B.L. Cabrera, J.A. Cabral, S.E. Beck and J.M. Carethers RAS/ERK modulates TGFbeta-regulated PTEN expression in human pancreatic adenocarcinoma cells, *Carcinogenesis* 28 (2007) 2321-2327.
- [173] M. Escrava, S. Peiro, N. Herranz, P. Villagrana, N. Dave, B. Montserrat-Sentis, S.A. Murray, C. Franci, T. Gridley, I. Virtanen and A. Garcia de Herreros Repression of PTEN phosphatase by Snail1 transcriptional factor during gamma-radiation-induced apoptosis, *Mol Cell Biol* (2008).
- [174] L. Simpson and R. Parsons PTEN: life as a tumor suppressor, *Exp Cell Res* 264 (2001) 29-41.
- [175] T. Saito, Y. Oda, K. Kawaguchi, K. Sugimachi, H. Yamamoto, N. Tateishi, K. Tanaka, S. Matsuda, Y. Iwamoto, M. Ladanyi and M. Tsuneyoshi E-cadherin mutation and Snail overexpression as alternative mechanisms of E-cadherin inactivation in synovial sarcoma, *Oncogene* 23 (2004) 8629-8638.
- [176] A. Tsutsumida, J. Hamada, M. Tada, T. Aoyama, K. Furuuchi, Y. Kawai, Y. Yamamoto, T. Sugihara and T. Moriuchi Epigenetic silencing of E- and P-cadherin gene expression in human melanoma cell lines, *Int J Oncol* 25 (2004) 1415-1421.
- [177] R. Villa, D. Pasini, A. Gutierrez, L. Morey, M. Occhionorelli, E. Vire, J.F. Nomdedeu, T. Jenuwein, P.G. Pelicci, S. Minucci, F. Fuks, K. Helin and L. Di Croce Role of the polycomb repressive complex 2 in acute promyelocytic leukemia, *Cancer Cell* 11 (2007) 513-525.
- [178] A.M. Al-Khouri, Y. Ma, S.H. Togo, S. Williams and T. Mustelin Cooperative phosphorylation of the tumor suppressor phosphatase and tensin homologue (PTEN) by casein kinases and glycogen synthase kinase 3beta, *J Biol Chem* 280 (2005) 35195-35202.
- [179] L. Odriozola, G. Singh, T. Hoang and A.M. Chan Regulation of PTEN activity by its carboxyl-terminal autoinhibitory domain, *J Biol Chem* 282 (2007) 23306-23315.

- [180] W.P. Roos and B. Kaina DNA damage-induced cell death by apoptosis, *Trends Mol Med* 12 (2006) 440-450.
- [181] J. Bartek and J. Lukas DNA damage checkpoints: from initiation to recovery or adaptation, *Curr Opin Cell Biol* 19 (2007) 238-245.
- [182] Y. Shiloh ATM and related protein kinases: safeguarding genome integrity, *Nat Rev Cancer* 3 (2003) 155-168.
- [183] S. Bekker-Jensen, C. Lukas, R. Kitagawa, F. Melander, M.B. Kastan, J. Bartek and J. Lukas Spatial organization of the mammalian genome surveillance machinery in response to DNA strand breaks, *J Cell Biol* 173 (2006) 195-206.
- [184] J. Falck, N. Mailand, R.G. Syljuasen, J. Bartek and J. Lukas The ATM-Chk2-Cdc25A checkpoint pathway guards against radioresistant DNA synthesis, *Nature* 410 (2001) 842-847.
- [185] C.Y. Peng, P.R. Graves, R.S. Thoma, Z. Wu, A.S. Shaw and H. Piwnica-Worms Mitotic and G2 checkpoint control: regulation of 14-3-3 protein binding by phosphorylation of Cdc25C on serine-216, *Science* 277 (1997) 1501-1505.
- [186] M. Perez-Caro, C. Bermejo-Rodriguez, I. Gonzalez-Herrero, M. Sanchez-Beato, M.A. Piris and I. Sanchez-Garcia Transcriptomal profiling of the cellular response to DNA damage mediated by Slug (Snai2), *Br J Cancer* 98 (2008) 480-488.
- [187] A. Deffie, H. Wu, V. Reinke and G. Lozano The tumor suppressor p53 regulates its own transcription, *Mol Cell Biol* 13 (1993) 3415-3423.
- [188] Y. Ogawara, S. Kishishita, T. Obata, Y. Isazawa, T. Suzuki, K. Tanaka, N. Masuyama and Y. Gotoh Akt enhances Mdm2-mediated ubiquitination and degradation of p53, *J Biol Chem* 277 (2002) 21843-21850.
- [189] J. Hoh, S. Jin, T. Parrado, J. Edington, A.J. Levine and J. Ott The p53M^H algorithm and its application in detecting p53-responsive genes, *Proc Natl Acad Sci U S A* 99 (2002) 8467-8472.
- [190] R. Kumar, A.E. Gururaj and C.J. Barnes p21-activated kinases in cancer, *Nat Rev Cancer* 6 (2006) 459-471.
- [191] M. Freeman Feedback control of intercellular signalling in development, *Nature* 408 (2000) 313-319.
- [192] D. Sakai, T. Suzuki, N. Osumi and Y. Wakamatsu Cooperative action of Sox9, Snai2 and PKA signaling in early neural crest development, *Development* 133 (2006) 1323-1333.
- [193] J. Capdevila, K.J. Vogan, C.J. Tabin and J.C. Izpisua Belmonte Mechanisms of left-right determination in vertebrates, *Cell* 101 (2000) 9-21.
- [194] A. Monsoro-Burq and N. Le Douarin Left-right asymmetry in BMP4 signalling pathway during chick gastrulation, *Mech Dev* 97 (2000) 105-108.
- [195] J.K. Dale, P. Malapert, J. Chal, G. Vilhais-Neto, M. Maroto, T. Johnson, S. Jayasinghe, P. Trainor, B. Herrmann and O. Pourquie Oscillations of the snail genes in the presomitic mesoderm coordinate segmental patterning and morphogenesis in vertebrate somitogenesis, *Dev Cell* 10 (2006) 355-366.

Bibliography

- [196] S. Kuphal, I. Poser, C. Jobin, C. Hellerbrand and A.K. Bosserhoff Loss of E-cadherin leads to upregulation of NF-kappaB activity in malignant melanoma, *Oncogene* 23 (2004) 8509-8519.
- [197] C. Jamora, P. Lee, P. Kocieniewski, M. Azhar, R. Hosokawa, Y. Chai and E. Fuchs A signaling pathway involving TGF-beta2 and snail in hair follicle morphogenesis, *PLoS Biol* 3 (2005) e11.
- [198] M.L. Grootclaes and S.M. Frisch Evidence for a function of CtBP in epithelial gene regulation and anoikis, *Oncogene* 19 (2000) 3823-3828.
- [199] K.M. Hajra, D.Y. Chen and E.R. Fearon The SLUG zinc-finger protein represses E-cadherin in breast cancer, *Cancer Res* 62 (2002) 1613-1618.
- [200] Y. Fujita, G. Krause, M. Scheffner, D. Zechner, H.E. Leddy, J. Behrens, T. Sommer and W. Birchmeier Hakai, a c-Cbl-like protein, ubiquitinates and induces endocytosis of the E-cadherin complex, *Nat Cell Biol* 4 (2002) 222-231.
- [201] S. Julien, I. Puig, E. Caretti, J. Bonaventure, L. Nelles, F. van Roy, C. Dargemont, A.G. de Herreros, A. Bellacosa and L. Larue Activation of NF-kappaB by Akt upregulates Snail expression and induces epithelium mesenchyme transition, *Oncogene* 26 (2007) 7445-7456.
- [202] K.M. Yamada and M. Araki Tumor suppressor PTEN: modulator of cell signaling, growth, migration and apoptosis, *J Cell Sci* 114 (2001) 2375-2382.
- [203] M. Tamura, J. Gu, T. Takino and K.M. Yamada Tumor suppressor PTEN inhibition of cell invasion, migration, and growth: differential involvement of focal adhesion kinase and p130Cas, *Cancer Res* 59 (1999) 442-449.
- [204] J. Liliental, S.Y. Moon, R. Lesche, R. Mamillapalli, D. Li, Y. Zheng, H. Sun and H. Wu Genetic deletion of the Pten tumor suppressor gene promotes cell motility by activation of Rac1 and Cdc42 GTPases, *Curr Biol* 10 (2000) 401-404.
- [205] S. Funamoto, R. Meili, S. Lee, L. Parry and R.A. Firtel Spatial and temporal regulation of 3-phosphoinositides by PI 3-kinase and PTEN mediates chemotaxis, *Cell* 109 (2002) 611-623.
- [206] M. Iijima and P. Devreotes Tumor suppressor PTEN mediates sensing of chemoattractant gradients, *Cell* 109 (2002) 599-610.
- [207] V. Stambolic, A. Suzuki, J.L. de la Pompa, G.M. Brothers, C. Mirtsos, T. Sasaki, J. Ruland, J.M. Penninger, D.P. Siderovski and T.W. Mak Negative regulation of PKB/Akt-dependent cell survival by the tumor suppressor PTEN, *Cell* 95 (1998) 29-39.
- [208] M.P. Myers, I. Pass, I.H. Batty, J. Van der Kaay, J.P. Stolarov, B.A. Hemmings, M.H. Wigler, C.P. Downes and N.K. Tonks The lipid phosphatase activity of PTEN is critical for its tumor suppressor function, *Proc Natl Acad Sci U S A* 95 (1998) 13513-13518.
- [209] M. Tamura, J. Gu, K. Matsumoto, S. Aota, R. Parsons and K.M. Yamada Inhibition of cell migration, spreading, and focal adhesions by tumor suppressor PTEN, *Science* 280 (1998) 1614-1617.
- [210] T. Muller, A. Choidas, E. Reichmann and A. Ullrich Phosphorylation and free pool of beta-catenin are regulated by tyrosine kinases and tyrosine phosphatases during epithelial cell migration, *J Biol Chem* 274 (1999) 10173-10183.

Bibliography

- [211] S. Persad, A.A. Troussard, T.R. McPhee, D.J. Mulholland and S. Dedhar Tumor suppressor PTEN inhibits nuclear accumulation of beta-catenin and T cell/lymphoid enhancer factor 1-mediated transcriptional activation, *J Cell Biol* 153 (2001) 1161-1174.

PUBLISHED PAPERS

Escrivà M, Peiró S, Herranz N, Villagrasa P, Dave N, Montserrat-Sentís B, Murray SA, Francí C, Gridley T, Virtanen I, García de Herreros A.

[Repression of PTEN phosphatase by Snail1 transcriptional factor during gamma radiation-induced apoptosis.](#)

Mol Cell Biol. 2008 Mar;28(5):1528-40. Epub 2008 Jan 2.

Francí C, Takkunen M, Dave N, Alameda F, Gómez S, Rodríguez R, Escrivà M, Montserrat-Sentís B, Baró T, Garrido M, Bonilla F, Virtanen I, García de Herreros A.

[Expression of Snail protein in tumor-stroma interface.](#)

Oncogene. 2006 Aug 24;25(37):5134-44. Epub 2006 Mar 27.